

DISS. ETH NO. 25794

Brain metabolic sensing and energy homeostasis

A thesis submitted to attain the degree of
DOCTOR OF SCIENCES of ETH ZURICH
(Dr. sc. ETH Zurich)

presented by
NADJA WEISSFELD

M.Sc., Universität Potsdam (Germany)

born on 18.02.1988
citizen of Germany

accepted on the recommendation of

Prof. Dr. Wolfgang Langhans, examiner
Prof. Dr. Barry Levin, co-examiner
Prof. Dr. Thomas Lutz, co-examiner
Dr. Abdelhak Mansouri, co-examiner

2019

“I cannot teach anybody anything; I can only make them think.”

Socrates

ACKNOWLEDGEMENTS

My greatest gratitude goes to you, Wolfgang. Without you, I would not be where I am writing this acknowledgment, feeling enriched in so many ways. I wish we would have been as close from the beginning as we are today. Thank you for encouraging and pushing me. Thank you for making me stronger and believe I can achieve anything, there is not more I could have wished for.

Abdelhak, there are no words describing my gratitude. Thank you, for being ALWAYS there for me, day and night, especially the last year. That is nothing one can take for granted and I will not. Your mentorship and friendship guided me to the finishing stretch, forming me into a better scientist. Thank you.

Barry and Thomas, thank you! I could not have asked for a better committee! Thank you not only for your scientific advice and support throughout the journey, but also for making me feel I can always turn to you. Unfortunately, I did not do so, but knowing I could was already worth a lot. Thank you.

Myrtha, thank you! Nothing ever was too much to ask for - you would always help and support. You are amazing and unique in so many ways, and I learned so much from you, thank you.

I wanted to keep this short; therefore, one more big THANK YOU to the former Langhans group as it was in June 2015! JP, Rosi, Shahana, Deepti, and Melanie! Special thanks to Nino and Sharon for scientific discussions, support, and friendship.

Marcella and Villi, I am grateful our paths crossed, winning lifetime friendships.

Big thanks to my awesome students Juliana and Julian!

Thanks to the whole SLA crowd - amazing, helpful, supporting, engaging and inspiring people!

Thanks to the whole SLA animal and technical service, obviously without them nothing would have been possible.

And the last, but most important, thank you to my parents Maid and Smilja Bjelopoljak, my sister Jasmina Roch, and brother in law Alexander Roch. Without you, I (born Nadja Bjelopoljak) would not be here today, and it would not mean anything. Your unconditional love, encouragement, and support giving me the strength to make it through this journey to my goal are inexpressible. THANK YOU, I LOVE YOU.

TABLE OF CONTENT

ACKNOWLEDGEMENTS.....	1
TABLE OF CONTENT	3
LIST OF ABBREVIATIONS	5
SUMMARY	9
ZUSAMMENFASSUNG.....	11
CHAPTER 1: GENERAL INTRODUCTION.....	15
1. Obesity.....	16
2. Peripheral signals modulating food intake	16
2.1. General	16
2.2. GI peptides.....	17
2.3. Adiposity signals	18
2.4. Metabolic signals	18
3. Gut-brain-axis	20
3.1. General	20
3.2. Enteric nervous system.....	20
3.3. Parasympathetic and sympathetic innervation.....	21
3.4. Role of the vagus nerve in the control of food intake	22
4. CNS control of energy balance	24
4.1. General	24
4.2. Neuronal circuits	24
4.3. Astrocytes, helper or master	27
4.4. Astrocyte metabolism.....	30
5. Aims of the thesis	31
6. References	33
CHAPTER 2: MONOCARBOXYLATE TRANSPORTER-2 KNOCKDOWN IN NODOSE GANGLIA AFFECTS EATING.....	45
Introduction	46
Methods	49
Results	54
Discussion.....	62
References.....	68

CHAPTER 3: ROLE OF ASTROCYTE SIRTUIN-3 IN ENERGY HOMEOSTASIS...	73
Introduction	74
Methods	77
Results	83
Discussion	107
References	114
CHAPTER 4: GENERAL DISCUSSION	121
1. Overview of the findings.....	122
2. VAN MCT2 in the control of food intake.....	124
3. Astrocyte SIRT3 in energy homeostasis	128
4. References	134
CURRICULUM VITAE	141

LIST OF ABBREVIATIONS

AAV	adeno-associated-viral construct
Adh1/1	alcohol dehydrogenase-1
AgRP	agouti-related peptide
AgRP	agouti-related peptide
Aif1	allograft Inflammatory Factor-1
AMPK	AMP-activated protein kinase
ANS	autonomic nervous system
ARC	arcuate nucleus
BHB	β -hydroxybutyrate
BL	baseline
BW	body weight
CART	cocaine-amphetamine-regulated-transcript
CCK	cholecystokinin
CD	control diet
Cd68	cluster of differentiation 68
Chol	cholesterol
CNS	central nervous system
CPT 1A	carnitine palmitoyltransferase-1A
CPT1	carnitine palmitoyltransferase-1
CR	caloric restriction
CTR	control
DAPI	4', 6-diamidino-2-phenylindole
DGAT-1i	diacylglycerol acyltransferase-1 inhibitor
DIO	diet-induced obesity
DRG	dorsal root ganglia
EE	energy expenditure
EEC	enteroendocrine cells
EH	energy homeostasis
ENS	enteric nervous system
FA	fatty acids
FAO	fatty acid oxidation
FI	food intake

GFAP	glial fibrillary acidic protein
GI	gastrointestinal
Gjc2	gap junction gamma-2
Gjic2	gap junctional intercellular communication-2
GK	glucokinase
GLP-1	glucagon-like peptide-1
GPCR	G-protein-coupled receptors
he	hemizygous
HFD	high fat diet
HMGCoAS2	3-hydroxy-3-methylglutaryl-CoA synthase 2
ho	homozygous
IC	indirect calorimetry
IP	intraperitoneal
IST	insulin sensitivity test
Itgam	integrin subunit alpha-M
KB	ketone bodies
KG	ketogenesis
ki	knock-in
ko	knock-out
LCAD	long-chain acyl-CoA dehydrogenase
LCFA	long-chain fatty acid
LH	lateral hypothalamus
LHA	lateral hypothalamic area
MA	mercaptoacetate
MCH	melanin-concentrating hormone
MCR	melanocortin receptors
MCT2	monocarboxylate transporter-2
MCT2kd	MCT2 knockdown
MCTs	monocarboxylate transporters
Mog	myelin oligodendrocyte glycoprotein
MRI	magnetic resonance imaging
NEFA	non-esterified fatty acids
Nefl	neurofilament light
NG	nodose ganglia

NPY	neuropeptide Y
ns	not significant
NTS	nucleus tractus solitarii
OEA	oleoylethanolamine
OGTT	oral glucose tolerance test
PGC-1 α	activated receptor gamma coactivator 1-alpha
PNS	parasympathetic system
POMC	proopiomelanocortin
PP	postprandial
PPAR α	proliferator-activated receptor-alpha
PVN	paraventricular nucleus
PYY	peptide tyrosine tyrosine
RER	respiratory exchange ratio
ROS	reactive oxygen species
SDA	subdiaphragmatic vagal deafferentation
SEM	standard error mean
shRNA	short hairpin - RNA
SIRT3	Sirtuin3
Snap25	synaptosomal-associated protein-25
SNS	sympathetic nervous system
Syt1	synaptogamin-1
TAG	triacylglycerol
TAM	tamoxifen
Tmem119	transmembrane protein-119
VAN	vagal afferent neurons
Vim	vimentin
VL	voluntary locomotion
VMH	ventromedial hypothalamus
VTA	ventral tegmental area
w	weeks
ZNS	Zentralnervensystem
α -MSH	alpha-melanocyte-stimulating hormone

SUMMARY

The physiological mechanisms maintaining the balance between energy intake and energy expenditure are complex and not fully understood. Peripheral metabolic signals have long been implicated in the control of eating, but it is still unknown by which mechanisms metabolites or their utilization affect eating; do they trigger a signal that is transmitted to the brain via afferent nerves or are they metabolized in the brain to affect eating? In this thesis, we started to test both possibilities.

In the first part, we examined whether the monocarboxylate transporter-2 (MCT2) in vagal afferent neurons (VAN) plays a role in the control of eating. To this end, we knocked down the MCT2 by bilateral nodose ganglia injection of a viral vector with shRNA targeting MCT2, or a non-target sequence, and recorded food intake in rats eating chow or a high fat diet (HFD, 60% fat). The MCT2 transports monocarboxylates such as lactate, pyruvate and beta-hydroxybutyrate across cell membranes and thus provides the basis for these metabolites' intracellular utilization. The knockdown efficiency was only 28%. Nevertheless, when the animals were eating chow, the MCT2 knockdown (MCT2kd) prolonged average meal duration and, after a 16 h fast, it almost doubled the size and duration of the second meal, indicating a substantial contribution of VAN MCT2 to meal size control under this condition. After the animals were switched to HFD, MCT2kd rats temporarily increased 12 h light phase food intake by increasing meal number, suggesting a role of VAN MCT2 in satiety. Overall, by showing that VAN MCT2 is involved in the control of eating under certain conditions, our data indirectly support the idea of a peripheral metabolic contribution to the control of food intake by VAN signaling.

In the second part, we used the inducible CreERT2-loxP system to test whether overexpression or knock-out of Sirtuin3 (SIRT3) specifically in glial fibrillary acidic protein (GFAP) expressing astrocytes affects food intake and metabolism in mice fed a low fat control diet or a high fat diet (HFD, 60% energy from fat). SIRT3 is a major mitochondrial deacetylase that deacetylates and, hence, activates several mitochondrial enzymes involved in different metabolic pathways, but in particular in fatty acid oxidation and ketogenesis. The astrocyte-specific SIRT3 knock-out (SIRT3ko) did not affect energy homeostasis or eating under both feeding conditions. The same was true for the astrocyte-specific SIRT3 overexpression (SIRT3ki) in mice on the control diet. However, the SIRT3ki caused changes in energy homeostasis and glucose metabolism in mice fed the HFD for 12 weeks. These mice exhibited an overall anabolic state with increased food intake but decreased energy expenditure, and a hypersecretion of insulin. These findings suggest that SIRT3ki in GFAP astrocytes can modulate central nervous system (CNS) metabolic signaling and whole body energy homeostasis and metabolism. The failure to verify the SIRT3ko for technical reasons and the comparatively small SIRT3 overexpression of 20% limit these interpretations.

Taken together, our results suggest a possible contribution of VAN metabolic sensing to the control of eating under certain conditions. Furthermore, astrocyte SIRT3 presumably does not play a major role in CNS metabolic sensing as part of the regulation of energy homeostasis. However, because of the unconfirmed (SIRT3ko) and limited (SIRT3ki) changes in SIRT3 expression that were achieved, these interpretations may underestimate the role of astrocyte SIRT3.

ZUSAMMENFASSUNG

Die physiologischen Mechanismen, welche die Balance zwischen Energieaufnahme und Energieverbrauch sicherstellen, sind sehr komplex und bis heute nicht vollständig aufgeklärt. Periphere metabolische Signale sind schon seit langem mit der Steuerung des Essverhaltens in Verbindung gebracht, dennoch ist bis heute nicht bekannt über welche Mechanismen Metaboliten oder deren Abbauprodukte die Nahrungsaufnahme beeinflussen; lösen sie ein Signal aus, welches über die vagalen Afferenzen zum Gehirn übertragen wird oder ist deren Verstoffwechslung im Gehirn für die Steuerung des Essverhaltens zuständig? In dieser Dissertation begannen wir, beide Möglichkeiten zu untersuchen.

Im ersten Teil der Arbeit untersuchten wir, ob der Monocarboxylat-Transporter-2 (MCT2) in den Afferenzen des Nervus vagus (VAN) eine Rolle bei der Steuerung des Essverhaltens spielt. Hierfür injizierten wir bei Ratten bilateral in die Ganglia nodosa einen viralen Vektor mit gegen MCT2 gerichteter shRNA oder (ungerichteter RNA) durch, um die Expression des MCT2 zu reduzieren (knock-down) und massen die Futteraufnahme von Ratten beim Verzehr einer Standard- oder Hochfettdiät (HFD, 60% Fett). Der MCT2 ist für den Transport von Monocarboxylaten wie Lactat, Pyruvat und Beta-Hydroxybutyrat über die Zellmembran zuständig und ermöglicht dadurch ihre intrazelluläre Verstoffwechslung. Die Knock-Down-Effizienz war nur 28%. Als die Tiere mit der Standarddiät gefüttert wurden, führte die Reduktion der Expression von MCT2 (MCT2kd) dennoch zu einer Verlängerung der mittleren Mahlzeitendauer. Nach einer 16-stündigen Fastenperiode war bei den MCT2kd-Ratten im Vergleich zu den Kontrollratten die zweite Mahlzeit deutlich vergrößert und verlängert, was für eine substantielle Beteiligung von VAN MCT2 an der Steuerung der Mahlzeitgröße unter

diesen Bedingungen spricht. Nach der Umstellung auf die HFD, zeigten die MCT2kd-Ratten vorübergehend während der 12-stündigen Hellphase eine erhöhte Mahlzeitenanzahl und Futteraufnahme. Dies weist darauf hin, dass der MCT2 in VAN unter diesen Bedingungen an der Aufrechterhaltung der Sättigung beteiligt ist.

Der Befund, dass der MCT2 in VAN unter bestimmten Bedingungen an der Steuerung der Nahrungsaufnahme beteiligt ist, unterstützt indirekt die Hypothese einer peripheren metabolischen Komponente der Steuerung der Nahrungsaufnahme über Signale in VAN.

Im zweiten Teil der Arbeit verwendeten wir das induzierbare CreERT2-loxP System, um zu untersuchen, ob eine Über- oder Unterexpression des Sirtuin3 (SIRT3), spezifisch in GFAP- (glial fibrillary acidic protein) exprimierenden Astrozyten, während der Aufnahme einer fettarmen oder fettreichen Diät (HFD), die Nahrungsaufnahme und den Metabolismus von Mäusen beeinflusst. SIRT3 ist eine wichtige Deacetylase, welche durch Deacetylierung mehrere mitochondriale Enzyme in unterschiedlichen Stoffwechselwegen, jedoch hauptsächlich in der Fettsäureoxidation und Ketogenese, aktiviert. Die Astrozyten-spezifische SIRT3 Unterexpression (SIRT3ko) zeigte unter beiden Fütterungsbedingungen keinen Einfluss auf die Nahrungsaufnahme oder Energie-Homöostase der Mäuse. Analoges traf auch bei Mäusen mit Astrozyten-spezifischer SIRT3 Überexpression bei fettarmer Fütterung zu. Die SIRT3 Überexpression führte hingegen bei Mäusen, die vorher 12 Wochen der HFD ausgesetzt waren, zu Veränderungen der Energie- und Glukosehomöostase. Mit erhöhter Futteraufnahme und verringertem Energieverbrauch zeigten diese Mäuse insgesamt das Bild einer anabolen Stoffwechsellage parallel zu einer Hypersekretion von Insulin. Diese Ergebnisse deuten darauf hin, dass die SIRT3 Überexpression in GFAP-Astrozyten metabolische Signale im Zentralnervensystem (ZNS) sowie die

Energiehomöostase des Organismus beeinflussen kann. Die missglückte Verifizierung des SIRT3ko aus technischen Gründen und die vergleichsweise geringe (20%) Überexpression von SIRT3 bei den SIRT3ki-Mäusen limitieren allerdings diese Interpretationen.

Insgesamt lassen unsere Ergebnisse unter bestimmten Bedingungen eine Beteiligung der VAN an der Erfassung und Weiterleitung peripherer metabolischer Signale bei der Steuerung der Nahrungsaufnahme vermuten. Des Weiteren deuten die Resultate darauf hin, dass SIRT3 in Astrozyten keine wesentliche Rolle bei der Registrierung metabolischer Signale im ZNS im Rahmen der Regulation der Energiehomöostase spielt. Wegen der unklaren (SIRT3ko) beziehungsweise limitierten (SIRT3ki) Veränderungen in der Expression von SIRT3 könnte diese Interpretation allerdings die Rolle von SIRT3 in Astrozyten unterschätzen.

CHAPTER 1: GENERAL INTRODUCTION

1. Obesity

Energy homeostasis (EH) results from a physiological regulatory process balancing energy intake and energy expenditure, but the exact mechanism remains not fully understood. A dysfunction in this regulatory system can cause an excessive accumulation of fat, leading to overweight or obesity. Comorbidities such as type 2 diabetes and cardiovascular diseases characterize the clinical picture of obesity, which is evolving into a major global health burden. A better understanding of how energy homeostasis is regulated might help identify the pathophysiology of obesity and guide the way to effective intervention (1).

2. Peripheral signals modulating food intake

2.1. General

For the control of food intake (FI) and energy expenditure (EE) the central nervous system (CNS) relies on receiving and processing numerous peripheral signals “reporting” on the metabolic status of the body. In this context, we distinguish between two categories of signals: i) Circulating nutrients, gastrointestinal peptides, and signals derived from mechanosensors in the stomach wall promote primarily meal termination (satiation) and are referred to as short-term acting satiation signals. ii) Long-term signals, on the other hand, are hormones released in proportion to the amount of stored fat. These adiposity signals provide “tonic” signals, which determine how potent short-acting satiation signals inhibit eating (2).

2.2. GI peptides

Enteroendocrine cells (EEC) are spread along the whole gastrointestinal (GI) tract and are localized among the gastric and intestinal epithelial cells. EEC are chemosensing cells that monitor the luminal nutrient content and secrete GI peptides in response to a meal (3). These gut-derived peptides signal nutrient availability to the brain either by acting directly on central nervous system receptors (endocrine fashion) or on afferent nerves of the autonomic nervous system, primarily on vagal afferent nerves (VAN) (paracrine fashion) (4). Cholecystokinin (CCK), glucagon-like peptide-1 (GLP-1), and peptide tyrosine tyrosine (PYY) are considered important GI satiation peptides, whereas ghrelin is the only GI peptide that stimulates eating (5, 6). Ghrelin is secreted primarily by X/A-like cells in the stomach during fasting and shortly before anticipated meals. It is an orexigenic hormone and acts mainly directly on the brain, on reward pathways to enhance the attractiveness of the available food. Ghrelin also increases GI motility (7). CCK is secreted from I-cells in the small intestine mainly in response to lipid and protein breakdown products and it potently inhibits eating by reducing meal size. This effect appears partly related to an inhibition of gastric emptying (8). GLP-1 is produced by L-cells in response to carbohydrates and fats. Intriguingly, L-cells increase in density throughout the small and large intestine. Similar to CCK, GLP-1 reduces meal size and inhibits gastric emptying, but also acts as an incretin, i.e., it enhances glucose-dependent insulin release (9). PYY is also produced by L-cells, where it is coexpressed and co-released with GLP-1. It is secreted in proportion to the caloric load (10, 11).

2.3. Adiposity signals

The circulating level of the prototypical adiposity signal leptin supposedly reflects the size of the available energy stores and thus enables the brain to adjust FI and EE accordingly (12). Leptin is produced by white adipocytes, and leptin plasma levels are approximately related to adipocyte size (13, 14). Leptin can inhibit FI and stimulate EE in large part by acting on its receptor in the arcuate nucleus (ARC) of the hypothalamus (15). A lack of leptin or its receptor results in a metabolic syndrome phenotype. Thus, leptin treatment of leptin-deficient mice reverses the phenotype (16). To influence food intake in individual meals, adiposity hormones must interact with satiation signals. Leptin and GI peptides interact at the level of the VAN and in the brain (17, 18). Leptin levels do scarcely change before or after a standard mixed mid-day-meal (1000 kcal) (19). Rather, leptin provides a “tonic” background signal in relation to the general energy status, thus determining how efficiently satiation signals act (20, 21). Moreover, it is important to note that low leptin levels are physiologically more relevant than high leptin levels because by not enhancing satiation signals, low leptin levels allow for an increase in meal size when energy stores are depleted. Medium or high leptin levels, on the other hand, display no differences in efficacy (22-26). Talking about adiposity signals, one must also mention insulin. Although insulin secretion changes in relation to meals, circulating insulin, and in particular cerebrospinal fluid insulin levels, reflect adiposity (27). Also similar to leptin, insulin enhances the effect of satiation signals.

2.4. Metabolic signals

The ultimate goal of eating is to provide energy and nutrients for the whole body to ensure normal function. Based on physiological principles of regulated systems it is therefore reasonable to assume that some measure of energy or energy availability

influences eating. Several hypotheses have been proposed in this context, which either focused on single metabolites (e.g., glucose) and their utilization or on a general measure of energy (e.g., fuel oxidation or the intracellular ADP/ATP ratio) (28-31).

Consistent with the original glucostatic hypothesis (32), parenteral glucose administrations often inhibited (33, 34), whereas an inhibition of glucose utilization stimulated (35-37), eating. Similar to the administration of glucose, also the parenteral administration of other metabolites, such as glycerol, L-malate, L-lactate, pyruvate or β -hydroxybutyrate (BHB) reduced FI in rats (38). Prandial lactate infusion into the hepatic portal vein or vena cava also reduced FI (39). The FI reducing effects of these metabolites were eliminated after hepatic branch vagotomy (elimination of most of the hepatic and part of the proximal intestinal vagal innervation) arguing for a VAN mediation of the eating inhibitory effects of these metabolites (40). Moreover, the reduction in FI was associated with the generation of reducing equivalents in the mitochondria produced by the first oxidative step of the injected metabolites (31). Reduced FI was also recorded after intraperitoneal (IP) administration of fatty acid oxidation (FAO) stimulators such as oleoylethanolamine (OEA) and WY-14643 (an exogenous peroxisome proliferator-activated receptor-alpha (PPAR α) agonist) (41, 42). Moreover, the interventions caused an increase in carnitine palmitoyltransferase-I (CPT1) and hydroxymethylglutaryl-CoA synthase-2 (HMGCOAS2) expression, the key FAO and ketogenesis (KG) enzymes, in the small intestine. Concomitantly, the treatments produced increased BHB levels in the hepatic portal vein. Intragastric infusion of a diacylglycerol acyltransferase-1 inhibitor (DGAT-1i), an enzyme involved in the last step of triglyceride synthesis, also increased circulating BHB levels and reduced FI (43). The observed effects of OEA, WY-14643, and DGAT-1i were not abolished after subdiaphragmatic vagal deafferentation (SDA), suggesting a non-vagal

mediation, but this needs to be further investigated (44). In another series of experiments, transgenic mice constitutively overexpressing the mitochondrial protein Sirtuin3 (SIRT3) specifically in the enterocytes and fed a high-fat diet (HFD) displayed increased KG associated with improved glucose homeostasis without changes in eating or body weight (45). Taken together, these data indicate that metabolic signals are involved in the control of FI and regulation of EH and suggest a possible role of intestinal FAO and KG. Nevertheless, in general, the idea that metabolic changes within the physiological range can affect eating is somewhat controversial, and in any case, metabolic signals are certainly only one component in the complex control of eating.

3. Gut-brain-axis

3.1. General

The autonomic nervous system (ANS) transfers information, encoded by many of the peripheral signals mentioned above, to the brain. In effect, these signals shape the efferent responses, i.e., modulate EE and eating behavior to regulate EH. The resulting bidirectional information flow between the GI tract and the brain is referred to as the “gut-brain-axis”. The ANS consists of the parasympathetic and sympathetic nervous system (PNS and SNS, respectively), which comprise the extrinsic innervation of the GI tract and the enteric nervous system (ENS), the intrinsic innervation of the GI tract.

3.2. Enteric nervous system

The ENS is referred to as the “gut-brain”. In humans, it is composed of 200-600 million neurons and consists of a “mesh-like-system” of neurons that govern GI functions.

ENS neurons are distributed in many thousands of small ganglia, the vast majority of which are found in the submucosal (Meissner's) and myenteric (Auerbach's) plexus. Most of the interactions between ENS and the extrinsic innervation occurs there (46). For instance, intestinofugal neurons, with their cell bodies in enteric ganglia and with their axons reaching the sympathetic ganglia, represent a significant connection between the intrinsic and extrinsic neurons, allowing for the transmission of intestinal signals to centers in the brain stem (47).

3.3. Parasympathetic and sympathetic innervation

The SNS and PNS generally act in a reciprocal or antagonistic fashion. The SNS stimulates the "fight or flight" response, mediating mainly catabolic processes; the PNS stimulates the "feed and breed" response, mainly mediating anabolic processes.

The sympathetic efferent innervation of the GI tract runs mostly in parallel with spinal nerves and spinal afferents. Spinal afferents pass through sympathetic prevertebral ganglia and synapse either with neurons of the myenteric or submucosal plexus of the ENS or terminate in the lamina propria of the mucosa of the GI tract (46). The cell bodies of sympathetic afferents, which relay the information to the spinal cord, are located in the dorsal root ganglia.

Vagal efferents convey motor signals mostly from the nucleus ambiguus and dorsal motor nucleus of the vagus to the GI tract (48). VAN, which relay the information to the nucleus tractus solitarii (NTS) in the brain stem, have their cell bodies located in the nodose ganglia (NG) (49). Approximately 80% of the vagal fibers are afferents (41). As the major CNS entry point of afferent nerves from the GI tract, the NTS constitutes a key component of the gut-brain axis (50). Distally, similar to sympathetic afferents,

vagal afferents synapse either with neurons of the myenteric or submucosal plexus of the ENS or terminate in the lamina propria of the mucosa of the GI tract (46).

3.4. Role of the vagus nerve in the control of food intake

Intestinal VAN, in essence, encode the amount and nutrient composition of a meal, thus providing an interface between the “food environment” and the body (51, 52). Gastric VAN react to gastric distension and thus convey mainly information about the volume of ingested food (53). In contrast, nutrient infusion into the proximal small intestine revealed a nutrient-specific pattern of activation in intestinal VAN, indicating that intestinal VAN are predominately involved in chemosensing rather than mechanosensing (54, 55). As a result, GI peptides released by EEC in relation to luminal nutrients act primarily on VAN relaying sensory input of the type of ingested nutrients (54). GI peptides are also able to modulate VAN mechanosensitivity, i.e., many VAN, in particular in the proximal small intestine, are polymodal, i.e., react to chemical as well as mechanical signals (56). Moreover, in addition to this kind of “indirect” sensing of volume and type of ingested food by VAN, they can also directly sense glucose, amino acids and fatty acids (FA) (57-59). Also direct sensing of metabolic intermediates such as lactate and KB by VAN has been proposed (38, 40, 44). Indeed, VAN are not only ideally positioned to sense the GI peptides released by EEC, but also to respond to digestion products or mediators released by enterocytes (60). First, VAN are present within the lamina propria and are thus in close proximity to intestinal epithelial cells (61). Second, in addition to GI peptide receptors, VAN also express receptors for a wide range of metabolites (57, 58, 62). Overall, VAN signaling appears to be mainly involved in the control of meal size and duration (63). Interestingly, VAN also express the leptin receptor, and leptin modulates GI satiation

signals already at the level of VAN (64). Thus, VAN are presumably also involved in the regulation of long-term energy balance.

Except for the mechanosensitivity of VAN in the stomach and proximal small intestine, all the mechanisms of VAN activation described so far are related to the binding of ligands (gut peptides or metabolites) to G-protein-coupled receptors (GPCR) or to enzyme-linked receptors (leptin and cytokines) located in the VAN membrane (62). There may however also be a mechanism of modulation of VAN activity related to the intracellular metabolism of fuels. For instance, Nijima showed more than 40 years ago that hepatic branch vagal afferent signaling is modulated by glucose metabolism (65). More recently, it was reported that VAN are able to sense glucose through intracellular glycolysis. Thus, GLUT3, Glucokinase, and K_{ATP} channels were detected and required for glucosensing in NG (66). Nevertheless, although glucose is the major energy substrate for the brain, under specific conditions such as during breast-feeding, starvation, and diabetes, ketone bodies (KB) provide an energy source as well (67). Also lactate is an essential energy substrate for neurons (67). Both, KB and lactate are produced in the brain (by astrocytes) or imported from the circulation to “feed” the neurons (68-71). In addition, both enter neurons via monocarboxylate transporters (72). Monocarboxylate transporters are a family of proton-linked transport proteins (72, 73) which are located in the plasma and mitochondrial membranes and transport metabolic intermediates such as pyruvate, lactate, and KB. Among those, the monocarboxylate transporter-2 (MCT2) is described as the essential transporter in neurons, which is required for lactate and KB to enter the cell (74, 75).

Whereas VAN glucose utilization has been implicated in the control of eating, it is so far unknown if changes in VAN utilization of lactate or KB can modulate VAN signaling

and, perhaps, also affect eating. We began to address this question by studying the role of VAN MCT2 in the control of FI (see CHAPTER 2).

4. CNS control of energy balance

4.1. General

Most of the original theories of the metabolic control of eating posited that the brain is a major, or even the only, place in the body where the availability or utilization of metabolites is sensed and processed to generate the adequate output. Importantly, however, peripheral signals also influence brain energy metabolism itself, which in turn affects the processing of metabolic inputs (76). Thus, brain energy metabolism “products” are involved in shaping the brain’s behavioral and autonomic output. Brain energy metabolism is seen as a neuroglial metabolic cooperation. A particular focus in this context is the astrocyte-neuron metabolic unit (77).

4.2. Neuronal circuits

Three functionally distinct, but highly connected brain areas are the key operators in the control of FI and regulation of energy homeostasis, i.e., the hypothalamus, the hindbrain, and the forebrain.

The hypothalamic circuit is a major regulator of energy homeostasis, being in charge of the maintenance of energy balance by integrating input on energy intake, energy storage and aligning it with the various energy-demanding activities such as sleep/wake cycle, thermoregulation and sexual activity (78, 79).

In the hypothalamus, metabolic mechanisms appear to be directly coupled to the control of FI. Andersson and colleagues showed that humoral or pharmacological activation or deactivation of the ubiquitous cellular energy sensor AMP kinase, which is activated in response to decreases in cellular energy availability, was sufficient to increase or decrease FI, respectively (80). Similar observations were made in the NTS (81, 82).

The hypothalamic circuit consists of several tightly interconnected nuclei, in particular i) the arcuate nucleus (ARC) ii) the paraventricular nucleus (PVN) iii) the ventromedial hypothalamus (VMH) and iv) the lateral hypothalamus (LH).

A primary function of the ARC is metabolic signaling and control of FI. Its position next to the third ventricle allows hormones and nutrients in the systemic circulation as well as the cerebrospinal fluid to access the ARC easily (83). Consequently, several ARC neurons are first-order neurons on which peripherally derived nutrients, but also hormones such as ghrelin, insulin and leptin, act. A portion of ARC neurons comprise two distinct neuronal populations: 1) Neurons expressing the orexigenic neuropeptides neuropeptide-Y (NPY) and agouti-related peptide (AgRP), and 2) neurons producing the anorexigenic neuropeptides alpha-melanocyte-stimulating hormone (α -MSH), derived from proopiomelanocortin (POMC), and cocaine-amphetamine-regulated-transcript (CART). AgRP and POMC neurons project to second-order neurons located in the PVN, VMH, and LH as well as in many other brain areas (84). When α -MSH is released and binds to the melanocortin receptors (MCR) 3 and 4 on these second-order neurons, catabolic pathways are activated, leading to an inhibition of FI and a stimulation of EE (85). In contrast, AgRP acts as an endogenous inverse agonist of MCR3 and MCR4, thus, in essence blocking the effects of α -MSH (86). ARC neurons are also able to sense glucose. They are in fact prototypic metabolic sensing neurons,

i.e., POMC neurons are excited by glucose, leptin and insulin, NPY neurons are inhibited by glucose, leptin and insulin (87, 88). Many of them can also sense fatty acids. All this is interesting because these neurons can therefore integrate metabolic and endocrine signals from the periphery. Glucosensing neurons in particular are scattered throughout the brain and take part in a wide spectrum of physiological, metabolic and behavioral processes (89-93).

The PVN consists of neurons producing and secreting primarily catabolic neuropeptides such as corticotrophin-releasing hormone, thyrotropin-releasing hormone, somatostatin, vasopressin, and oxytocin, and some of them are also metabolic sensing neurons. The PVN also stimulates the SNS (94, 95) and, consequently, PVN stimulation promotes lipolysis and FAO in peripheral metabolic organs.

The VMH is densely innervated by both populations of ARC neurons mentioned above. VMH neurons project to the dorsomedial hypothalamus, the LH and back to ARC as well as to the brain stem (96). Also many VMH neurons are metabolic sensing neurons, and the VMH is important for the maintenance of glucose homeostasis and the generation of satiety (97, 98).

The LH has long been considered a “feeding center”, as its destruction leads to hypophagia and weight loss (99). Two neuronal populations, both producing orexigenic neuropeptides, are located in the LH: melanin-concentrating hormone (MCH) and orexin also termed hypocretin (100).

The hindbrain circuit is involved in the processing of gastrointestinal sensory, oral sensory and motor events in relation to the act of eating. An important nucleus of the hindbrain is the NTS. The NTS receives GI tract-derived signals mainly via VAN and

via splanchnic afferents (101). However, the NTS is close to the area postrema, which is a circumventricular organ with a leaky blood-brain barrier and, hence, like the ARC in a supreme position to react to peripheral circulating signals (102). The NTS is mostly responsible for the control of meal size and meal duration. Strong bidirectional projections between the hindbrain and the hypothalamus account for the incorporation of eating circuits into the regulation of EH. The NTS also controls other efferent responses, regulating GI motility and EE (103).

Forebrain reward circuits are responsible for the hedonic control of FI based on palatability (104). The mesolimbic and mesocortical dopaminergic pathways are major components of these hedonic circuits. Palatable foods trigger dopamine release in the ventral tegmental area (VTA), which further activates neurons in the nucleus accumbens (105). In addition to ghrelin (see above) (106), also adiposity signals control hedonic eating. For instance, leptin and insulin can suppress FI by acting on dopaminergic neurons in the VTA (107).

In sum, in conditions of energy deficit the homeostatic circuitries increase the motivation to eat, whereas under conditions of energy abundance the hedonic control is responsible for the desire to consume highly palatable foods (104). Nevertheless, the overall energy status also determines the rewarding effects of food, illustrating the strong interconnection among all three circuits.

4.3. Astrocytes, helper or master

Although glia cells make up approximately half of the brain volume, neurons have long been considered the primary cell types of the CNS receiving, processing, and transmitting information, as well as being the only cells relevant for reasoning and

awareness. Nowadays, however, the significance of glial contribution to the formation of neuronal responses has become a focus of attention (76).

Oligodendrocyte, microglia, astrocytes, and tanycytes are different types of glia cells. All of them, to various degrees, contribute to the regulation of EH (108). Their functions differ substantially: Oligodendrocytes provide the myelin sheets of axons and are thus important for fast signal transmission. Microglia represent the brain's immune system, protecting against infections and dealing with harmed cells. Tanycytes are specialized ependymogial cells (classified as astroglia), which line the floor of the third ventricle and are involved in hypothalamic functions. Finally, the astrocytes' key functions are to nourish and support neurons (109).

In particular hypothalamic astrocytes appear to play a pivotal role in the regulation of whole-body EH (110). Astrocytes are the most abundant type of glial cells, and the cytological connections among astrocytes, brain capillary endothelial cells and neurons are crucial for the astrocytes' unique role (111, 112). Astrocytes surround brain capillaries through specialized "perivascular end-feet" (113). This indicates that astrocytes function as gatekeepers, forming the first cellular barrier that nutrients and humoral signals entering the brain parenchyma encounter. This location puts astrocytes also in a primary position to distribute energy substrates. Astrocytes also form processes that engulf synaptic contacts (114) and express receptors and uptake sites, which enable direct interaction with neurotransmitters during synaptic activity (115). Those two features allow astrocytes to monitor and influence synaptic activity. Taken together, astrocytes are ideally suited and positioned to link changes in energy metabolism with adaptations in neuronal activity. Those exquisite structural and functional characteristics endow astrocytes with the prerequisites for the following functions:

- i) Neurovascular coupling, which is the spatiotemporal coupling between neuronal activity and increased cerebral blood flow to ensure appropriate metabolic supply (116).
- ii) Neurotransmitter recycling and anaplerosis (replenishing of Krebs cycle intermediates), which is the removal of neurotransmitters from the synaptic cleft, terminating synaptic transmission, thus maintaining neuronal excitability (117-119).
- iii) The glutamate-glutamine shuttle; glutamate is the primary excitatory neurotransmitter in the brain, and overstimulation of neurons is neurotoxic (excitotoxicity). Astrocytes take up glutamate, convert it to glutamine by the astrocyte-specific enzyme glutamine synthetase, and transfer the glutamine back to neurons where it is re-converted into glutamate to fill the neurotransmitter pool (119).
- iv) The glutamate-stimulated uptake of glucose by astrocytes provides the direct coupling of synaptic activity to glucose utilization (120).
- v) The astrocyte-neuron lactate shuttle; compared to glucose, lactate is a “ready to use” energy fuel that is energetically favored, in particular in situations of high-energy demand, when maintenance of high ATP levels are critical (70).
- vi) The astrocyte-neuron ketone body shuttle; astrocytes are the only cell type in the brain oxidizing FA for KB synthesis. During specific conditions such as suckling and starvation, the neurons rely on KB utilization (121, 122).
- vii) Glycogen storage; storage of energy in the brain is exclusively localized in astrocytes. During metabolic needs, glycogen breakdown mostly results in lactate production and release for the uptake by neurons (123, 124).

Those prerequisites emphasize the close functional metabolic partnership between astrocytes and neurons representing the astrocyte-neuron metabolic unit, which underlines the astrocytes' significance in brain energy metabolism.

In addition to those local tasks, further astrocyte features are emerging that highlight the astrocytes' involvement in whole-body energy homeostasis. These include the following:

- i) Hypothalamic astrocytes are involved in glucose sensing and in forming the neuronal response to fluctuations in glucose availability (125-127).
- ii) Hypothalamic astrocyte-derived KB influence neuronal signaling and FI. KB thus even override glucose and fatty acid sensing (71).
- iii) Lactate, most probably derived from astrocytes, also functions as an intracellular signaling molecule modulating FI (128).
- iv) Astrocytes express receptors for hormones involved in EH such as GLP-1, ghrelin, leptin, and insulin, and astrocyte-specific insulin receptor knockdown revealed the astrocytes' involvement in EH (129-132).

In summary, there is growing evidence that interactions between astrocytes and neurons are not only dedicated to fueling actions but also to signaling events, hence participating in neuronal signaling and whole-body EH.

4.4. Astrocyte metabolism

As mentioned above, neurons and astrocytes prefer different metabolic pathways, which is partly related to cell-type specific expression patterns of key metabolic regulatory genes. Thus, neurons and astrocytes differ with respect to their metabolic profiles; they are complementary and, as a result, pave the way for an indispensable

metabolic cooperation (77). The three key metabolic differences are i) the exclusive glycogen storage by astrocytes (123) ii) their high glycolytic rate (133, 134) and iii) their ability to oxidize FA and produce KB (71, 135, 136).

Astrocytes and neurons possess equal capacity to oxidize glucose and/or lactate (137), but neurons sustain a higher rate of oxidative metabolism compared to glia cells, whereas astrocytes display a higher glycolytic rate (133). Unlike astrocytes, neurons also metabolize lactate, which enables them to use the lactate provided by astrocytes due to their high glycolytic rate (124, 138). In addition, astrocytes store the surplus energy as glycogen, a phenomenon called the “glycogen shunt” (139, 140). Moreover, astrocytes are the only cell type in the brain able to oxidize fatty acids for the synthesis of KB. As mentioned above, KB, like lactate, are implicated as signaling molecules (71).

Sirtuin 3 (SIRT3) an NAD⁺ dependent mitochondrial deacetylase deacetylates, and thereby activates, numerous enzymes involved in several metabolic pathways (141). Prominent is its function to upregulate FAO and KG while downregulating glycolysis (142). Investigating the involvement of SIRT3 in astrocyte mitochondrial metabolism and, in particular, KG might allow for a better understanding of the roles of SIRT3 and astrocytes in whole-body energy homeostasis.

5. Aims of the thesis

This thesis aims at a better understanding of the possible involvement of intracellular metabolism in the sensing and signaling of energy availability in the periphery and the CNS with respect to energy homeostasis.

1) Based on early work suggesting that mitochondrial oxidation of various metabolites, including lactate (38), affected eating via VAN signaling (40), and prompted by recent findings suggesting a role of enterocyte-derived KB in the control of eating (44), we started to address the possible role of VAN MCT2 in the control of eating. More specifically, we knocked down MCT2 specifically in VAN of rats by bilateral NG injections of an AAV-shRNA targeting rat MCT2 and characterized the animals' eating behavior on chow and after the switch to HFD (CHAPTER 2).

2) Accumulating evidence indicates that astrocytes play a role in CNS metabolic sensing and in the regulation of energy homeostasis (76). Following up on studies implicating astrocyte fatty acid oxidation and KB production in the control of eating (71), we attempted to manipulate astrocyte metabolism by downregulating or overexpressing Sirtuin3 (SIRT3), specifically in GFAP expressing astrocytes, using the inducible CreERT2-loxP system in mice fed either low fat or HFD. SIRT3 deacetylates and, hence, activates various mitochondrial enzymes involved in several metabolic pathways, in particular in fatty acid oxidation and ketogenesis (CHAPTER 3).

6. References

1. **González-Muniesa P, Martínez-González M-A, Hu FB, Després J-P, Matsuzawa Y, Loos RJF, et al.** Obesity. *Nature Reviews Disease Primers*. 2017;3:17034.
2. **Havel PJ.** Peripheral signals conveying metabolic information to the brain: short-term and long-term regulation of food intake and energy homeostasis. *Experimental Biology and Medicine (Maywood, N.J.)*. 2001;226(11):963-77.
3. **Psichas A, Reimann F, Gribble FM.** Gut chemosensing mechanisms. *Journal of Clinical Investigation*. 2015;125(3):908-17.
4. **Woods SC, Benoit SC, Clegg DJ, Seeley RJ.** Clinical endocrinology and metabolism. Regulation of energy homeostasis by peripheral signals. *Best Practice & Research: Clinical Endocrinology & Metabolism*. 2004;18(4):497-515.
5. **Cummings DE, Overduin J.** Gastrointestinal regulation of food intake. *Journal of Clinical Investigation*. 2007;117(1):13-23.
6. **Wren AM, Seal LJ, Cohen MA, Brynes AE, Frost GS, Murphy KG, et al.** Ghrelin enhances appetite and increases food intake in humans. *Journal of Clinical Endocrinology and Metabolism*. 2001;86(12):5992.
7. **Stengel A, Tache Y.** Ghrelin - a pleiotropic hormone secreted from endocrine x/a-like cells of the stomach. *Frontiers in Neuroscience*. 2012;6:24.
8. **Raybould HE.** Mechanisms of CCK signaling from gut to brain. *Current Opinion in Pharmacology*. 2007;7(6):570-4.
9. **Wang X, Liu H, Chen J, Li Y, Qu S.** Multiple Factors Related to the Secretion of Glucagon-Like Peptide-1. *International Journal of Endocrinology*. 2015;2015:651757-.
10. **Habib AM, Richards P, Rogers GJ, Reimann F, Gribble FM.** Co-localisation and secretion of glucagon-like peptide 1 and peptide YY from primary cultured human L cells. *Diabetologia*. 2013;56(6):1413-6.
11. **Degen L, Oesch S, Casanova M, Graf S, Ketterer S, Drewe J, et al.** Effect of peptide YY3-36 on food intake in humans. *Gastroenterology*. 2005;129(5):1430-6.
12. **Park H-K, Ahima RS.** Physiology of leptin: energy homeostasis, neuroendocrine function and metabolism. *Metabolism: Clinical and Experimental*. 2015;64(1):24-34.
13. **Considine RV, Sinha MK, Heiman ML, Kriauciunas A, Stephens TW, Nyce MR, et al.** Serum immunoreactive-leptin concentrations in normal-weight and obese humans. *New England Journal of Medicine*. 1996;334(5):292-5.

14. **Cammisotto PG, Bukowiecki LJ.** Mechanisms of leptin secretion from white adipocytes. *American Journal of Physiology: Cell Physiology.* 2002;283(1):C244-50.
15. **Bjørbaek C.** Central leptin receptor action and resistance in obesity. *Journal of investigative medicine : the official publication of the American Federation for Clinical Research.* 2009;57(7):789-94.
16. **Harris RB.** Parabiosis between db/db and ob/ob or db/+ mice. *Endocrinology.* 1999;140(1):138-45.
17. **Wang L, Barachina MD, Martinez V, Wei JY, Tache Y.** Synergistic interaction between CCK and leptin to regulate food intake. *Regulatory Peptides.* 2000;92(1-3):79-85.
18. **Owyang C, Heldsinger A.** Vagal control of satiety and hormonal regulation of appetite. *Journal of Neurogastroenterology and Motility.* 2011;17(4):338-48.
19. **Korbonits M, Trainer PJ, Little JA, Edwards R, Kopelman PG, Besser GM, et al.** Leptin levels do not change acutely with food administration in normal or obese subjects, but are negatively correlated with pituitary-adrenal activity. *Clinical Endocrinology.* 1997;46(6):751-7.
20. **Moran TH, Ladenheim EE.** Physiologic and Neural Controls of Eating. *Gastroenterology Clinics of North America.* 2016;45(4):581-99.
21. **Geary N.** Endocrine controls of eating: CCK, leptin, and ghrelin. *Physiology and Behavior.* 2004;81(5):719-33.
22. **Kelesidis T, Kelesidis I, Chou S, Mantzoros CS.** Narrative review: the role of leptin in human physiology: emerging clinical applications. *Annals of Internal Medicine.* 2010;152(2):93-100.
23. **Zhang J, Matheny MK, Tümer N, Mitchell MK, Scarpace PJ.** Leptin antagonist reveals that the normalization of caloric intake and the thermic effect of food after high-fat feeding are leptin dependent. *American Journal of Physiology-Regulatory, Integrative and Comparative Physiology.* 2007;292(2):R868-R74.
24. **Rosenbaum M, Goldsmith R, Bloomfield D, Magnano A, Weimer L, Heymsfield S, et al.** Low-dose leptin reverses skeletal muscle, autonomic, and neuroendocrine adaptations to maintenance of reduced weight. *Journal of Clinical Investigation.* 2005;115(12):3579-86.
25. **Schwartz MW, Woods SC, Seeley RJ, Barsh GS, Baskin DG, Leibel RL.** Is the energy homeostasis system inherently biased toward weight gain? *Diabetes.* 2003;52(2):232-8.
26. **Velkoska E, Morris MJ, Burns P, Weisinger RS.** Leptin reduces food intake but does not alter weight regain following food deprivation in the rat. *International Journal of Obesity and Related Metabolic Disorders.* 2003;27(1):48-54.

27. **Bagdade JD, Bierman EL, Porte D, Jr.** The significance of basal insulin levels in the evaluation of the insulin response to glucose in diabetic and nondiabetic subjects. *Journal of Clinical Investigation*. 1967;46(10):1549-57.
28. **Friedman MI.** Control of energy intake by energy metabolism. *American Journal of Clinical Nutrition*. 1995;62(5 Suppl):1096s-100s.
29. **Booth DA.** Postabsorptively induced suppression of appetite and the energostatic control of feeding. *Physiology and Behavior*. 1972;9(2):199-202.
30. **Langhans W, Scharrer E.** Metabolic control of eating. *World Review of Nutrition and Dietetics*. 1992;70:1-67.
31. **Russek M.** Participation of hepatic glucoreceptors in the control of intake of food. *Nature*. 1963;197:79-80.
32. **Mayer J.** Glucostatic mechanism of regulation of food intake. *New England Journal of Medicine*. 1953;249(1):13-6.
33. **Walls EK, Koopmans HS.** Differential effects of intravenous glucose, amino acids, and lipid on daily food intake in rats. *American Journal of Physiology*. 1992;262(2 Pt 2):R225-34.
34. **Glick Z, Modan M.** Control of food intake during continuous injection of glucose into the upper duodenum and the upper ileum of rats. *Physiological Psychology*. 1977;5(1):7-10.
35. **Houpt TR, Hance HE.** Stimulation of food intake in the rabbit and rat by inhibition of glucose metabolism with 2-deoxy-D-glucose. *Journal of Comparative and Physiological Psychology*. 1971;76(3):395-400.
36. **Zhou L, Yueh C-Y, Lam DD, Shaw J, Osundiji M, Garfield AS, et al.** Glucokinase inhibitor glucosamine stimulates feeding and activates hypothalamic neuropeptide Y and orexin neurons. *Behavioural Brain Research*. 2011;222(1):274-8.
37. **Flynn FW, Grill HJ.** Fourth ventricular phlorizin dissociates feeding from hyperglycemia in rats. *Brain Research*. 1985;341(2):331-6.
38. **Langhans W, Damaske U, Scharrer E.** Different metabolites might reduce food intake by the mitochondrial generation of reducing equivalents. *Appetite*. 1985;6(2):143-52.
39. **Silberbauer CJ, Surina-Baumgartner DM, Arnold M, Langhans W.** Prandial lactate infusion inhibits spontaneous feeding in rats. *American Journal of Physiology: Regulatory, Integrative and Comparative Physiology*. 2000;278(3):R646-53.
40. **Langhans W, Egli G, Scharrer E.** Selective hepatic vagotomy eliminates the hypophagic effect of different metabolites. *Journal of the Autonomic Nervous System*. 1985;13(3):255-62.

41. **Azari EK, Ramachandran D, Weibel S, Arnold M, Romano A, Gaetani S, et al.** Vagal afferents are not necessary for the satiety effect of the gut lipid messenger oleoylethanolamide. *American Journal of Physiology: Regulatory, Integrative and Comparative Physiology*. 2014;307(2):R167-78.
42. **Karimian Azari E, Leitner C, Jaggi T, Langhans W, Mansouri A.** Possible Role of Intestinal Fatty Acid Oxidation in the Eating-Inhibitory Effect of the PPAR- α Agonist Wy-14643 in High-Fat Diet Fed Rats. *PloS One*. 2013;8(9):e74869.
43. **Schober G, Arnold M, Birtles S, Buckett LK, Pacheco-López G, Turnbull AV, et al.** Diacylglycerol acyltransferase-1 inhibition enhances intestinal fatty acid oxidation and reduces energy intake in rats. *Journal of Lipid Research*. 2013;54(5):1369-84.
44. **Mansouri A, Langhans W.** Enterocyte-afferent nerve interactions in dietary fat sensing. *Diabetes, Obesity & Metabolism*. 2014;16 Suppl 1:61-7.
45. **Ramachandran D, Clara R, Fedele S, Hu J, Lackzo E, Huang J-Y, et al.** Intestinal SIRT3 overexpression in mice improves whole body glucose homeostasis independent of body weight. *Mol Metab*. 2017;6(10):1264-73.
46. **Furness JB, Callaghan BP, Rivera LR, Cho HJ.** The enteric nervous system and gastrointestinal innervation: integrated local and central control. *Advances in Experimental Medicine and Biology*. 2014;817:39-71.
47. **Furness JB.** Novel gut afferents: Intrinsic afferent neurons and intestinofugal neurons. *Autonomic Neuroscience*. 2006;125(1-2):81-5.
48. **Yuan H, Silberstein SD.** Vagus Nerve and Vagus Nerve Stimulation, a Comprehensive Review: Part I. Headache. 2016;56(1):71-8.
49. **Berthoud HR, Neuhuber WL.** Functional and chemical anatomy of the afferent vagal system. *Autonomic Neuroscience*. 2000;85(1-3):1-17.
50. **Browning KN, Travagli RA.** Central nervous system control of gastrointestinal motility and secretion and modulation of gastrointestinal functions. *Comprehensive Physiology*. 2014;4(4):1339-68.
51. **de Lartigue G, Diepenbroek C.** Novel developments in vagal afferent nutrient sensing and its role in energy homeostasis. *Current Opinion in Pharmacology*. 2016;31:38-43.
52. **Bates SL, Sharkey KA, Meddings JB.** Vagal involvement in dietary regulation of nutrient transport. *American Journal of Physiology*. 1998;274(3 Pt 1):G552-60.
53. **Willing AE, Berthoud HR.** Gastric distension-induced c-fos expression in catecholaminergic neurons of rat dorsal vagal complex. *American Journal of Physiology*. 1997;272(1 Pt 2):R59-67.
54. **Berthoud HR.** Vagal and hormonal gut-brain communication: from satiation to satisfaction. *Neurogastroenterology and Motility*. 2008;20 Suppl 1:64-72.

55. **Schwartz GJ, Moran TH.** Duodenal nutrient exposure elicits nutrient-specific gut motility and vagal afferent signals in rat. *American Journal of Physiology.* 1998;274(5 Pt 2):R1236-42.
56. **Williams EK, Chang RB, Strohlic DE, Umans BD, Lowell BB, Liberles SD.** Sensory Neurons that Detect Stretch and Nutrients in the Digestive System. *Cell.* 2016;166(1):209-21.
57. **Darling RA, Zhao H, Kinch D, Li A-J, Simasko SM, Ritter S.** Mercaptoacetate and fatty acids exert direct and antagonistic effects on nodose neurons via GPR40 fatty acid receptors. *American journal of physiology. Regulatory, integrative and comparative physiology.* 2014;307(1):R35-R43.
58. **Babic T, Troy AE, Fortna SR, Browning KN.** Glucose-dependent trafficking of 5-HT₃ receptors in rat gastrointestinal vagal afferent neurons. *Neurogastroenterology and motility : the official journal of the European Gastrointestinal Motility Society.* 2012;24(10):e476-e88.
59. **Jordi J, Herzog B, Camargo SM, Boyle CN, Lutz TA, Verrey F.** Specific amino acids inhibit food intake via the area postrema or vagal afferents. *Journal of Physiology.* 2013;591(22):5611-21.
60. **Berthoud HR, Blackshaw LA, Brookes SJH, Grundy D.** Neuroanatomy of extrinsic afferents supplying the gastrointestinal tract. *Neurogastroenterology and Motility.* 2004;16(s1):28-33.
61. **Berthoud HR, Kressel M, Raybould HE, Neuhuber WL.** Vagal sensors in the rat duodenal mucosa: distribution and structure as revealed by in vivo Dil-tracing. *Anatomy and Embryology.* 1995;191(3):203-12.
62. **Egerod KL, Petersen N, Timshel PN, Rekling JC, Wang Y, Liu Q, et al.** Profiling of G protein-coupled receptors in vagal afferents reveals novel gut-to-brain sensing mechanisms. *Mol Metab.* 2018;12:62-75.
63. **de Lartigue G.** Role of the vagus nerve in the development and treatment of diet-induced obesity. *The Journal of Physiology.* 2016;594(20):5791-815.
64. **de Lartigue G, Ronveaux CC, Raybould HE.** Deletion of leptin signaling in vagal afferent neurons results in hyperphagia and obesity. *Mol Metab.* 2014;3(6):595-607.
65. **Niijima A.** The effect of D-glucose on the firing rate of glucose-sensitive vagal afferents in the liver in comparison with the effect of 2-deoxy-D-glucose. *Journal of the Autonomic Nervous System.* 1984;10(3-4):255-60.
66. **Grabauskas G, Zhou S-Y, Lu Y, Song I, Owyang C.** Essential elements for glucosensing by gastric vagal afferents: immunocytochemistry and electrophysiology studies in the rat. *Endocrinology.* 2013;154(1):296-307.
67. **J. Magistretti P, Allaman I.** Brain Energy and Metabolism. In: Pfaff DW, Volkow ND, editors. *Neuroscience in the 21st Century: From Basic to Clinical.* New York, NY: Springer New York; 2016. p. 1879-909.

68. **Boumezbeur F, Petersen KF, Cline GW, Mason GF, Behar KL, Shulman GI, et al.** The contribution of blood lactate to brain energy metabolism in humans measured by dynamic ¹³C nuclear magnetic resonance spectroscopy. *The Journal of neuroscience : the official journal of the Society for Neuroscience*. 2010;30(42):13983-91.
69. **Puchalska P, Crawford PA.** Multi-dimensional Roles of Ketone Bodies in Fuel Metabolism, Signaling, and Therapeutics. *Cell Metabolism*. 2017;25(2):262-84.
70. **Pellerin L, Pellegrini G, Bittar PG, Charnay Y, Bouras C, Martin JL, et al.** Evidence supporting the existence of an activity-dependent astrocyte-neuron lactate shuttle. *Developmental Neuroscience*. 1998;20(4-5):291-9.
71. **Le Foll C, Dunn-Meynell AA, Miziorko HM, Levin BE.** Regulation of hypothalamic neuronal sensing and food intake by ketone bodies and fatty acids. *Diabetes*. 2014;63(4):1259-69.
72. **Pierre K, Pellerin L.** Monocarboxylate transporters in the central nervous system: distribution, regulation and function. *Journal of Neurochemistry*. 2005;94(1):1-14.
73. **Halestrap AP.** Monocarboxylic acid transport. *Comprehensive Physiology*. 2013;3(4):1611-43.
74. **Broer S, Broer A, Schneider HP, Stegen C, Halestrap AP, Deitmer JW.** Characterization of the high-affinity monocarboxylate transporter MCT2 in *Xenopus laevis* oocytes. *Biochemical Journal*. 1999;341 (Pt 3):529-35.
75. **Rafiki A, Boulland JL, Halestrap AP, Ottersen OP, Bergersen L.** Highly differential expression of the monocarboxylate transporters MCT2 and MCT4 in the developing rat brain. *Neuroscience*. 2003;122(3):677-88.
76. **García-Cáceres C, Balland E, Prevot V, Luquet S, Woods SC, Koch M, et al.** Role of astrocytes, microglia, and tanycytes in brain control of systemic metabolism. *Nature Neuroscience*. 2018.
77. **Bélanger M, Allaman I, Magistretti Pierre J.** Brain Energy Metabolism: Focus on Astrocyte-Neuron Metabolic Cooperation. *Cell Metabolism*. 2011;14(6):724-38.
78. **Waterson Michael J, Horvath Tamas L.** Neuronal Regulation of Energy Homeostasis: Beyond the Hypothalamus and Feeding. *Cell Metabolism*. 2015;22(6):962-70.
79. **Roh E, Song DK, Kim MS.** Emerging role of the brain in the homeostatic regulation of energy and glucose metabolism. *Experimental and Molecular Medicine*. 2016;48:e216.
80. **Andersson U, Filipsson K, Abbott CR, Woods A, Smith K, Bloom SR, et al.** AMP-activated protein kinase plays a role in the control of food intake. *Journal of Biological Chemistry*. 2004;279(13):12005-8.

81. **Hayes M, Leichner T, Zhao S, S Lee G, Chowansky A, Zimmer D, et al.** Intracellular Signals Mediating the Food Intake-Suppressive Effects of Hindbrain Glucagon-like Peptide-1 Receptor Activation 2011. 320-30 p.
82. **Hayes MR, Skibicka KP, Bence KK, Grill HJ.** Dorsal Hindbrain 5'-Adenosine Monophosphate-Activated Protein Kinase as an Intracellular Mediator of Energy Balance. *Endocrinology*. 2009;150(5):2175-82.
83. **Broadwell RD, Brightman MW.** Entry of peroxidase into neurons of the central and peripheral nervous systems from extracerebral and cerebral blood. *Journal of Comparative Neurology*. 1976;166(3):257-83.
84. **Schwartz MW, Woods SC, Porte D, Jr., Seeley RJ, Baskin DG.** Central nervous system control of food intake. *Nature*. 2000;404(6778):661-71.
85. **Huszar D, Lynch CA, Fairchild-Huntress V, Dunmore JH, Fang Q, Berkemeier LR, et al.** Targeted disruption of the melanocortin-4 receptor results in obesity in mice. *Cell*. 1997;88(1):131-41.
86. **Ollmann MM, Wilson BD, Yang YK, Kerns JA, Chen Y, Gantz I, et al.** Antagonism of central melanocortin receptors in vitro and in vivo by agouti-related protein. *Science*. 1997;278(5335):135-8.
87. **Levin BE, Routh VH, Kang L, Sanders NM, Dunn-Meynell AA.** Neuronal Glucosensing. *Diabetes*. 2004;53(10):2521.
88. **Levin BE, Kang L, Sanders NM, Dunn-Meynell AA.** Role of Neuronal Glucosensing in the Regulation of Energy Homeostasis. *Diabetes*. 2006;55(Supplement 2):S122.
89. **Routh VH.** Glucosensing neurons in the ventromedial hypothalamic nucleus (VMN) and hypoglycemia-associated autonomic failure (HAAF). *Diabetes/Metabolism Research and Reviews*. 2003;19(5):348-56.
90. **Roper J, Ashcroft FM.** Metabolic inhibition and low internal ATP activate K-ATP channels in rat dopaminergic substantia nigra neurones. *Pflügers Archiv. European Journal of Physiology*. 1995;430(1):44-54.
91. **Ritter S, Dinh TT, Zhang Y.** Localization of hindbrain glucoreceptive sites controlling food intake and blood glucose. *Brain Research*. 2000;856(1-2):37-47.
92. **Sakurai T, Amemiya A, Ishii M, Matsuzaki I, Chemelli RM, Tanaka H, et al.** Orexins and orexin receptors: a family of hypothalamic neuropeptides and G protein-coupled receptors that regulate feeding behavior. *Cell*. 1998;92(4):573-85.
93. **Tritos NA, Vicent D, Gillette J, Ludwig DS, Flier ES, Maratos-Flier E.** Functional interactions between melanin-concentrating hormone, neuropeptide Y, and anorectic neuropeptides in the rat hypothalamus. *Diabetes*. 1998;47(11):1687.

94. **Lee SK, Ryu PD, Lee SY.** Differential distributions of neuropeptides in hypothalamic paraventricular nucleus neurons projecting to the rostral ventrolateral medulla in the rat. *Neuroscience Letters*. 2013;556:160-5.
95. **Foster MT, Song CK, Bartness TJ.** Hypothalamic paraventricular nucleus lesion involvement in the sympathetic control of lipid mobilization. *Obesity (Silver Spring)*. 2010;18(4):682-9.
96. **Bouret SG, Draper SJ, Simerly RB.** Formation of projection pathways from the arcuate nucleus of the hypothalamus to hypothalamic regions implicated in the neural control of feeding behavior in mice. *Journal of Neuroscience*. 2004;24(11):2797-805.
97. **Routh VH.** Glucose sensing neurons in the ventromedial hypothalamus. *Sensors (Basel, Switzerland)*. 2010;10(10):9002-25.
98. **King BM.** The rise, fall, and resurrection of the ventromedial hypothalamus in the regulation of feeding behavior and body weight. *Physiology and Behavior*. 2006;87(2):221-44.
99. **Milam KM, Stern JS, Storlien LH, Keesey RE.** Effect of lateral hypothalamic lesions on regulation of body weight and adiposity in rats. *American Journal of Physiology*. 1980;239(3):R337-43.
100. **Broberger C, De Lecea L, Sutcliffe JG, Hokfelt T.** Hypocretin/orexin- and melanin-concentrating hormone-expressing cells form distinct populations in the rodent lateral hypothalamus: relationship to the neuropeptide Y and agouti gene-related protein systems. *Journal of Comparative Neurology*. 1998;402(4):460-74.
101. **Schwartz GJ.** The role of gastrointestinal vagal afferents in the control of food intake: current prospects. *Nutrition*. 2000;16(10):866-73.
102. **Stanley S, Wynne K, McGowan B, Bloom S.** Hormonal regulation of food intake. *Physiological Reviews*. 2005;85(4):1131-58.
103. **Grill HJ, Hayes MR.** The nucleus tractus solitarius: a portal for visceral afferent signal processing, energy status assessment and integration of their combined effects on food intake. *International Journal of Obesity (2005)*. 2009;33 Suppl 1:S11-5.
104. **Lutter M, Nestler EJ.** Homeostatic and hedonic signals interact in the regulation of food intake. *The Journal of Nutrition*. 2009;139(3):629-32.
105. **Hsu TM, McCutcheon JE, Roitman MF.** Parallels and Overlap: The Integration of Homeostatic Signals by Mesolimbic Dopamine Neurons. *Frontiers in Psychiatry*. 2018;9(410).
106. **Abizaid A, Liu Z-W, Andrews ZB, Shanabrough M, Borok E, Elsworth JD, et al.** Ghrelin modulates the activity and synaptic input organization of midbrain dopamine neurons while promoting appetite. *The Journal of clinical investigation*. 2006;116(12):3229-39.

107. **Hommel JD, Trinko R, Sears RM, Georgescu D, Liu ZW, Gao XB, et al.** Leptin receptor signaling in midbrain dopamine neurons regulates feeding. *Neuron*. 2006;51(6):801-10.
108. **Douglass JD, Dorfman MD, Thaler JP.** Glia: silent partners in energy homeostasis and obesity pathogenesis. *Diabetologia*. 2017;60(2):226-36.
109. **Jäkel S, Dimou L.** Glial Cells and Their Function in the Adult Brain: A Journey through the History of Their Ablation. *Frontiers in Cellular Neuroscience*. 2017;11:24-.
110. **Camandola S.** Astrocytes, emerging stars of energy homeostasis. *Cell stress*. 2018;2(10):246-52.
111. **Weber B, Barros LF.** The Astrocyte: Powerhouse and Recycling Center. *Cold Spring Harbor Perspectives in Biology*. 2015;7(12).
112. **Sofroniew MV, Vinters HV.** Astrocytes: biology and pathology. *Acta Neuropathologica*. 2010;119(1):7-35.
113. **Mathiisen TM, Lehre KP, Danbolt NC, Ottersen OP.** The perivascular astroglial sheath provides a complete covering of the brain microvessels: an electron microscopic 3D reconstruction. *Glia*. 2010;58(9):1094-103.
114. **Halassa MM, Fellin T, Takano H, Dong JH, Haydon PG.** Synaptic islands defined by the territory of a single astrocyte. *Journal of Neuroscience*. 2007;27(24):6473-7.
115. **Porter JT, McCarthy KD.** Astrocytic neurotransmitter receptors in situ and in vivo. *Progress in Neurobiology*. 1997;51(4):439-55.
116. **Gordon GR, Choi HB, Rungta RL, Ellis-Davies GC, MacVicar BA.** Brain metabolism dictates the polarity of astrocyte control over arterioles. *Nature*. 2008;456(7223):745-9.
117. **Schousboe A, Westergaard N, Waagepetersen HS, Larsson OM, Bakken IJ, Sonnewald U.** Trafficking between glia and neurons of TCA cycle intermediates and related metabolites. *Glia*. 1997;21(1):99-105.
118. **Rothman DL, De Feyter HM, Maciejewski PK, Behar KL.** Is there in vivo evidence for amino acid shuttles carrying ammonia from neurons to astrocytes? *Neurochemical Research*. 2012;37(11):2597-612.
119. **Bak LK, Schousboe A, Waagepetersen HS.** The glutamate/GABA-glutamine cycle: aspects of transport, neurotransmitter homeostasis and ammonia transfer. *Journal of Neurochemistry*. 2006;98(3):641-53.
120. **Pellerin L, Magistretti PJ.** Glutamate uptake into astrocytes stimulates aerobic glycolysis: a mechanism coupling neuronal activity to glucose utilization. *Proceedings of the National Academy of Sciences of the United States of America*. 1994;91(22):10625-9.
121. **Blázquez MGaC.** Is there an astrocyte–neuron ketone

body shuttle? *Trends in Endocrinology and Metabolism*. 2001;12.

122. **Chowdhury GMI, Jiang L, Rothman DL, Behar KL.** The contribution of ketone bodies to basal and activity-dependent neuronal oxidation in vivo. *Journal of cerebral blood flow and metabolism : official journal of the International Society of Cerebral Blood Flow and Metabolism*. 2014;34(7):1233-42.
123. **Brown AM.** Brain glycogen re-awakened. *Journal of Neurochemistry*. 2004;89(3):537-52.
124. **Dringen R, Gebhardt R, Hamprecht B.** Glycogen in astrocytes: possible function as lactate supply for neighboring cells. *Brain Research*. 1993;623(2):208-14.
125. **Chari M, Yang CS, Lam CK, Lee K, Mighiu P, Kokorovic A, et al.** Glucose transporter-1 in the hypothalamic glial cells mediates glucose sensing to regulate glucose production in vivo. *Diabetes*. 2011;60(7):1901-6.
126. **Marty N, Dallaporta M, Foretz M, Emery M, Tarussio D, Bady I, et al.** Regulation of glucagon secretion by glucose transporter type 2 (glut2) and astrocyte-dependent glucose sensors. *Journal of Clinical Investigation*. 2005;115(12):3545-53.
127. **Allard C, Carneiro L, Grall S, Cline BH, Fioramonti X, Chrétien C, et al.** Hypothalamic astroglial connexins are required for brain glucose sensing-induced insulin secretion. *Journal of cerebral blood flow and metabolism : official journal of the International Society of Cerebral Blood Flow and Metabolism*. 2014;34(2):339-46.
128. **Lam CK, Chari M, Wang PY, Lam TK.** Central lactate metabolism regulates food intake. *American Journal of Physiology: Endocrinology and Metabolism*. 2008;295(2):E491-6.
129. **Cheunsuang O, Morris R.** Astrocytes in the arcuate nucleus and median eminence that take up a fluorescent dye from the circulation express leptin receptors and neuropeptide Y Y1 receptors. *Glia*. 2005;52(3):228-33.
130. **Fuente-Martin E, Garcia-Caceres C, Argente-Arizon P, Diaz F, Granado M, Freire-Regatillo A, et al.** Ghrelin Regulates Glucose and Glutamate Transporters in Hypothalamic Astrocytes. *Scientific Reports*. 2016;6:23673.
131. **Reiner DJ, Mietlicki-Baase EG, McGrath LE, Zimmer DJ, Bence KK, Sousa GL, et al.** Astrocytes Regulate GLP-1 Receptor-Mediated Effects on Energy Balance. *Journal of Neuroscience*. 2016;36(12):3531-40.
132. **Garcia-Caceres C, Quarta C, Varela L, Gao Y, Gruber T, Legutko B, et al.** Astrocytic Insulin Signaling Couples Brain Glucose Uptake with Nutrient Availability. *Cell*. 2016;166(4):867-80.
133. **Itoh Y, Esaki T, Shimoji K, Cook M, Law MJ, Kaufman E, et al.** Dichloroacetate effects on glucose and lactate oxidation by neurons and astroglia in vitro and on glucose utilization by brain in vivo. *Proceedings of the*

- National Academy of Sciences of the United States of America. 2003;100(8):4879-84.
134. **Bittner CX, Loaiza A, Ruminot I, Larenas V, Sotelo-Hitschfeld T, Gutierrez R, et al.** High resolution measurement of the glycolytic rate. *Frontiers in Neuroenergetics*. 2010;2.
 135. **Edmond J.** Energy metabolism in developing brain cells. *Canadian Journal of Physiology and Pharmacology*. 1992;70 Suppl:S118-29.
 136. **Taib B, Bouyakdan K, Hryhorczuk C, Rodaros D, Fulton S, Alquier T.** Glucose regulates hypothalamic long-chain fatty acid metabolism via AMP-activated kinase (AMPK) in neurons and astrocytes. *Journal of Biological Chemistry*. 2013;288(52):37216-29.
 137. **Zielke HR, Zielke CL, Baab PJ.** Direct measurement of oxidative metabolism in the living brain by microdialysis: a review. *Journal of Neurochemistry*. 2009;109 Suppl 1(Suppl 1):24-9.
 138. **Bouzier-Sore AK, Voisin P, Bouchaud V, Bezancon E, Franconi JM, Pellerin L.** Competition between glucose and lactate as oxidative energy substrates in both neurons and astrocytes: a comparative NMR study. *European Journal of Neuroscience*. 2006;24(6):1687-94.
 139. **Shulman RG, Hyder F, Rothman DL.** Cerebral energetics and the glycogen shunt: neurochemical basis of functional imaging. *Proceedings of the National Academy of Sciences of the United States of America*. 2001;98(11):6417-22.
 140. **Walls AB, Heimbürger CM, Bouman SD, Schousboe A, Waagepetersen HS.** Robust glycogen shunt activity in astrocytes: Effects of glutamatergic and adrenergic agents. *Neuroscience*. 2009;158(1):284-92.
 141. **Hirschey MD, Shimazu T, Huang JY, Schwer B, Verdin E.** SIRT3 regulates mitochondrial protein acetylation and intermediary metabolism. *Cold Spring Harbor Symposia on Quantitative Biology*. 2011;76:267-77.
 142. **Nogueiras R, Habegger KM, Chaudhary N, Finan B, Banks AS, Dietrich MO, et al.** Sirtuin 1 and sirtuin 3: physiological modulators of metabolism. *Physiological Reviews*. 2012;92(3):1479-514.

**CHAPTER 2: MONOCARBOXYLATE TRANSPORTER-2
KNOCKDOWN IN NODOSE GANGLIA AFFECTS EATING**

Introduction

The “energostatic hypothesis” proposed that a common metabolic measure of energy rather than the concentration or utilization of a single nutrient controls eating (1). This hypothesis remained controversially discussed over the years, but is recently gaining new attention (2). Back in 1986 Langhans and Scharrer demonstrated that intraperitoneal (IP) injection of the fatty acid oxidation (FAO) inhibitor mercaptoacetate (MA) stimulated food intake (FI) in rats fed ad libitum a fat-enriched (18% fat) diet (3). The original idea was that the effects of FAO inhibitors originate in the liver and that the generated signal reaches the brain via vagal afferents (4, 5). Yet, changes in hepatic FAO proved to be neither necessary nor sufficient for FAO inhibitors to stimulate eating (6, 7), and liver parenchyma scarcely contains any vagal afferent fibers (8). Moreover, it was shown that a constitutively enhanced hepatic FAO in mice stimulated rather than inhibited eating (9). On the other hand, MA failed to stimulate eating in rats after subdiaphragmatic vagal deafferentation (SDA), a procedure that eliminates all vagal afferents from below the diaphragm. This finding therefore indicates that the effect of MA originates in the abdominal cavity, but “outside” the liver. In several studies, a pharmacological stimulation of FAO inhibited FI and induced the protein expression of key enzymes involved in FAO and ketogenesis, such as carnitine palmitoyltransferase-1A (CPT 1A) and mitochondrial 3-hydroxy-3-methylglutaryl-CoA synthase (HMGCoAS2), in the small intestine, but not in the liver (10-13). Furthermore, in some of these studies, the treatments increased hepatic portal vein β -hydroxybutyrate (BHB) levels without a concomitant change in circulating non-esterified fatty acid (NEFA) levels (10, 13). These and other findings suggest that oxidation of dietary-derived fatty acids in enterocytes generates a signal that modulates eating. Enterocytes can produce ketone bodies (KB), and BHB has often

been shown to inhibit eating after exogenous administration. For instance, subcutaneously injected BHB inhibited eating in rats fed chow diet ad libitum presumably through a metabolic mechanism and via a vagus nerve-mediated path (14-16). Recent findings (17) further support this view in confirming that hepatic branch vagotomy eliminated the hypophagic effect of intraperitoneally injected BHB also in mice. Moreover, the effect observed in WT mice was also present in mice deficient of the GPR109A, the major BHB receptor (18, 19), indicating that the vagal afferent signal generated was not due to activation of a membrane receptor. In other studies, hepatic branch vagotomy not only blocked the hypophagic effect of BHB, but also that of other subcutaneously injected metabolites such as glycerol, L-malate, L-lactate or pyruvate (15). Prandial lactate infusions into the hepatic portal vein or vena cava lead to similar decreases in meal size, supporting the idea of an extrahepatic sensing mechanism (20). Finally, the observed reduction in food intake caused by different metabolites appeared to be linked to the generation of reducing equivalents in the mitochondria produced by the first oxidative step of the injected metabolite (21).

Based on all these studies, it is reasonable to speculate that enterocyte-derived KB or lactate may be taken up by intestinal VAN to affect signaling and, hence, eating via a metabolic mechanism. Lactate and KB may enter the VAN via one of the monocarboxylate transporters (MCTs), with the most likely one being the MCT2 (22). Therefore, we first examined whether rat vagal afferent primary neurons express MCT2. Then we knocked down MCT2 expression in nodose ganglia (NG) by injecting an AAV-shRNA targeting rat MCT2 and assessed food intake (FI) and body weight (BW) on chow and with high-fat diet (HFD) feeding. The MCT2 knockdown distinctly affected meal patterns under both feeding conditions (chow and HFD): On chow, it prolonged dark phase meal duration, and after food deprivation, it increased meal size

as well, whereas after the switch to HFD it increased meal number specifically during the light phase. The latter effect translated into increased 24 h FI and increased BW during the first week after the switch to HFD. Overall, our findings suggest that the MCT2 in VAN is involved in the control of eating. The MCT2 knockdown may stimulate eating by limiting the VAN uptake and metabolization of intermediates such as BHB and lactate produced in enterocytes from ingested nutrients.

Methods

Animals and housing

The cell culture and immunohistochemistry experiment was performed by Myrtha Arnold in Professor Helen Raybould's laboratory at UC Davis (Davis, CA, USA). Male Sprague Dawley rats (Harlan Industries, Indianapolis, IN), weighing 207 ± 1 g upon arrival were group-housed (four animals/cage) in a climate-controlled room (22 ± 2 °C and $55 \pm 5\%$ relative humidity) with a 12/12 dark/light cycle and ad libitum access to water and food (standard chow diet; Lab Diet 5001 rodent diet, St. Louis, USA; crude protein 23.0%, crude fat 4.5%, nitrogen free extract (NFE) 48.7%). All experimental procedures were in accordance with protocols approved by the Institutional Animal Care and Use Committee (University of California, Davis).

The NG shRNA injection experiment with food intake monitoring was performed in our laboratory at *ETH* Zürich in Schwerzenbach. Male Sprague-Dawley rats (Charles River, Sulzfeld, Germany), weighing 140-180 g upon arrival, were group-housed (four animals/cage) in a climate-controlled room (22 ± 2 °C and $55 \pm 5\%$ relative humidity) with a 12/12 dark/light cycle and ad libitum access to water and food, unless otherwise noted (standard chow diet #3433 or 3436 Kliba-Nafag, Switzerland; crude protein 18.5%, dry matter 88%, crude fat 4.5%, NFE 54.2% or 54.0% respectively). Animals were adapted to the housing conditions for at least 7 days prior to the surgical procedure (see below) and then single-caged for 10 days before food intake recordings began. In the experiment, rats were fed either standard chow (#3433 or 3436 Kliba-Nafag, Switzerland; crude protein 18.5%, dry matter 88%, crude fat 4.5%, NFE 54.2% or 54.0% respectively) or high-fat diet (HFD, #E15742-34 Ssniff, Germany; 60 kJ % fat; crude protein 24.4%, crude fat 34.6%, crude fibre 6%, crude ash 5.5%, starch

0.1%, sugar 9.4%). All experimental procedures were approved by the Veterinary Office of the Canton of Zürich.

Cell culture and immunohistochemistry

After an overnight (light phase) food deprivation animals were euthanized with CO₂. Harvested nodose ganglia (NG) were dissected under aseptic conditions and digested for 2 h at 37°C in HBSS (Ca²⁺ and Mg²⁺ free Hank's balanced salt solution) containing 2 mg/ml collagenase A (Roche Diagnostics, Indianapolis, IN). Cells were dispersed, washed twice with HEPES-buffered DMEM containing 10% fetal calf serum supplemented with 3% antibiotic/antimycotic solution, and plated onto four-well chamber slides (Millipore E-Z 4-chamber slides). Cells were maintained in DMEM (+ supplements, see above) at 37°C in 5.5% CO₂. The medium was changed every 48 h. After 3 days, the cultured vagal afferent neurons (VAN) were fixed in 4% para-formaldehyde in PBS, processed for immunohistochemistry, and stained for MCT2 (1:100, sc-14926, Santa Cruz, Dallas, USA) and Pan cadherin (1:100, Abcam 6528, Cambridge, UK). The samples were mounted in Vectashield with 4',6-diamidino-2-phenylindole (DAPI; Vector Laboratories, Peterborough, UK) for nuclear localization. Staining was visualized under the microscope (Olympus Production Fluorescence Microscope).

Virus details and NG injection

An adeno-associated-viral construct (AAV) expressing either a scrambled shRNA or a shRNA targeting MCT2 (2.5 x 10⁷ infectious particles (InP)/μl) (AAV-MCT2) was provided by Prof. Luc Pellerin, University of Lausanne, Switzerland. Rats (weighing

200-260 g on surgery day) were anesthetized with isoflurane (IsoFlo, Abbott Laboratories), and nodose ganglia (NG) were exposed. With a Picospritzer III injector (Parker Hannifin) and a glass capillary (50 μm tip), 1.5 μl of viral solution, AAV-MCT2 or scrambled shRNA, was administered into each NG at a speed of 0.5 $\mu\text{L}/\text{min}$, followed by additional 3 min resting time (23). Animals were allowed to recover for 2 weeks before body weight monitoring was used for data collection.

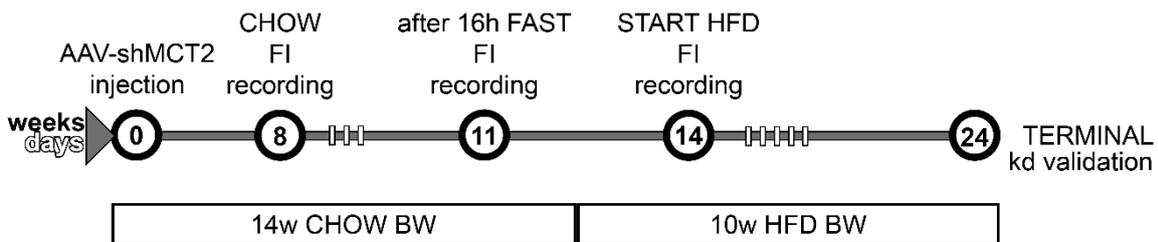
Food intake and meal pattern recording

Feeding cups were placed on scales (XS4001S; Mettler-Toledo) and accessible through a niche in the cage. A custom-designed software (LabX meal analyzer 1.4; Mettler Toledo) on a computer connected to the scales continuously recorded the weight of the feeding cups, allowing for precise meal pattern analysis. A minimum food removal of 0.3 g separated from other food removals by at least 15 min of eating inactivity was defined as a meal. Food recordings always started with dark phase onset and lasted for 23 hrs. Recording recess was necessary for food cup refill or scale reset to 0.0 and body weight monitoring. Food intake recordings during chow feeding started 8 weeks after virus injection to ensure expression of the viral construct (24). Food intake data are presented as means of individual animal averages of three recording days. In a second experiment three weeks later, animals had no access to food for 16 h (12 h light phase and 4 h dark phase) before the food intake measurement. Fourteen weeks after virus injection the animals were switched from chow to HFD at dark onset, and food intake recording was started. Food intake recording data of the first day on HFD are presented as a single independent experiment.

NG collection and gene expression analysis

Animals were anesthetized with isoflurane (IsoFlo, Abbott Laboratories) and transcardially perfused with PBS (RT, Gibco # 10010-15-015 pH 7.4) for 5 min at a speed of 30 ml/min. Both NG were harvested, pooled, immediately frozen in liquid nitrogen and stored at -80 °C. RNA was extracted using Trizol (Life Technologies) and transcribed to cDNA using the High-Capacity cDNA Reverse Transcription kit (ThermoFisher, 4368814). RT-qPCR was performed using FAST SYBER green in a Vii7 Real Time PCR system machine (Applied Biosystems). Data were analyzed using the 2ddCt method with β -actin (FW 5': aaggccaaccgtgaaaagat; RV 5': accagaggcatacagggaca) as the reference gene and MCT2 (FW 5': ctggctgtcatgtacgcagga; RV 5': aagccgacggtgaggtaaagt) as the gene of interest.

Experimental design



Schematic timeline of the experiments.

BW = body weight; FI = food intake; HFD = high-fat diet; kd= knockdown; w = weeks.

Statistical analysis

GraphPad Prism (version 7.03) was used for all statistical analyses and graph generation. Data normality was verified using the Shapiro-Wilk test, and outliers were detected using the Grubb's test. For unpaired, normally distributed values of equal

variance, differences were analyzed using the Student t-test. Where the dependent variable was affected by two factors, data were analyzed using two-way ANOVA. Post-hoc analyses were performed using the Bonferroni/Sidak correction. Data are presented as means \pm SEM. Differences were considered significant when $p < 0.05$.

Results

Rat VAN express MCT2, and AAV-MCT2sh RNA injection decreased MCT2 gene expression in NG of rats

As MCT2 expression varies among species and tissues (25), MCT2 expression in rat VAN was examined in primary rat NG neurons (Fig 1A). Staining for MCT2 revealed MCT2 expression along cell body and axons. The bilateral NG injection of AAVshMCT2 led to a 28% reduction in MCT2 mRNA expression compared to control treated animals injected with an AAV carrying a scrambled shRNA (Figure 1B).

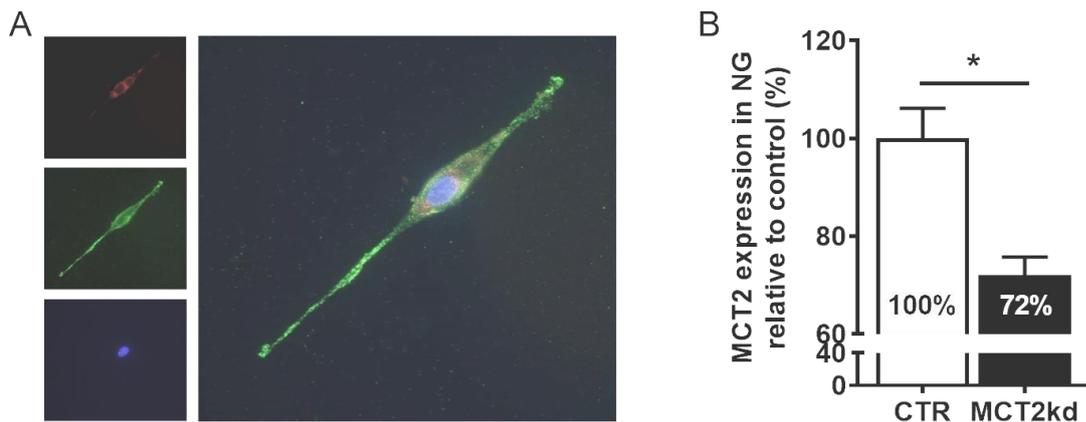


Figure 1: Rat VAN express MCT2, and AAV-MCT2sh RNA injection decreased MCT2 gene expression in NG of rats

(A) Visualization of MCT2 protein expression (green), calcium-dependent adhesion transmembrane proteins (Pan cadherin, red), and nucleus (DAPI, blue), in a rat vagal afferent primary cell culture neuron; representative picture. **(B)** Relative MCT2 mRNA expression in nodose ganglia of MCT2 knockdown (MCT2kd) and control animals (CTR) (n=6/7), Student's t-test, $p < 0.05$. Results are presented as means \pm SEM; * = $p < 0.05$.

NG MCT2 knockdown did not affect cumulative food intake, but prolonged meal duration when rats were fed chow diet ad libitum

To investigate the role of VAN MCT2 in the control of eating, we first assessed whether the NG MCT2 knockdown influenced eating in rats fed chow diet ad libitum. MCT2 knockdown did not affect 24 h food intake, nor dark- or light phase food intake (Fig 2A-C), but it prolonged meal duration specifically during the dark phase (Fig 2D-F). Dark phase meal size tended to be increased, but this effect did not reach significance (Fig 2H). Also, the number of meals remained unaffected (Fig 2J-L)). The MCT2 knockdown also did not affect first and second dark phase meal parameters (data not shown). After a 16 h fast, MCT2 knockdown animals showed a markedly increased and prolonged 2nd meal (Fig 3B and 3D). Four-hour cumulative food intake and 12 as well as 24 h food intake were unaffected (data not shown).

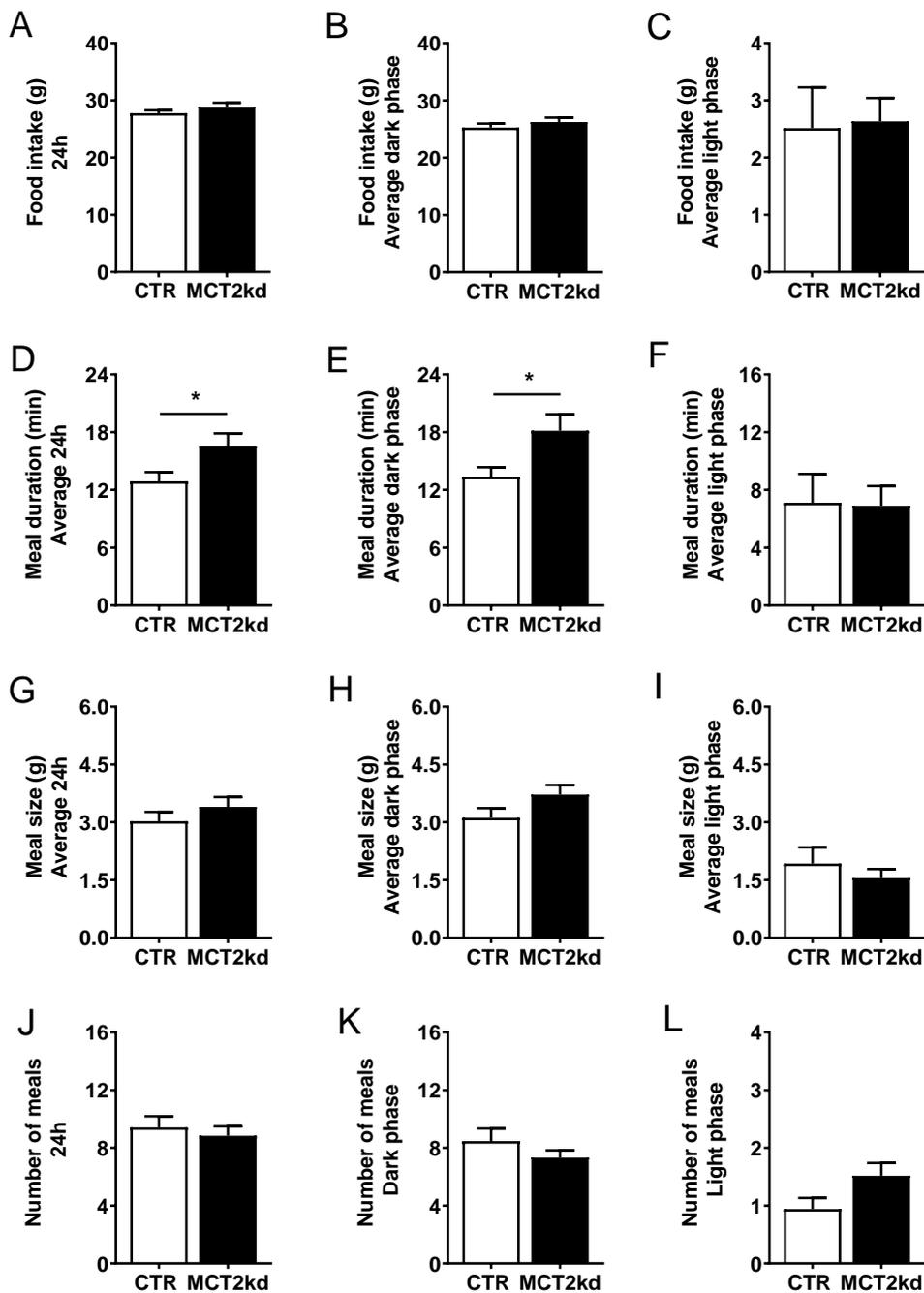


Figure 2: NG MCT2kd animals on chow displayed a prolonged meal duration but no difference in meal size or meal number.

A-M: Food intake of MCT2kd and control animals on ad libitum chow, presented as means of individual animal averages of 3 days of recordings (n=6/7). **(A)** 24 h food intake, **(B)** 12 h dark phase and **(C)** 12 h light phase, Student's t-test, all ns. **(D)** Average meal duration over 24 h, **(E)** 12 h dark phase and **(F)** 12 h light phase, Student's t-test, $p < 0.05$, $p < 0.05$, and ns, respectively. **(G)** Average meal size over 24 h, **(H)** 12 h dark phase and **(I)** 12 h light phase, Student's t-test, all ns. **(J)** Number of meals over 24 h, **(K)** 12 h dark phase and **(L)** 12 h light

phase, Student's t-test, all ns. Results are presented as means \pm SEM; ns = not significant; * = $p < 0.05$.

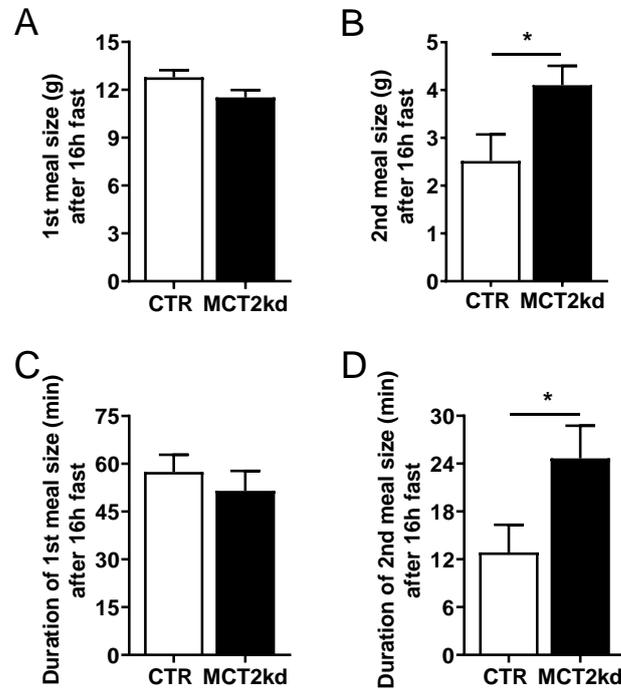


Figure 3: After a 16 h fast NG MCT2kd animals on chow showed bigger and longer 2nd meals.

A-D: Meal pattern recording of MCT2kd and control animals on ad libitum chow after 16 h of fasting (n=6/7). **(A)** 1st meal size dark phase, **(B)** 2nd meal size dark phase, Student's t-test, ns, $p < 0.05$, respectively. **(C)** Duration of 1st meal, **(D)** Duration of 2nd meal, Student's t-test, ns, $p < 0.05$, respectively. Results are presented as means \pm SEM; ns = not significant; * = $p < 0.05$.

NG MCT2 knockdown did not affect body weight when rats were fed chow diet ad libitum

Body weight and body weight gain did not differ between MCT2 knockdown and control rats during the entire duration of the experiment when they were fed chow diet (Fig 4A and 4B).

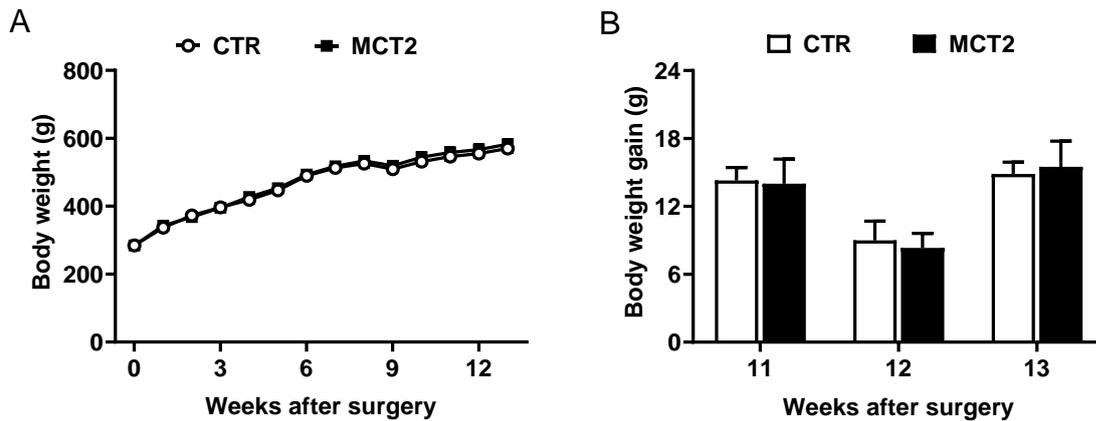


Figure 4: NG MCT2kd animals on chow showed no difference in body weight and body weight gain.

(A) Body weight of MCT2kd and control animals monitored over 13 weeks on chow feeding after surgery (n=6/7), 2 way-ANOVA, time x group ns, time $p < 0.0001$, group ns. **(B)** Consecutive weekly body weight gains over the last 3 weeks on chow diet (n=6/7), Student's t-tests, all ns. Results are presented as means \pm SEM; ns = not significant; * = $p < 0.05$.

When switched to the HFD, the MCT2 knockdown rats increased light phase food intake by increasing the number of meals

Different from what we saw when the animals were fed chow, on the day they were switched to HFD, MCT2 knockdown rats ate more than control rats during the light phase, but not during the dark phase (Fig 5A-C). The increase in food intake during light phase was big enough to increase 24 h food intake, and it was due to an increase in the number of meals (Fig 5L), whereas meal size and meal duration remained unaffected (Fig 5D-I). MCT2 knockdown did also not affect 1st and 2nd meal size when animals were fed a high-fat diet (data not shown).

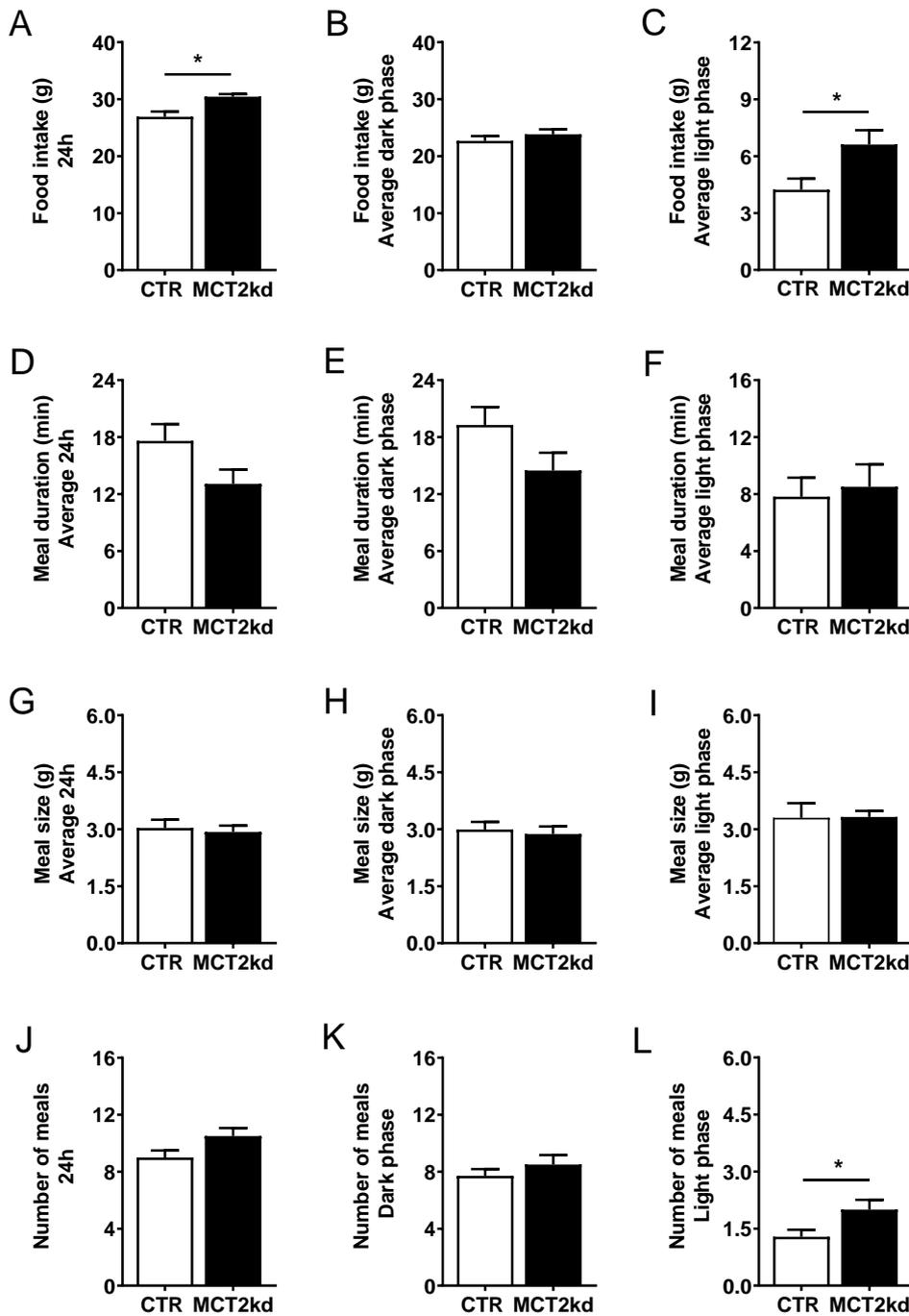


Figure 5: When switched to high-fat diet, NG MCT2kd animals displayed increased 12 h light phase food intake which was also reflected in increased 24 h food intake and due to a greater number of meals during 12 h light phase.

A-M: Food intake and meal patterns of MCT2kd and control animals on 1st day of ad libitum high-fat diet (n=6/7). **(A)** 24 h food intake, **(B)** 12 h dark phase and **(C)** 12 h light phase, Student's t-test, p < 0.05, ns, p < 0.05, respectively. **(D)** Average meal duration over 24 h, **(E)** 12 h dark phase and **(F)** 12 h light phase, Student's t-test, all ns. **(G)** Average meal size over 24 h, **(H)** 12 h dark phase and **(I)** 12 h light phase, Student's t-test, all ns; **(J)** Number of meals

over 24 h. (K) 12 h dark phase and (L) 12 h light phase, Student's t-test, ns, ns, $p < 0.05$, respectively. Results are presented as means \pm SEM; ns = not significant; * = $p < 0.05$.

When switched to the HFD, the MCT2 knockdown rats showed increased 5 day cumulative FI and increased BW

The MCT2 knockdown animals did not compensate for the increased food intake shown in the first 24 h on HFD. Rather, a continuous small, non-significant daily difference added up to a significant cumulative food intake difference on Days four and five after the diet switch (Fig 6A). Thereafter, when 24 h food intake was recorded once a week until week 5 after the switch to HFD, no difference between MCT2 knockdown and control animals was observed (Fig 6B).

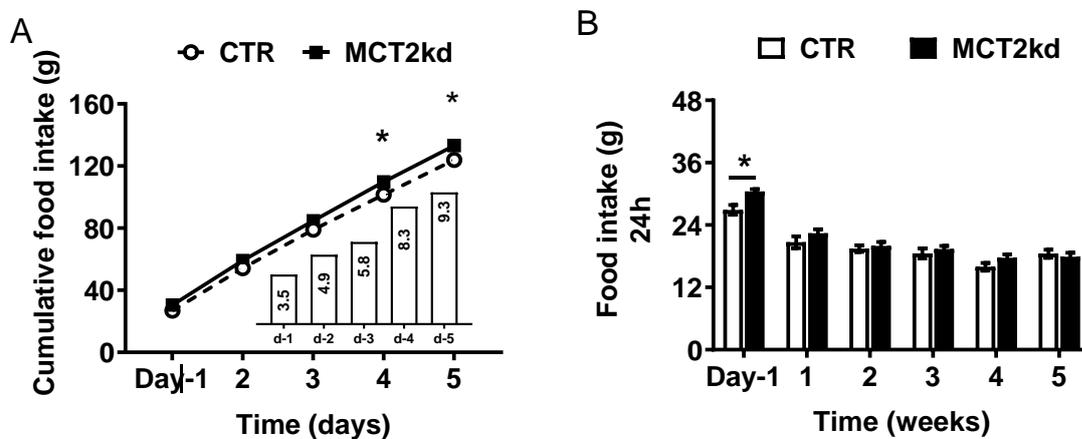


Figure 6: NG MCT2kd animals increased 5 day cumulative FI after switch to HFD.

(A) Cumulative food intake of MCT2kd and control animals monitored over 5 days after the switch to HFD ($n=6/7$), bars represent the exact average difference in cumulative FI on each day, 2 way-ANOVA, time x group $p < 0.05$, time $p < 0.0001$, group $p < 0.05$; Multiple t-test, day 1-3 ns, day 4 and 5 $p < 0.05$. (B) 24 h food intake recorded once a week for 5 weeks after the switch to HFD ($n = 6/7$), Student's t-tests, Day 1 $p < 0.05$, week 1 – 5, all ns. Results are presented as means \pm SEM; ns = not significant; * = $p < 0.05$.

In the first week after the switch from chow to HFD, MCT2 knockdown animals gained more weight than control animals. In line with the disappearance of the increased food

intake of MCT2 knockdown animals, there was also no difference in body weight gain beyond the 1st week of HFD feeding (Fig 7B). Overall body weight assessed over 10 weeks on HFD revealed no significant differences between MCT2 knockdown and control animals (Fig 7A).

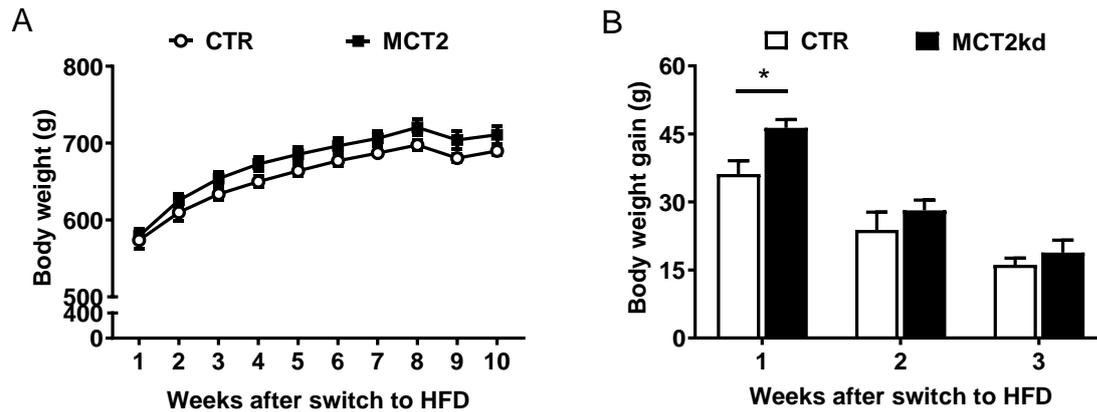


Figure 7: NG MCT2kd animals showed increased body weight gain in the first week after the switch to HFD.

(A) Body weight of MCT2kd and control animals monitored over 10 weeks of high-fat diet feeding ($n=6/7$), 2 way-ANOVA, time x group ns, time $p < 0.0001$, group ns. **(B)** Consecutive body weight gain over the first 3 weeks of 10 monitored weeks ($n = 6/7$), Student's t-tests, $p < 0.05$, ns, ns, respectively. Results are presented as means \pm SEM; ns = not significant; * = $p < 0.05$.

Discussion

VAN signaling is involved in the control of eating, but to which extent VAN also relay energy-related metabolic signals to the brain is debatable. MCT2, the key neuronal pyruvate, lactate and KB transporter supposedly links neuroenergetics with neuronal signaling. Here we addressed the role of VAN MCT2 in the control of eating and demonstrate that a moderate knockdown of MCT2 in the NG has subtle effects on meal patterns and temporarily promotes eating when animals are food deprived or switched from chow to HFD.

So far, the MCT2 has been shown to be expressed in various areas of the mouse brain (26, 27), but, to our knowledge, little is known about its distribution in the peripheral or in the autonomic nervous system. There is one report on MCT2 expression in mouse dorsal root ganglia (DRG) neurons (28). However, considering that MCT2 is scarcely conserved across species and differs in tissue expression profile (25, 29), we first examined whether MCT2 is also present in the rat NG. Visualization with immunocytochemistry revealed that rat primary NG neurons express MCT2 and that it is distributed all over the cell body and axon as described previously for Purkinje cells (30). This also indicates that neurons are the major cell type in NG that expresses MCT2. The moderate MCT2kd (28%) in NG in vivo induced by bilateral NG injection of an AAV-shMCT2 was sufficient to cause subtle changes in meal patterns, i.e., an increase in meal duration and size (after food deprivation) when the rats were eating chow, and an increase in light phase meal number, when rats were switched to HFD. In the latter situation, the increase in meal number also caused a transient increase in 24 h food intake and body weight. The NG MCT2kd did however not affect energy balance chronically. Of course, we cannot exclude that a more pronounced knockdown could have caused greater effects on food intake and, perhaps, body weight. To our

knowledge, there are scarcely any directly comparable studies, except for the NG GLP-1-receptor knockdown study from our own laboratory by Krieger et al. (23). They achieved a 52.5 % knockdown with a bilateral NG injection of a lentivirus containing a GLP-1-R- targeting shRNA construct and found a sustained increase in meal size, whereas total 24 h FI remained unaffected because of a concomitant reduction in meal frequency. Body weight was unaffected too. Thus, it is not unusual to see only changes in meal patterns after interfering with vagal afferent signaling.

In the present experiment, with chow feeding, the MCT2kd prolonged meal duration specifically in the dark phase, indicating that in this situation the diminished presence of MCT2 in VAN delayed satiation. Meal size tended to be increased, but this difference did not reach significance. The small number of meals during the light phase may have prevented the detection of small differences in meal duration and/or meal size, if they existed, during this part of the diurnal cycle. Interestingly, after food deprivation, second meal size and duration, both, increased substantially in MCT2kd rats, indicating that in this situation the VAN MCT2 was an essential part of the normal control of meal size. We can only speculate why this effect did not manifest itself in the first meal: Perhaps the first meal was simply too big (around 12 g) and too long (> 50 min) for any further increase to occur (ceiling effect). In any case, considering the comparatively small knockdown efficiency, the fact that after food deprivation second meal size and duration basically doubled in MCT2kd rats reflects a substantial contribution of VAN MCT2 to meal size control under these conditions, i.e., when the system is challenged by prior food deprivation and the subsequent initial hyperphagia. This also suggests a role of VAN intracellular metabolism in meal size control. Nevertheless, these effects were obviously short-lived because no differences in 24 h food intake or body weight were observed at any time.

The monocarboxylate involved in this effect under these conditions was presumably lactate rather than BHB because with chow feeding the intestine has been shown to be a net producer of lactate, i.e., to primarily produce lactate during meals (31), whereas BHB levels drop substantially in all blood vessels as soon as a chow meal starts (31). The enterocytes release lactate into the interstitial fluid, which bathes the VAN terminals in the wall of the small intestine, i.e., VAN could easily take up enterocyte-derived lactate. Silberbauer and colleagues reported that lactate (1 or 1.5 mmol) infused during the first spontaneous dark phase meal into the hepatic portal vein or the vena cava decreased meal size, and the higher dose of lactate also decreased meal duration. These results correspond to our observation and indicate that lactate can have an immediate effect on meal size. The study by Silberbauer and colleagues did not allow differentiating whether lactate triggered an eating-inhibitory signal by acting on the lactate receptor GPR81 (18) or whether lactate uptake and metabolism was involved. However, the GPR81 has been shown to be expressed in the brain (32), but does not appear to be expressed in VAN (33). This appears to be more consistent with an effect based on uptake and metabolism. Together with previous findings with exogenous lactate and pyruvate (15, 20, 21, 31), also our study provides indirect evidence supporting the latter possibility. The MCT2kd in our model presumably reduces the transport of lactate across the VAN plasma membrane as well as the transport of pyruvate across the VAN mitochondrial membrane (29, 34), hence affecting VAN metabolism because it limits fuel availability, i.e., the entrance of glucose or lactate-derived pyruvate into the mitochondria to enter the TCA cycle. Therefore, the decreased mitochondrial pyruvate uptake in our MCT2kd model would ultimately decrease ATP production from carbohydrates. This appears to be consistent with

previous findings (24) and the idea of an energostatic (1) or ischymetric (35, 36) contribution to the control of eating involving VAN metabolic sensing.

When switched to the HFD, MCT2kd rats temporarily increased meal number, indicating that in this case the maintenance of satiety after meals was compromised, in particular during the light phase. This suggests a role of VAN MCT2 and, hence, enterocyte-derived monocarboxylates and/or their oxidative metabolism in satiety. The effect resulted in a transient increase in 24 h food intake and even body weight. In this situation, the enterocyte-derived monocarboxylate might be predominantly BHB rather than lactate because HFD intake was shown to increase enterocyte oxidation of dietary-derived fatty acids that enter the cell through the apical membrane (37) and to release BHB in response to a meal. Interestingly, detailed analysis of HFD meal-induced changes in hepatic portal vein and intestinal lymphatic metabolites showed that the enterocytes apparently start producing and releasing BHB after a HFD fat meal with the most pronounced production of BHB between 1 and 2 hours after meal termination (M. Arnold, unpublished results). These dynamics may be related to the fact that in this case postprandial satiety rather than satiation was affected in the MCT2kd rats, but further studies are needed to examine this possibility. That the diminished uptake and, presumably, intracellular utilization of endogenous BHB in VAN can increase food intake is consistent with several findings of decreased food intake after peripheral administration of exogenous BHB (12, 14, 42). It should be mentioned in this context that similar to CNS neurons, peripheral nerves are able to oxidize ketone bodies (16, 38).

That the observed increase in FI was primarily due to an increase in meal number during the light phase is reminiscent of the eating-stimulatory effect of the FAO inhibitor MA, which initiated eating, i.e., shortened satiety, and did so with greater potency

during the light phase than during the dark phase (39). Although it is clear that MA stimulates food intake mainly by acting on the GPR40 rather than by inhibiting fatty acid oxidation (40, 41), it is equally clear that MA requires intact abdominal vagal afferents to stimulate eating (42). The MA findings therefore indicate that VAN signaling is also involved in the maintenance of satiety. The observed circadian differences in the MCT2kd effect on FI during dark and light phase may be related to circadian clock-driven changes in metabolism, with lipolysis and FAO prevailing during the inactive phase of the light cycle. The circadian clock machinery controls the expression of enzymes that regulate the rate-limiting steps of metabolic pathways or nuclear receptors and nutrient sensors (43, 44), such as PPAR α , a key regulatory nuclear factor of FAO and ketogenesis. In nocturnal rodents such as rats and mice, PPAR α is upregulated during the light, when animals are generally in a fasting state that requires KB, and inhibited during dark, when food-derived hexoses are the primary fuel source (45, 46). Thus, in a metabolic state when FAO and KB utilization is favored, the compromised transport into and, hence, reduced utilization inside VAN may stimulate eating, whereas these effects do not suffice to stimulate eating during dark, when the organism is tuned into other metabolic fuels. Circadian variations in the phenotype of VAN are ascertained (47). Although not specifically in VAN, circadian regulation of BHB dehydrogenase was reported as well (48). Certainly, its regulation by the circadian clock in VAN needs to be tested, but if so, this could provide additional support for the idea proposed above.

The effects of chronic HFD exposure on vagal afferent sensitivity may explain the transient nature of the eating stimulatory effect of the MCT2kd when the rats were switched to the HFD. One day of HFD feeding is enough to introduce changes in the VAN phenotype. Thus, 24 h HFD exposure caused an upregulation of mRNA

expressions of the proinflammatory biomarkers Emr1, Iba1, Il6, and TNF α in the nodose ganglia and hypothalamus of mice (49). Only three days of HFD consumption reduced the percentage of VAN in which glucose modulates vagal afferent responses to 5-HT (50).

Clearly, our study had several limitations. First, the n of 6-7 rats/group might have hampered detection of the overall rather subtle changes in meal patterns, which are notoriously variable. Second, the switch from chow to HFD took place 14 weeks after the AAV injection. Adeno-associated viruses do not integrate into the genome, and although neurons do not replicate, a loss of knockdown efficiency might already have occurred at this time point, compromising the findings with the HFD. Third, given the various examples of changes in overall metabolism in relation to pharmacological or genetic manipulations of enterocyte metabolism (11, 13, 51) it would be very interesting to have assessments of insulin sensitivity as well as energy expenditure measurements. Both should be performed in follow-up studies. Last, but not least, it would be interesting to address the possible influence of compromised learning mechanisms on the transient effects observed after the switch to the HFD. As many peripheral signals in the control of eating require learning (52), it is conceivable that the MCT2kd rats took longer to gauge the energy content of the HFD than the control rats because they were lacking important afferent signals derived from monocarboxylate uptake into, and utilization in, VAN.

In summary, our study demonstrates for the first time that VAN MCT2 are involved in the control of eating, at least under certain conditions. In doing so, our findings indirectly support and provide novel aspects in relation to “old” ideas of a peripheral metabolic contribution to the control of eating that depends on VAN signaling. Further studies are required to examine the exact mechanisms involved.

References

1. **Booth DA.** Postabsorptively induced suppression of appetite and the energostatic control of feeding. *Physiology and Behavior.* 1972;9(2):199-202.
2. **de Lartigue G, Diepenbroek C.** Novel developments in vagal afferent nutrient sensing and its role in energy homeostasis. *Current Opinion in Pharmacology.* 2016;31:38-43.
3. **Scharrer E, Langhans W.** Control of food intake by fatty acid oxidation. *American Journal of Physiology.* 1986;250(6 Pt 2):R1003-6.
4. **Friedman MI, Harris RB, Ji H, Ramirez I, Tordoff MG.** Fatty acid oxidation affects food intake by altering hepatic energy status. *American Journal of Physiology.* 1999;276(4 Pt 2):R1046-53.
5. **Langhans W, Scharrer E.** Evidence for a vagally mediated satiety signal derived from hepatic fatty acid oxidation. *Journal of the Autonomic Nervous System.* 1987;18(1):13-8.
6. **Brandt K, Arnold M, Geary N, Langhans W, Leonhardt M.** Beta-adrenergic-mediated inhibition of feeding by mercaptoacetate in food-deprived rats. *Pharmacology, Biochemistry and Behavior.* 2006;85(4):722-7.
7. **Brandt K, Geary N, Langhans W, Leonhardt M.** Mercaptoacetate fails to block the feeding-inhibitory effect of the beta3-adrenergic receptor agonist CGP 12177A. *Physiology and Behavior.* 2006;89(2):128-32.
8. **Berthoud HR.** Anatomy and function of sensory hepatic nerves. *Anatomical Record. Part A: Discoveries in Molecular, Cellular, and Evolutionary Biology.* 2004;280(1):827-35.
9. **Mansouri A, Pacheco-López G, Ramachandran D, Arnold M, Leitner C, Prip-Buus C, et al.** Enhancing hepatic mitochondrial fatty acid oxidation stimulates eating in food-deprived mice. *American Journal of Physiology - Regulatory, Integrative and Comparative Physiology.* 2015;308(2):R131-R7.
10. **Azari EK, Ramachandran D, Weibel S, Arnold M, Romano A, Gaetani S, et al.** Vagal afferents are not necessary for the satiety effect of the gut lipid messenger oleoylethanolamide. *American Journal of Physiology: Regulatory, Integrative and Comparative Physiology.* 2014;307(2):R167-78.
11. **Schober G, Arnold M, Birtles S, Buckett LK, Pacheco-López G, Turnbull AV, et al.** Diacylglycerol acyltransferase-1 inhibition enhances intestinal fatty acid oxidation and reduces energy intake in rats. *Journal of Lipid Research.* 2013;54(5):1369-84.
12. **Clara R, Schumacher M, Ramachandran D, Fedele S, Krieger JP, Langhans W, et al.** Metabolic Adaptation of the Small Intestine to Short- and Medium-Term High-Fat Diet Exposure. *Journal of Cellular Physiology.* 2016.

13. **Karimian Azari E, Leitner C, Jaggi T, Langhans W, Mansouri A.** Possible Role of Intestinal Fatty Acid Oxidation in the Eating-Inhibitory Effect of the PPAR- α Agonist Wy-14643 in High-Fat Diet Fed Rats. *PLoS One*. 2013;8(9):e74869.
14. **Langhans W, Wiesenreiter F, Scharrer E.** Different effects of subcutaneous D,L-3-hydroxybutyrate and acetoacetate injections on food intake in rats. *Physiology and Behavior*. 1983;31(4):483-6.
15. **Langhans W, Egli G, Scharrer E.** Selective hepatic vagotomy eliminates the hypophagic effect of different metabolites. *Journal of the Autonomic Nervous System*. 1985;13(3):255-62.
16. **Fisler JS, Egawa M, Bray GA.** Peripheral 3-hydroxybutyrate and food intake in a model of dietary-fat induced obesity: effect of vagotomy. *Physiology and Behavior*. 1995;58(1):1-7.
17. **Hepler C, Foy CE, Higgins MR, Renquist BJ.** The hypophagic response to heat stress is not mediated by GPR109A or peripheral beta-OH butyrate. *American Journal of Physiology: Regulatory, Integrative and Comparative Physiology*. 2016;310(10):R992-8.
18. **Husted AS, Trauelsen M, Rudenko O, Hjorth SA, Schwartz TW.** GPCR-Mediated Signaling of Metabolites. *Cell Metabolism*. 2017;25(4):777-96.
19. **Taggart AK, Kero J, Gan X, Cai TQ, Cheng K, Ippolito M, et al.** (D)-beta-Hydroxybutyrate inhibits adipocyte lipolysis via the nicotinic acid receptor PUMA-G. *Journal of Biological Chemistry*. 2005;280(29):26649-52.
20. **Silberbauer CJ, Surina-Baumgartner DM, Arnold M, Langhans W.** Prandial lactate infusion inhibits spontaneous feeding in rats. *American Journal of Physiology: Regulatory, Integrative and Comparative Physiology*. 2000;278(3):R646-53.
21. **Langhans W, Damaske U, Scharrer E.** Different metabolites might reduce food intake by the mitochondrial generation of reducing equivalents. *Appetite*. 1985;6(2):143-52.
22. **Halestrap AP.** Monocarboxylic acid transport. *Comprehensive Physiology*. 2013;3(4):1611-43.
23. **Krieger JP, Arnold M, Pettersen KG, Lossel P, Langhans W, Lee SJ.** Knockdown of GLP-1 Receptors in Vagal Afferents Affects Normal Food Intake and Glycemia. *Diabetes*. 2016;65(1):34-43.
24. **Kollarik M, Carr MJ, Ru F, Ring CJ, Hart VJ, Murdock P, et al.** Transgene expression and effective gene silencing in vagal afferent neurons in vivo using recombinant adeno-associated virus vectors. *Journal of Physiology*. 2010;588(Pt 21):4303-15.
25. **Jackson VN, Price NT, Carpenter L, Halestrap AP.** Cloning of the monocarboxylate transporter isoform MCT2 from rat testis provides evidence

- that expression in tissues is species-specific and may involve post-transcriptional regulation. *Biochemical Journal*. 1997;324 (Pt 2):447-53.
26. **Pierre K, Parent A, Jayet P-Y, Halestrap AP, Scherrer U, Pellerin L.** Enhanced expression of three monocarboxylate transporter isoforms in the brain of obese mice. *The Journal of Physiology*. 2007;583(Pt 2):469-86.
 27. **Suzuki A, Stern SA, Bozdagi O, Huntley GW, Walker RH, Magistretti PJ, et al.** Astrocyte-neuron lactate transport is required for long-term memory formation. *Cell*. 2011;144(5):810-23.
 28. **Domenech-Estevez E, Baloui H, Repond C, Rosafio K, Medard JJ, Tricaud N, et al.** Distribution of monocarboxylate transporters in the peripheral nervous system suggests putative roles in lactate shuttling and myelination. *Journal of Neuroscience*. 2015;35(10):4151-6.
 29. **Halestrap AP, Meredith D.** The SLC16 gene family-from monocarboxylate transporters (MCTs) to aromatic amino acid transporters and beyond. *Pflügers Archiv. European Journal of Physiology*. 2004;447(5):619-28.
 30. **Bergersen L, Waerhaug O, Helm J, Thomas M, Laake P, Davies AJ, et al.** A novel postsynaptic density protein: the monocarboxylate transporter MCT2 is co-localized with delta-glutamate receptors in postsynaptic densities of parallel fiber-Purkinje cell synapses. *Experimental Brain Research*. 2001;136(4):523-34.
 31. **Langhans W.** Hepatic and intestinal handling of metabolites during feeding in rats. *Physiology and Behavior*. 1991;49(6):1203-9.
 32. **Morland C, Lauritzen KH, Puchades M, Holm-Hansen S, Andersson K, Gjedde A, et al.** The lactate receptor, G-protein-coupled receptor 81/hydroxycarboxylic acid receptor 1: Expression and action in brain. *Journal of Neuroscience Research*. 2015;93(7):1045-55.
 33. **Egerod KL, Petersen N, Timshel PN, Rekling JC, Wang Y, Liu Q, et al.** Profiling of G protein-coupled receptors in vagal afferents reveals novel gut-to-brain sensing mechanisms. *Mol Metab*. 2018;12:62-75.
 34. **Hashimoto T, Hussien R, Cho HS, Kaufer D, Brooks GA.** Evidence for the mitochondrial lactate oxidation complex in rat neurons: demonstration of an essential component of brain lactate shuttles. *PloS One*. 2008;3(8):e2915.
 35. **Nicolaidis S, Rowland N.** Metering of intravenous versus oral nutrients and regulation of energy balance. *American Journal of Physiology*. 1976;231(3):661-8.
 36. **Nicolaidis S, Even PC.** The ischymetric control of feeding. *International Journal of Obesity*. 1990;14 Suppl 3:35-49; discussion 50-2.
 37. **Storch J, Zhou YX, Lagakos WS.** Metabolism of apical versus basolateral sn-2-monoacylglycerol and fatty acids in rodent small intestine. *Journal of Lipid Research*. 2008;49(8):1762-9.

38. **Greene DA, Winegrad AI.** In vitro studies of the substrates for energy production and the effects of insulin on glucose utilization in the neural components of peripheral nerve. *Diabetes*. 1979;28(10):878-87.
39. **Langhans W, Scharrer E.** Role of fatty acid oxidation in control of meal pattern. *Behavioral and Neural Biology*. 1987;47(1):7-16.
40. **Darling RA, Zhao H, Kinch D, Li AJ, Simasko SM, Ritter S.** Mercaptoacetate and fatty acids exert direct and antagonistic effects on nodose neurons via GPR40 fatty acid receptors. *American Journal of Physiology: Regulatory, Integrative and Comparative Physiology*. 2014;307(1):R35-43.
41. **Li AJ, Wiater MF, Wang Q, Wank S, Ritter S.** Deletion of GPR40 fatty acid receptor gene in mice blocks mercaptoacetate-induced feeding. *American Journal of Physiology: Regulatory, Integrative and Comparative Physiology*. 2016;310(10):R968-74.
42. **Brandt K, Arnold M, Geary N, Langhans W, Leonhardt M.** Vagal afferents mediate the feeding response to mercaptoacetate but not to the beta (3) adrenergic receptor agonist CL 316,243. *Neuroscience Letters*. 2007;411(2):104-7.
43. **Eckel-Mahan K, Sassone-Corsi P.** Metabolism and the circadian clock converge. *Physiological Reviews*. 2013;93(1):107-35.
44. **Sahar S, Sassone-Corsi P.** Regulation of metabolism: the circadian clock dictates the time. *Trends in Endocrinology and Metabolism*. 2012;23(1):1-8.
45. **Yang X, Downes M, Yu RT, Bookout AL, He W, Straume M, et al.** Nuclear receptor expression links the circadian clock to metabolism. *Cell*. 2006;126(4):801-10.
46. **Lee CH, Olson P, Evans RM.** Minireview: lipid metabolism, metabolic diseases, and peroxisome proliferator-activated receptors. *Endocrinology*. 2003;144(6):2201-7.
47. **Kentish SJ, Frisby CL, Kennaway DJ, Wittert GA, Page AJ.** Circadian variation in gastric vagal afferent mechanosensitivity. *Journal of Neuroscience*. 2013;33(49):19238-42.
48. **Young ME, Brewer RA, Peliciari-Garcia RA, Collins HE, He L, Birky TL, et al.** Cardiomyocyte-specific BMAL1 plays critical roles in metabolism, signaling, and maintenance of contractile function of the heart. *Journal of Biological Rhythms*. 2014;29(4):257-76.
49. **Waise TMZ, Toshinai K, Naznin F, NamKoong C, Md Moin AS, Sakoda H, et al.** One-day high-fat diet induces inflammation in the nodose ganglion and hypothalamus of mice. *Biochemical and Biophysical Research Communications*. 2015;464(4):1157-62.

50. **Troy AE, Simmonds SS, Stocker SD, Browning KN.** High fat diet attenuates glucose-dependent facilitation of 5-HT₃ -mediated responses in rat gastric vagal afferents. *The Journal of Physiology*. 2016;594(1):99-114.
51. **Ramachandran D, Clara R, Fedele S, Hu J, Lackzo E, Huang J-Y, et al.** Intestinal SIRT3 overexpression in mice improves whole body glucose homeostasis independent of body weight. *Mol Metab*. 2017;6(10):1264-73.
52. **Woods SC, Ramsay DS.** Food intake, metabolism and homeostasis. *Physiology and Behavior*. 2011;104(1):4-7.

CHAPTER 3: ROLE OF ASTROCYTE SIRTUIN-3 IN ENERGY HOMEOSTASIS

Introduction

Accumulating evidence indicates a fundamental role of glia cells in brain and whole body energy homeostasis. This also identifies new mechanisms for a possible involvement of glia cells in the development of obesity. To understand the possible role of glia cells in this regard, it is crucial to explore the effect of nutrient availability on glia cell metabolism and the conceivable involvement of glia cell metabolism in whole body energy homeostasis and, in particular, the control of eating (1, 2).

Astrocytes constitute a major part of the glia cell population. They are versatile, and their predominant functions such as modulation of synaptic transmission and transport of nutrients and other circulating factors from the blood vessels to neurons attract attention regarding energy homeostasis (3). Astrocytes are called the “metabolic workhorses of the brain”, providing not only for themselves but also for neurons and other glia cells (3). The astrocytes’ metabolic profile differs from that of the other glia cells and neurons mainly because of three major characteristics: i) Their substantial pool of glucose, where a surplus of pyruvate is converted into lactate as an efficient oxidative fuel for neurons, in the so called astrocyte-lactate shuttle (4). ii) Astrocytes are the only cells providing an energy reservoir in the brain by storing glycogen (5). iii) Last, but not least, astrocytes oxidize fatty acids and produce ketone bodies (6). Therefore, it is reasonable to hypothesize that astrocyte-derived metabolites might affect brain function. Indeed, it was shown that astrocyte-derived lactate activates lateral hypothalamic orexin/hypocretin neurons (7). During periods of fasting or high-fat diet feeding, a surplus of fatty acids is taken up into the astrocytes (8-10). Intriguingly, some studies observed changes in food intake and hepatic glucose production upon central inhibition or stimulation of key enzymes involved in fatty acid synthesis and fatty acid oxidation, without targeting a specific cell type (11, 12). Whereas the neuronal ability to oxidize fatty acids is still debatable, the astrocytes’ capability to do so and to produce ketone bodies is well established (6, 13). Therefore, the observed effects in response to manipulations of central nervous system fatty acid metabolism were most likely due to changes in astrocytes’ fatty acid metabolism. Le Foll and colleagues provided evidence for a role of astrocyte-derived ketone bodies in the control of eating in rats (13), whereas others showed that disruption of lipid uptake into astrocytes exacerbates diet-induced obesity (DIO) (14). Moreover, viral-mediated astrocyte-specific knockdown of mitochondrial 3-hydroxy-3-methylglutaryl-CoA

synthase 2 (HMGCOA2), the rate-limiting enzyme in ketogenesis, in the basolateral hypothalamus of rats was sufficient to enhance satiation and decrease the respiratory exchange ratio in animals fed a low-fat diet. When switched to high-fat diet (HFD), HMGCOAS2 knockdown animals exhibited a prolonged latency to eat (Fedele et al. unpublished). The astrocytes' indispensability in overall metabolic signaling was nicely demonstrated several times (15-17). For instance, astrocyte-specific insulin receptor knock-down reduced glucose sensing in the hypothalamus, impaired whole-body glucose homeostasis and influenced food intake (18). This suggests that insulin resistance occurring at the level of the astrocyte contributes to the development of obesity and is worth investigating.

To further unravel how astrocyte metabolism participates in systemic metabolic control, we aimed at testing whether increasing or decreasing astrocyte mitochondrial metabolic function affects whole-body energy homeostasis in diet-induced obesity (DIO). Sirtuin-3 (SIRT3), the primary ubiquitous mitochondrial NAD⁺-dependent deacetylase, acts as a cellular energy sensor and modulates metabolic processes. SIRT3 is activated by high NAD⁺ levels, caused by a low cellular energy status. Hence, SIRT3 inhibits glycolysis, while stimulating fatty acid oxidation and ketogenesis. Naturally, SIRT3 expression is upregulated in fasting or caloric restriction, whereas it is downregulated in the obese state (19). Many beneficial effects of caloric restriction have been related to increased SIRT3 levels (20), and whole body SIRT3 knockdown mice exhibited exacerbated DIO (21). Consequently, SIRT3 activation supposedly protects against the metabolic syndrome (22). Therefore, elucidating SIRT3's role in astrocyte metabolism and examining the possible consequences for whole-body energy homeostasis might provide new insights into the pathogenesis of DIO. To this end, we used a tamoxifen-inducible CreERT2-LoxP system with a glial-acid protein (GFAP) promoter to knock-in or knock-out SIRT3 specifically in astrocytes. We found the astrocyte SIRT3 knock-out to increase glucose tolerance in mice fed control (low-fat) diet, but not when the mice were fed a 60% high fat diet, which was introduced immediately after tamoxifen injection. On the other hand, astrocyte-specific SIRT3 overexpression did not produce any metabolic changes when mice were fed the control diet. When the astrocyte-specific SIRT3 overexpression (SIRT3ki) was initiated after the mice had been exposed to HFD for 12 weeks, the SIRT3ki produced a distinct phenotype: SIRT3ki mice showed improved glucose tolerance and insulin sensitivity as well as an increased insulin secretion. Concomitantly, SIRT3ki mice stored more

fat, which was reflected in greater body weight gain compared to control mice. Finally, SIRT3 overexpression increased the respiratory exchange ratio (RER), decreased energy expenditure (EE) and locomotor activity and, concomitantly, increased food intake. Overall, our results suggest that astrocyte SIRT3 can affect whole body energy homeostasis.

Methods

Animals

Mice with an inducible astrocyte-specific SIRT3 overexpression hemizygous (he) for the knock-in of SIRT3 (SIRT3ki; cre/+ fl/+) were generated by crossing hemizygous transgenic mice with a floxed STOP cassette preceding an additional SIRT3 gene (FIKi; fl/+) (23) (mice were received from the laboratory of Professor Eric Verdin at UC San Francisco (San Francisco, CA, USA)) with hemizygous hGFAP-Cre-ERT2 mice expressing Cre recombinase under the astrocyte-specific promoter GFAP (Cre; cre/+) (24) (mice were received from the laboratory of Professor Frank Kirchhoff at University of Saarland, Germany). The mice with an inducible astrocyte-specific SIRT3 knock-out (SIRT3ko; cre/+ fl/fl) were generated in two breeding steps. First, hemizygous transgenic mice floxing the SIRT3 gene itself (FIKo-he; fl/+) (mice were received from the laboratory of Professor Eric Verdin at UC San Francisco (San Francisco, CA, USA)) were crossed with hemizygous hGFAP-Cre-ERT2 mice (Cre; cre/+). These mice (cre/+ fl/+) were, in a second step, crossed once again with hemizygous FIKo-he (fl/+) mice or later with homozygous (ho) FIKo-ho (fl/fl) mice to obtain inducible astrocyte-specific SIRT3 knock-out animals homozygous for the knock-out of SIRT3 and heterozygous for Cre recombinase expression (SIRT3ko; cre/+ fl/fl). Cre and Fl mice were used as controls, and wild-type mice were used for the isolation of primary astrocytes. Genotyping of all mice was performed at the age of 3 to 4 weeks immediately after weaning and reconfirmed post mortem. Gene recombination was achieved by repetitive intraperitoneal injection of Tamoxifen (Sigma) every 24 h over 5 days (100 μ l of 20 mg/ml Tamoxifen in corn oil and 10% ethanol per adult mouse). All mice were on C57Bl6/J background, and all the breedings were carried out in our in-house specified and opportunistic pathogen free (SOPF) animal facility. After weaning mice were fed autoclaved chow diet (#3807, Kliba-Nafag, Switzerland; crude protein 24.0%, dry matter 88.1%, crude fat 4.9%, NFE 47.5%) in the SOPF breeding facility.

Male mice at the age of 8-10 weeks were moved into the experimental rooms with a 12h/12h dark/light cycle and controlled temperature and humidity (22 ± 2 °C and 55 ± 5 %, respectively). All animals had ad libitum access to chow and water unless otherwise specified, and their body weights were monitored on a regular basis as

indicated. Mice were group-housed (2-4 animals per cage) before they were single caged 5 days prior indirect calorimetry measurements. Animals were fed standard chow diet (#3430 Kliba-Nafag, Switzerland; crude protein 18.5%, dry matter 88%, crude fat 4.5%, NFE 54.2%) before being switched to either a low-fat control diet (CD, #S9213-E001 Ssniff, Germany; 10 kJ % fat; crude protein 18.2%, crude fat 4.3%, crude fibre 4.8%, crude ash 5.3%, starch 42.7%, sugar 7.5%) or a high-fat diet (HFD, #E15742-34 Ssniff, Germany; 60 kJ % fat; crude protein 24.4%, crude fat 34.6%, crude fibre 6%, crude ash 5.5%, starch 0.1%, sugar 9.4%). All experimental animal procedures were approved by the Veterinary Office of the Canton of Zürich.

Primary astrocyte isolation

Viable primary astrocytes of adult mice were isolated by combining two isolation methods. First, the “Cold Spring Harbour Protocol of Purification of Rat and Mouse Astrocytes by immunopanning” (25) was applied to obtain a single cell suspension of a whole brain lysate. This astrocyte isolation protocol is designed to preserve the viability of the fragile astrocytes during isolation, but is limited to the isolation of astrocytes from 10 day post-natal mice or rats. Therefore, we proceeded with the Anti-ASCA-2 Microbead Kit mouse (MACS Miltenyi Biotec, 130-097-678) to isolate astrocytes out of the single cell suspension. With this, a magnetic field allows for the selection of ASCA-2 positive cells, which were magnetically labeled with anti-ASCA-2 microbeads. The obtained cell pellets with approximately 2×10^6 isolated cells per brain were frozen in liquid nitrogen and stored at $-80\text{ }^{\circ}\text{C}$ for further RNA analysis. Cells isolated from wild-type animals were used to determine the isolation efficiency and contamination with neurons or other glial cells. Cells isolated from SIRT3^{ki} or SIRT3^{ko} animals and their corresponding controls were used to verify astrocyte-specific SIRT3 overexpression or downregulation, respectively.

Real time quantitative polymerase chain reaction (RT-qPCR) analysis

The Trizol reagent (Life Technologies) was used to extract RNA from isolated astrocytes following the manufacturer’s protocol. Isolated RNA was further treated with DNase (Quiagen). cDNA was synthesized using the High-Capacity cDNA Reverse

Transcription Kit (Applied Biosystems) and RT- qPCR was performed using FAST SYBER green in a Vii7 Real-Time PCR system machine (Applied Biosystems). Data were analyzed using the 2ddCt method with GAPDH as the reference gene. Primers used are listed in Table 1.

Table 1: qPCR primer list

10-formyltetrahydrofolate dehydrogenase (Aldh111)	FW 5` GCAGGTACTTCTGGGTTGCT RW 5` GGAAGGCACCCAAGGTCAAA
Glial fibrillary acidic protein (GFAP)	FW 5` AGAAAGGTTGAATCGCTGGA RW 5` CGGCGATAGTCGTTAGCTTC
Vimentin (Vim)	FW 5` AGACCAGAGATGGACAGGTGA RW 5` TTGCGCTCCTGAAAACTGC
Myelin oligodendrocyte glycoprotein (Mog)	FW 5` CACCGAAGACTGGCAGGACA RW 5` CCACAGCAAAGAGGCCAATG
Gap junctional intercellular communication 2 (Gjic2)	FW 5` CTTGTGCATCTCCAGGTCCCA RW 5` TGTCAGCACAAATGCGGAAGA
Integrin subunit alpha M (Itgam)	FW 5` TGGCCTATAACAAGCTTGGCTTT RW 5` AAAGGCCGTTACTGAGGTGG
Transmembrane protein 119 (Tmem119)	FW 5` GTGTCTAACAGGCCCCAGAA RW 5` AGCCACGTGGTATCAAGGAG
Cluster of differentiation 68 (Cd68)	FW 5` ACTGGTGTAGCCTAGCTGGT RW 5` CCTTGGGCTATAAGCGGTCC
Allograft Inflammatory Factor 1 (Aif1)	FW 5` GGATCAACAAGCAATTCCTCGA RW 5` CTGAGAAAGTCAGAGTAGCTGA
Synatosomal associated protein 25 (Snap25)	FW 5` AGCAAGGCGAACAACCTCGAT RW 5` AGGCCACAGCATTTCCTAA
Synaptogamin-1 (Syt1)	FW 5` CGCTCCAGTTTCCCTCTGAAT RW 5` GGATGTTGGTTGTTTCGAGCG
Neurofilament light (Nefl)	FW 5` CAAGGACGAGGTGTCGGAAA RW 5` TGATTGTGTCCTGCATGGCG
Glycerinaldehyd-3-phosphat-Dehydrogenase (GAPDH)	FW 5` ATG GTG AAG GTC GGT GTG A RW 5` AAT CTC CAC TTT GCC ACT GC
SIRT3	FW 5` GCT GGA CAT AGG ATG ATC TGC RW 5` TCT TAT GCA GCG GGA ACG)
SIRT3-flag	FW 5` ACAAGAACTGCTGGATCTTATGC RW 5` CGTCATCCTTGTAATCTCTGTCC

Body composition

To assess body fat and lean mass, awake mice were scanned using the EchoMRI 3-1 analyzer (Echo-MRITM). Measurements were taken at various time points shown in the individual experimental timelines.

Oral glucose tolerance test (OGTT)

After food deprivation during the first 6 h of the dark phase, the mice received a bolus of 20% glucose solution (in water; 2 g/kg body weight) by gavage. Tail blood glucose levels were monitored using a glucometer (Accu-check Aviva, Roche) at baseline and 15, 30, 60, 90 and 120 min following glucose administration. For insulin measurements, an additional OGTT was performed on a separate experimental day. In this case, tail vein blood was collected using micro hematocrit capillaries (Sigma, Brand) at baseline and 15 and 120 min after glucose administration. Blood samples were centrifuged (8,700 g, 4 °C, 10 min) and plasma was collected and analyzed using a Mouse/Rat Insulin Kit (catalog no. K152BZC-2) for the Meso Scale MULTY-ARRAY Assay System (Meso Scale Discovery, USA). The tests were performed at times shown in the experimental timelines.

Insulin sensitivity test (IST)

Mice were food deprived 2 h after dark phase onset for 4 h before Actrapid HM human insulin (Novo Nordisk) was injected intraperitoneally (0.4 and 0.6 mU/g body weight insulin in NaCl, for CD- or HFD-fed mice, respectively). Tail blood glucose levels were measured at the time points indicated using a glucometer (Accu-check Aviva, Roche). The test was performed at the times shown in the experimental timelines.

Plasma Metabolites

Tail vein blood was collected using micro hematocrit capillaries (Sigma, Brand) at baseline (BL, considered as pre-prandial), 1 h before dark phase onset after an 11 h

light phase food deprivation, and in a fed state 4 h after dark phase onset (considered as postprandial, PP). Blood samples were centrifuged (8,700 g, 4 °C, 10 min) and plasma was collected and stored at -80°C until required. Standard colorimetric and enzymatic methods adapted for the Cobas MIRA auto analyzer (Hoffman LaRoche) were used to measure plasma glucose, non-esterified fatty acids (NEFA), β -hydroxybutyrate (BHB), cholesterol (Chol), triacylglycerol (TAG) and free glycerol. Free glycerol values were subtracted from the measured TAG values to obtain the final TAG values. The experiment was performed according to the corresponding experimental timelines.

Food intake and indirect calorimetry

Metabolic measurements were carried out in Promethion metabolic cages (SS, Sable Systems International). Mice were adapted in their housing room for 5 days to single housing in cages similar to the SS metabolic cages before being transferred to the corresponding system. Data were collected after an additional 3 days of habituation in the metabolic cage system. In both SIRT3ki experiments (with mice on CD or HFD), in addition to the SS recordings, food intake was measured manually every 12 h at the beginning of the dark or light phases at a later time point (please see the corresponding experimental timelines).

Statistical analysis

All statistical analyses and graph generation were performed using GraphPad Prism (Version 8.0). Data normality was verified using the Shapiro-Wilk test, while outliers were detected using the Grubb's test. Student t-test was applied to analyze differences of unpaired normally distributed values of equal variance. A one-way ANOVA was used to analyze differences for sample groups > 2 if normality was met. Multiple comparisons were assessed with Tukey's test. Where the dependent variable was affected by two factors, data were analyzed using a two-way ANOVA. Post-hoc analyses were performed using the Bonferroni/Sidak correction. Data are presented as mean \pm SEM. Differences were considered significant when $p < 0.05$.

Results

Isolated primary astrocytes were contaminated with oligodendrocytes but free of neurons and microglia

Primary astrocytes from wild type mice were isolated to validate the isolation method (25). The purity of the isolated astrocyte fraction was tested by assessing gene expression of neuronal, microglial, oligodendrocyte and astrocyte markers compared to whole brain lysate. The isolated astrocyte fraction was devoid of neurons according to the three neuronal marker genes *Snap25*, *Syt1* and *Nefl* (Figure 1A). We detected contamination with microglia (approximately 25%) when we screened for four microglial marker genes (*Itgam*, *Tmem119*, *Cd68* and *Aif1*; Figure 1B). However, the astrocyte fraction contained as many oligodendrocytes as astrocytes, judging by the threefold higher expression of oligodendrocyte and astrocyte-specific marker genes *Mog* and *Gjc2* or *Adh1/1* and *Vim*, respectively, than control (Figure 1C, D). We found *Gfap*, the astrocyte-specific marker used in our transgenic mouse model as promoter for specific astrocyte SIRT3 knock-in or knock-out, to be 50% less expressed compared to control (Figure 1D).

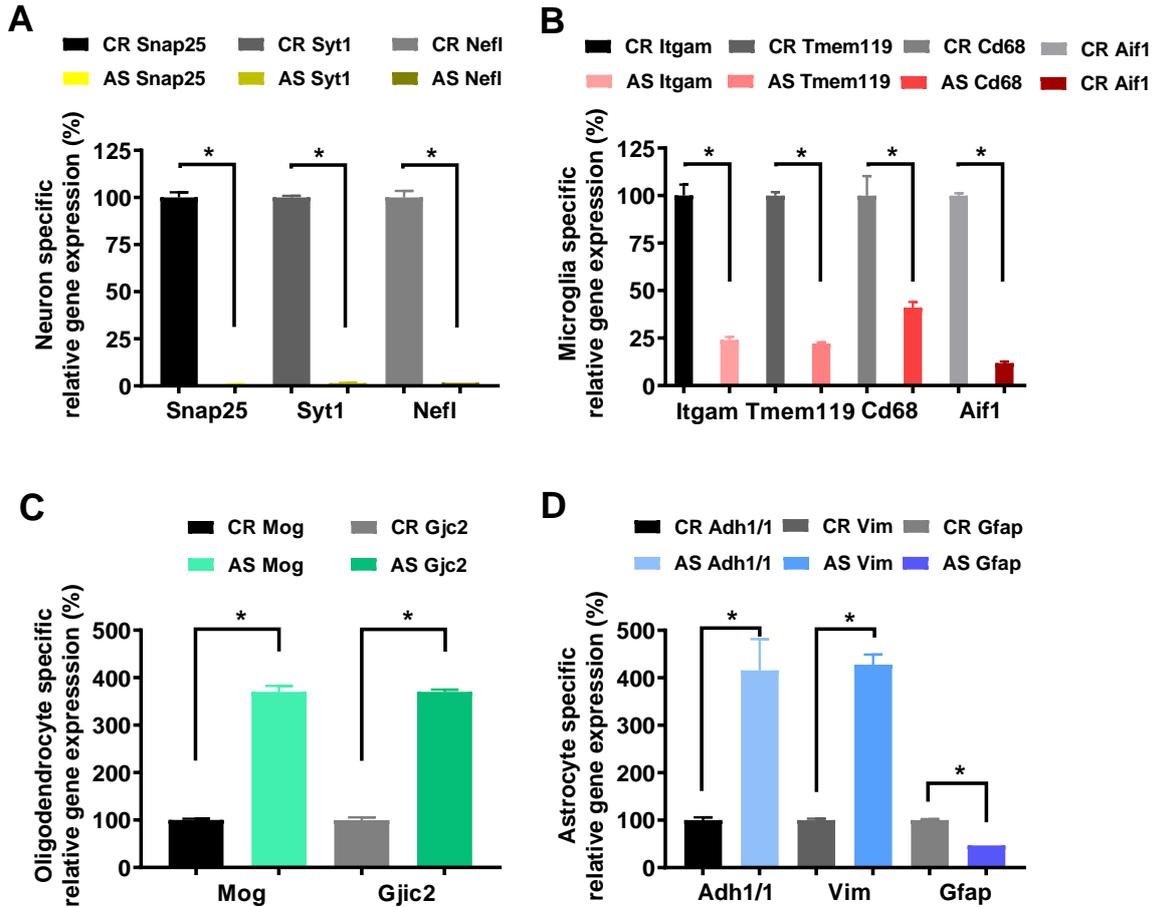


Figure 1: Validation of the astrocyte isolation method revealed oligodendrocyte contamination but purity for neurons and microglia.

A-D: Relative mRNA expression of specific neuronal, microglial, oligodendrocyte and astrocyte genes in the fraction of primary isolated astrocytes (AS) or whole brain lysate (CR) from a wild type, chow-fed mouse ($n = 1$; normalized to GAPDH; SEM corresponds to technical triplicates). **(A)** Neuron specific genes; Snap25: Synaptosomal-associated protein-25; Syt1: Synaptogamin-1; Nefl: Neurofilament light. **(B)** Microglia specific genes; Itgam: Integrin subunit alpha-M; Tmem119: Transmembrane protein-119; Cd68: Cluster of differentiation 68; Aif1: Allograft Inflammatory Factor-1. **(C)** Oligodendrocyte specific genes; Mog: Myelin oligodendrocyte glycoprotein; Gjc2: gap junctional intercellular communication-2. **(D)** Astrocyte specific genes: Adh1/1: Alcohol dehydrogenase-1; Vim: Vimentin; Gfap: Glial Fibrillary Acidic Protein. Results are presented as means \pm SEM and data were analyzed using Student's t-test, * = $p < 0.05$.

SIRT3 knock-in study on control diet



Figure 2: Experimental design of SIRT3ki on control diet

Schematic timeline of the experiments. Measurements and tests: BW = body weight; FI = food intake; IC = indirect calorimetry; IST = insulin sensitivity test; MRI = magnetic resonance imaging; OGTT = oral glucose tolerance test; TAM = tamoxifen injections; VL = voluntary locomotion; w = weeks.

No difference in glucose tolerance was observed between SIRT3ki and control animals (Cre mice and FIKi mice) when fed CD

The study started when the mice were switched from chow to control diet (CD) at the age of 8 weeks. After 14 weeks of CD feeding a first oral glucose tolerance test (OGTT-1) was performed to examine the glucose responses of all three genotypes, Cre, FIKi, and SIRT3ki, before TAM injections, i.e., prior to the induction of astrocyte SIRT3 overexpression in SIRT3ki animals (Figure 3A). A follow-up OGTT-2 performed 4 weeks after TAM injection revealed unchanged similar glucose tolerance of all three genotypes (Figure 3B). An insulin sensitivity test (IST) performed 6 weeks after TAM injection showed also no genotype differences (Figure 3C).

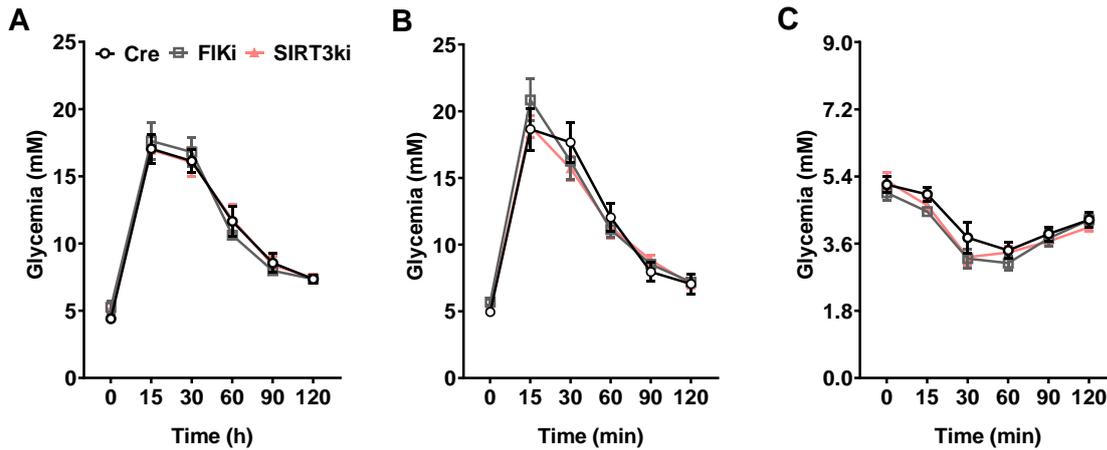


Figure 3: Glucose tolerance of SIRT3ki, Cre, and FIKi mice on control diet was similar.

A-B: Oral glucose tolerance tests (OGTT-1 and OGTT-2) (n=4-8). **(A)** OGTT-1: Tail blood glucose values measured at the time points indicated after an oral bolus of glucose (2 g/kg/BW) after 14 weeks on CD and before TAM injection; 2-way ANOVA, genotype ns, time $p < 0.0001$, genotype x time ns. **(B)** OGTT-2: Tail blood glucose values measured at the time points indicated after an oral bolus of glucose (2 g/kg/BW) after 20 weeks on CD or 4 weeks after the last TAM injection; 2-way ANOVA, genotype ns, time $p < 0.0001$, genotype x time ns. **(C)** Insulin sensitivity test (IST), tail blood glucose values measured at the time points indicated after an intraperitoneal injection of insulin (0.4 mU/g body weight) after 22 weeks on CD or 6 weeks after the last TAM injection (n = 4-8); 2-way ANOVA, genotype ns, time $p < 0.0001$, genotype x time ns. Data are presented as means \pm SEM; ns = not significant.

Similar levels of circulating pre- and postprandial metabolites were observed between SIRT3ki and control animals (Cre mice and FIKi mice) when fed CD

Plasma metabolite analyses from tail vein blood samples collected 2 weeks after TAM injections, after an 11 h food deprivation during the light phase, one hour before dark phase onset (pre-prandial=baseline (BL)), and 4 h after dark phase onset (postprandial (PP)) revealed no differences in concentrations of glucose, non-esterified free fatty acids (NEFA) or β -hydroxybutyrate (BHB) among the three genotypes (Figure 4A-C).

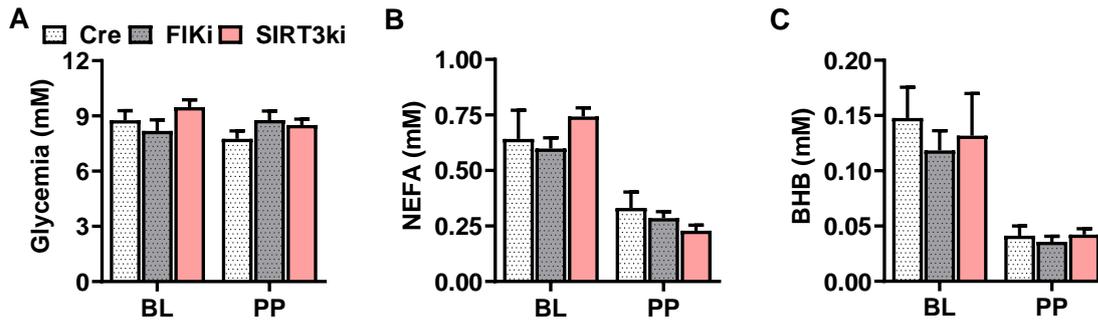


Figure 4: Baseline and postprandial blood plasma metabolite levels of SIRT3ki animals and control animals (Cre mice and FIKi mice) on CD measured 2 weeks after TAM injection were similar.

A-C: Tail vein blood plasma metabolite levels 2 weeks after TAM injection, at baseline (BL= pre-prandial) corresponding to levels obtained after an 11 h fast during the light phase and postprandial (PP) metabolite levels obtained from tail vein blood plasma collected 4 h after dark-phase onset (n = 4-8). **(A)** Glucose; BL and PP One-way ANOVA all ns. **(B)** Non-esterified fatty acids (NEFA); BL and PP One-way ANOVA all ns. **(C)** β -hydroxybutyrate (BHB); BL and PP One-way ANOVA all ns. Data are presented as means \pm SEM; ns = not significant.

A similar metabolic profile was observed between SIRT3ki and control animals (Cre mice and FIKi mice) when fed CD

Indirect calorimetry was performed 5 weeks after the last TAM injection. Data of 48 h recording did not reveal any statistically significant genotype differences in RER (Figure 5A), EE (Figure 5B), cumulative voluntary locomotor activity or cumulative food intake (Figure 5C and D, respectively).

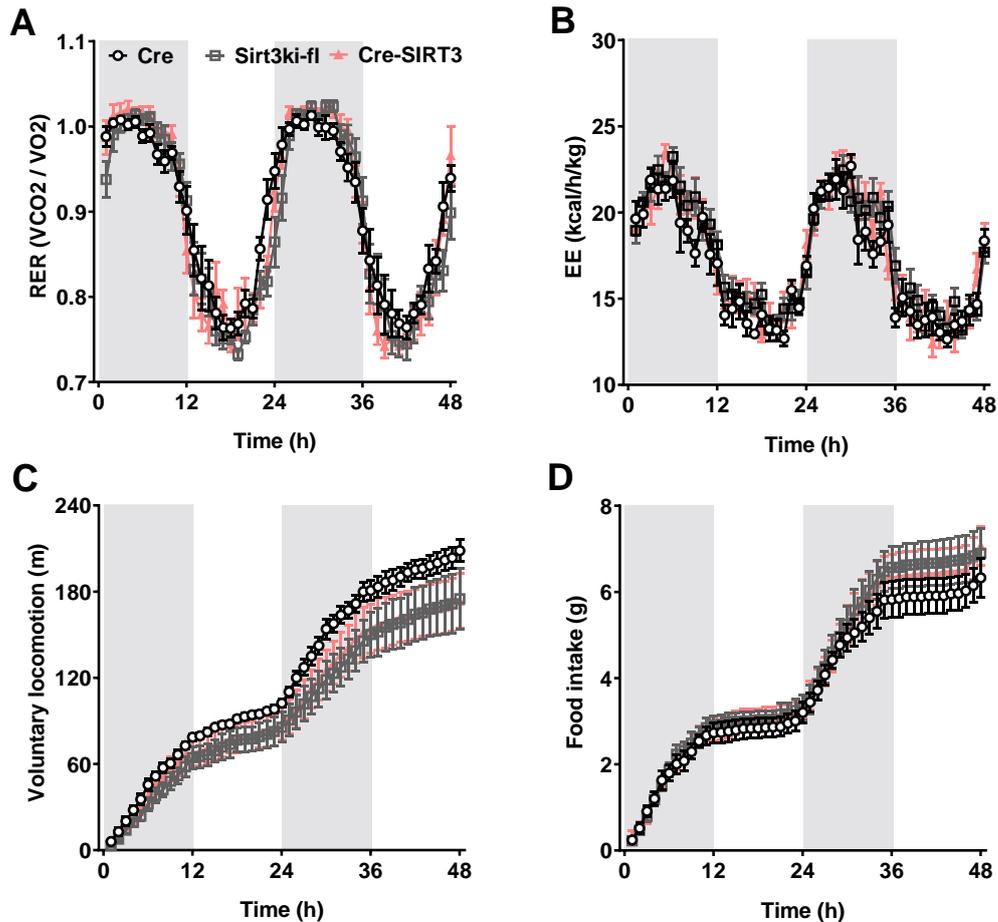


Figure 5: The metabolic profile of SIRT3ki animals and control animals (Cre mice and FIKi mice) on CD measured 5 weeks after TAM injection was similar.

A-D: Indirect calorimetry data (Sable System) of SIRT3ki animals compared to Cre and FIKi animals 5 weeks after TAM injection ($n = 6-7$). The white and grey background areas represent the light or dark phases, respectively. **(A)** Respiratory exchange ratio (RER) as mean values of 1 h bins; 2-way ANOVA, genotype ns, time $p < 0.0001$, genotype \times time $p < 0.05$. **(B)** Energy expenditure (EE) as mean values of 1 h bins; 2-way ANOVA, genotype ns, time $p < 0.0001$, genotype \times time ns. **(C)** Cumulative locomotor activity of 1 h bins; 2-way ANOVA, genotype ns, time $p < 0.0001$, genotype \times time $p < 0.05$. **(D)** Cumulative food intake of 1 h bins; 2-way ANOVA, genotype ns, time $p < 0.0001$, genotype \times time ns. Data are presented as means \pm SEM; ns = not significant.

No change in body composition was observed between SIRT3ki and control animals (Cre mice and FIKi mice) when fed CD

An Echo MRI performed after 14 weeks of CD feeding before TAM injection showed no difference in body composition among all three genotypes (Cre, FIKi and SIRT3ki

mice) at baseline (Figure 6A). The delta MRI data, which represent the difference between body composition data measured at baseline and 6 weeks after the last TAM injection, also revealed no differences among the genotypes (Figure 6B). Further, body weight gain at 3 or 6 weeks after TAM injection as well as food intake measured in the 7th week after TAM injection showed no differences among genotypes (Figure 6C and D, respectively).

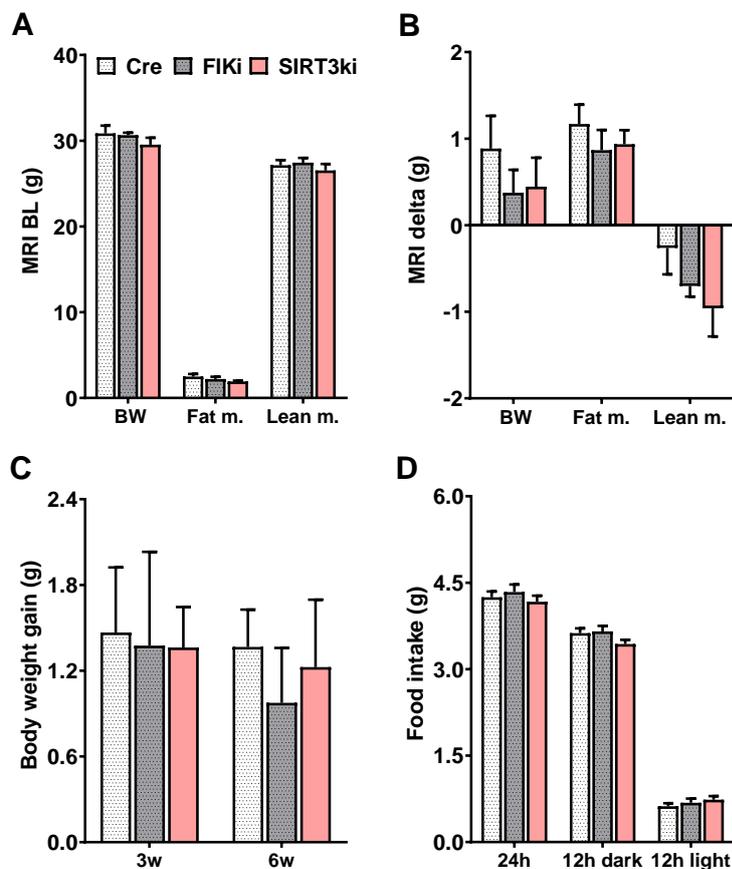


Figure 6: The body composition of SIRT3ki animals and control animals (Cre mice and FIKi mice) on CD measured 6 weeks after TAM injection was similar.

(A-B) Body composition assessed by a mouse Echo MRI ($n = 4-8$). **(A)** Baseline MRI performed after 14 weeks on CD, before TAM injection; One-way ANOVA BW, all ns; One-way ANOVA Fat mass, all ns; One-way ANOVA Lean mass, all ns. **(B)** Delta MRI = MRI performed 6 weeks after TAM injection minus baseline MRI data; One-way ANOVA BW, all ns; One-way ANOVA Fat mass, all ns; One-way ANOVA Lean mass, all ns. **(C)** Body weight gain 3 and 6 weeks after the last TAM injection ($n = 4-8$); 2-way ANOVA, genotype ns, time ns, genotype x time ns; One-way ANOVA 3 w, all ns, One-way ANOVA 6 w, all ns. **(D)** Manually collected food intake data in the 7th week after the last TAM injection ($n = 4-8$); 2-way ANOVA,

genotype ns, time $p < 0.0001$, genotype x time $p < 0.05$. One-way ANOVA 24 h, all ns; One-way ANOVA 12 h dark, all ns; One-way ANOVA 12 h light, all ns. Data are presented as means \pm SEM; ns = not significant.

SIRT3 knock-in study on high-fat diet

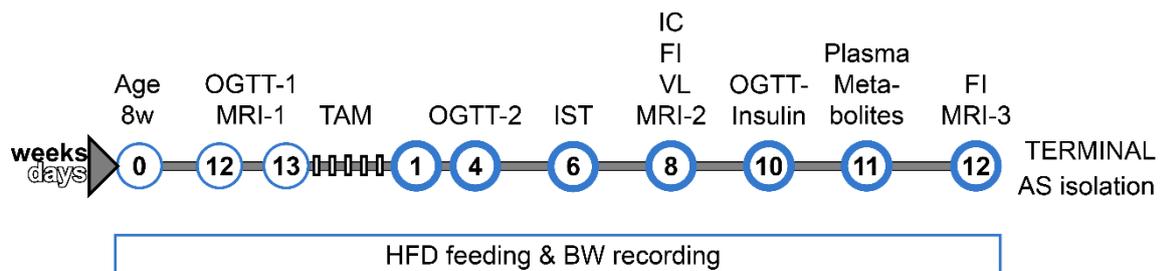


Figure 7: Experimental design of SIRT3ki on high-fat diet

Schematic timeline of the experiments. Measurements and tests: AS = astrocytes; BW = body weight; FI = food intake; HFD = high-fat diet; IC = indirect calorimetry; IST = insulin sensitivity test; MRI = magnetic resonance imaging; OGTT = oral glucose tolerance test; TAM = tamoxifen injections; VL = voluntary locomotion; w = weeks.

An improved glucose tolerance was observed in SIRT3ki compared to control animals (Cre mice and FIKi mice) when fed HFD

The study started as mice were switched from chow to HFD at the age of 8 weeks. After 12 weeks on HFD, we performed a first oral glucose tolerance test (OGTT-1) to examine the glucose response of all three genotypes Cre, FIKi, and SIRT3ki before TAM injections, i.e., prior to the induction of astrocyte SIRT3 overexpression in SIRT3ki animals (Figure 8A). Four weeks after the last TAM injection, we performed the OGTT-2 and found a better glucose tolerance ($p < 0.05$, at 30 min after glucose bolus) in SIRT3ki mice than in Cre and FIKi control mice (Figure 8B). The IST at 6 weeks after the last TAM injection revealed a more pronounced glucose response to insulin at 15, 60 and 90 min after injection in SIRT3ki animals than in Cre and FIKi control mice (Figure 8C). The OGTT-3 at 10 weeks after the last TAM injection, in which we also

measured insulin at baseline and 15 and 120 min after the glucose bolus, showed a greater insulin release ($p < 0.05$ at 15 min) in SIRTki animals than in Cre control mice (Figure 8D).

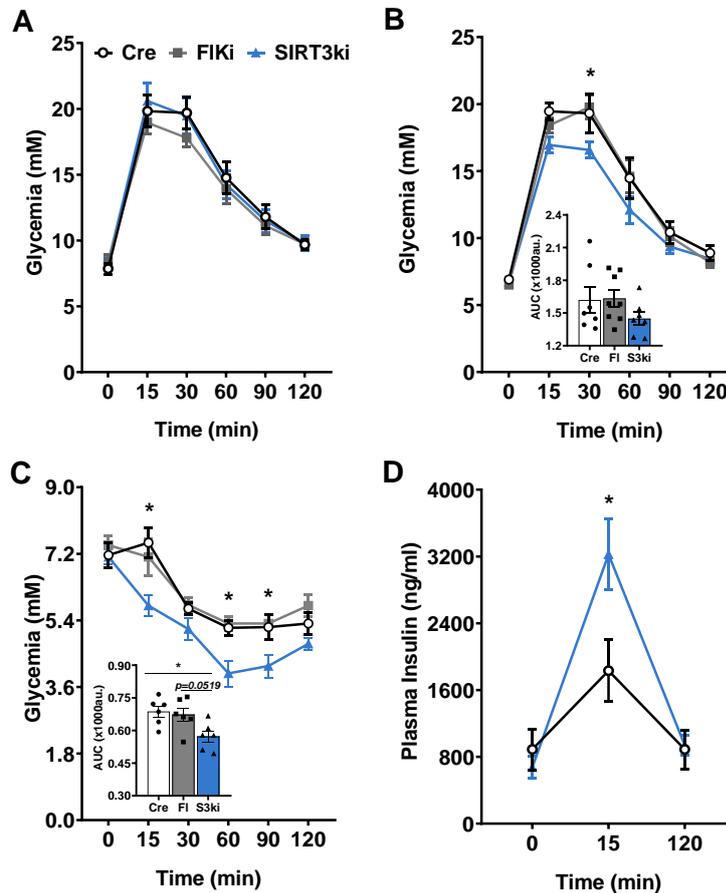


Figure 8: An improved glucose homeostasis was observed in SIRT3ki mice compared to control animals (Cre and FIKi mice) on HFD.

A-B: Oral glucose tolerance tests (OGTT) ($n = 6-8$). **(A)** OGTT-1: Tail blood glucose values measured at the time points indicated after an oral bolus of glucose (2 g/kg/BW) after 12 weeks on HFD and before TAM injection; 2-way ANOVA, genotype ns, time $p < 0.0001$, genotype x time ns. **(B)** OGTT-2: Tail blood glucose values measured at the time points indicated after an oral bolus of glucose (2 g/kg/BW) after 18 weeks on HFD or 4 weeks after the last TAM injection; 2-way ANOVA, genotype ns, time $p < 0.0001$, genotype x time ns, followed by Tukey's multiple comparison test at 30 min, Cre vs. FIKi ns, Cre vs. SIRT3ki $p < 0.05$, FIKi vs. SIRT3ki $p < 0.05$. Area under the curve (AUC) one-way ANOVA, all ns. **(C)** Insulin sensitivity test (IST), tail blood glucose values measured at the time points indicated after an intraperitoneal injection of insulin (0.6 mU/g body weight) after 20 weeks on HFD (6 weeks after the last TAM injection) ($n = 6$); 2-way ANOVA, genotype $p < 0.0001$, time $p < 0.0001$, genotype x time ns, followed by Tukey's multiple comparison test at 15, 60 and 90 min, Cre

vs. FIKi ns, Cre vs. SIRT3ki $p < 0.05$, FIKi vs. SIRT3ki $p < 0.05$. Area under the curve (AUC) with one-way ANOVA, Cre vs. FIKi ns, Cre vs. SIRT3ki $p = 0.0519$, FIKi vs. SIRT3ki $p < 0.05$. **(D)** OGTT-3 performed as in A or B after 24 weeks on HFD (10 weeks after the last TAM injection), tail vein blood plasma was collected at the time points indicated and plasma insulin measured ($n = 6-7$); Multiple t-test, at 0 min ns, at 15 min $p < 0.05$, at 120 min ns. Data are presented as means \pm SEM; ns = not significant; * = $p < 0.05$.

Overall differences in the metabolic profile were observed between SIRT3ki and control animals (Cre mice) when fed HFD

Indirect calorimetry was performed 8 weeks after the last TAM injection. Data of 48 h recording revealed no significant differences, but a trend towards a higher RER of SIRT3ki compared to Cre control mice (Figure 9A). On the other hand, SIRTki mice displayed a significantly lower EE than Cre control mice during the dark phase, but not during the light phase (Figure 9B-C). Further, SIRT3ki mice showed significantly lower cumulative voluntary locomotor activity than Cre control mice (Figure 9D, F). Finally, SIRT3ki animals displayed a lower cumulative food intake compared to Cre control mice (Figure 9E, F).

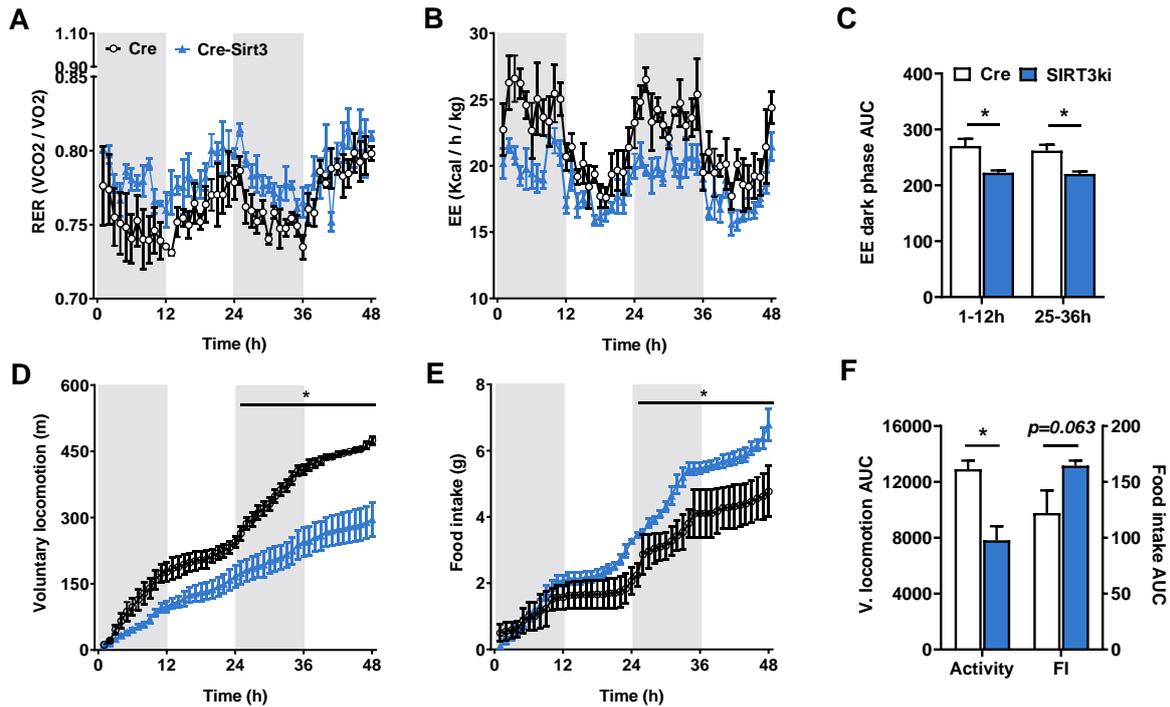


Figure 9: Overall differences in the metabolic profile of SIRT3ki and cre control mice were observed on HFD measured 8 weeks after TAM injection

A-D: Indirect calorimetry data (Sable System) of SIRT3ki mice compared to Cre control mice 8 weeks after TAM injection (on HFD for 22 weeks) ($n = 3-4$). The white and grey background areas represent the light or dark phases, respectively. **(A)** Respiratory exchange ratio (RER) as mean values of 1 h bins; 2-way ANOVA, genotype $p < 0.05$, time $p < 0.0001$, genotype \times time ns. **(B)** Energy expenditure (EE) as mean values of 1 h bins; 2-way ANOVA, genotype $p < 0.05$, time $p < 0.0001$, genotype \times time $p < 0.05$. **(C)** EE Area under the curve (AUC) with Student's t-test for the first and second dark phase, respectively $p < 0.05$, $p < 0.05$. **(D)** Cumulative voluntary locomotor activity of 1 h bins; 2-way ANOVA, genotype $p < 0.05$, time $p < 0.0001$, genotype \times time $p < 0.05$, followed by Sidak's multiple comparison test for 27- 48 h, Cre vs. SIRT3ki $p < 0.05$. Multiple t-test for 25-48 h, $p < 0.05$. **(E)** Cumulative food intake of 1 h bins; 2-way ANOVA, genotype ns, time $p < 0.0001$, genotype \times time $p < 0.05$, followed by Sidak's multiple comparison test for 33-34 h and 45- 48 h, Cre vs. SIRT3ki $p < 0.05$. Multiple t-test for 32-48 h, $p < 0.05$. **(F)** Cumulative voluntary locomotor activity of 1 h bins (= activity), area under the curve (AUC) with Student's t-test, $p < 0.05$; Cumulative food intake of 1 h bins, Area under the curve (AUC) with Student's t-test, $p = 0.063$. Data are presented as means \pm SEM; ns = not significant; * = $p < 0.05$.

Similar levels of circulating pre- and postprandial metabolites were observed in SIRT3ki and Cre control mice when fed HFD

Tail vein blood samples collected 11 weeks after the last TAM injection following 11 h food deprivation during the light phase, one hour before dark phase onset (preprandial = baseline (BL)) and 4 h after dark phase onset (postprandial (PP)) showed no differences in the concentrations of plasma glucose, non-esterified fatty acids (NEFA), β -hydroxybutyrate (BHB), triacylglycerol (TAG) and cholesterol (Chol) between SIRT3ki and Cre control mice (Figure 10A-E).

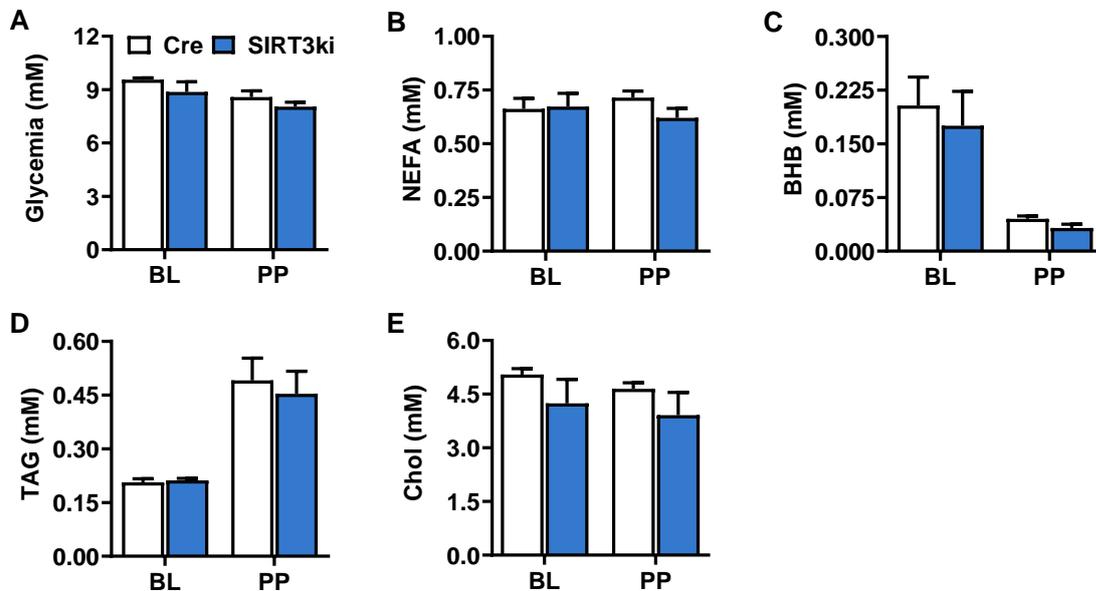


Figure 10: Similar baseline and postprandial blood plasma metabolite levels were measured in SIRT3ki mice and Cre control mice on HFD 11 weeks after TAM injection.

A-C: Tail vein blood plasma metabolite levels at baseline (BL= pre-prandial), obtained after an 11 h fast during the light phase, and postprandial (PP) metabolite levels obtained from tail vein blood plasma collected 4 h after dark-phase onset (25 weeks on HFD, 11 weeks after the last TAM injection) (n = 5-6). **(A)** Glucose; BL and PP Student's t-test ns and ns. **(B)** Non-esterified fatty acids (NEFA); BL and PP Student's t-test ns and ns. **(C)** β -hydroxybutyrate (BHB); BL and PP Student's t-test ns and ns. **(D)** Triglycerides (TAG); BL and PP Student t-test ns and ns. **(E)** Cholesterol (Chol); BL and PP Student's t-test ns and ns. Data are presented as means \pm SEM; ns = not significant.

Greater body weight gain and fat mass were observed in SIRT3ki mice compared to control animals (Cre and FIKi mice) when fed HFD

An Echo MRI performed after 12 weeks HFD feeding before TAM injection showed no difference in body composition among all three genotypes Cre, FIKi and SIRT3ki at baseline (Figure 11A). The delta MRI data, which represent the differences between body composition assessed at baseline and 12 weeks after the last TAM injection (after 26 weeks on HFD), revealed a greater body weight gain and fat mass of SIRT3ki mice compared to Cre and FIKi control mice (Figure 11B). Food intake, measured manually in Week 13 after the last TAM injection, did not differ among genotypes (Figure 11D).

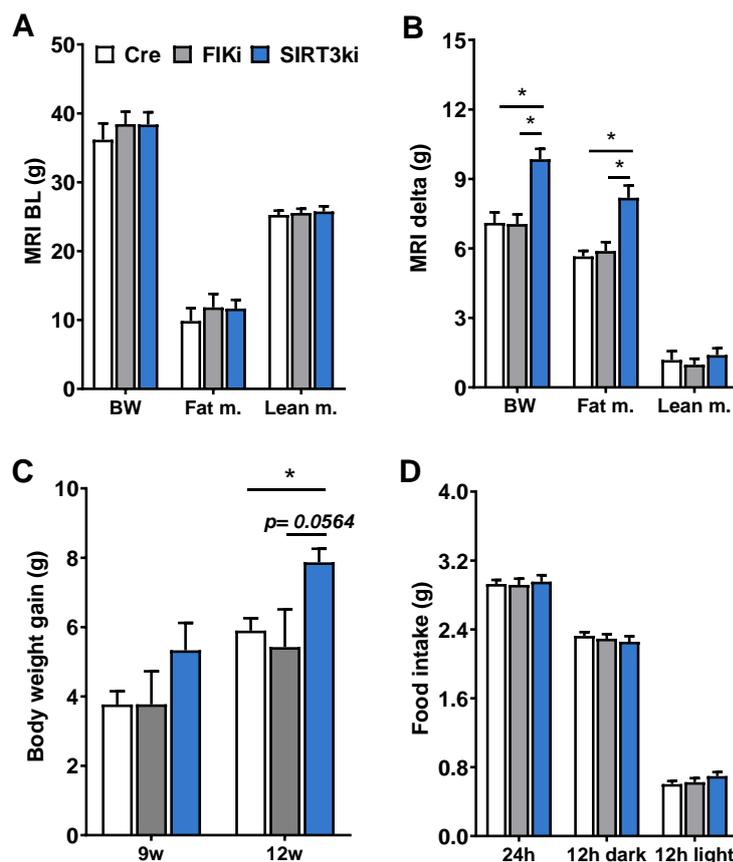


Figure 11: Greater body weight gain and fat mass of SIRT3ki animals compared to control animals (Cre and FIKi mice) were observed on HFD measured 12 weeks after TAM injection.

A-B: Body composition assessed by a mouse Echo MRI (n = 4-7). **(A)** Baseline MRI performed after 12 weeks on HFD, before TAM injection; One-way ANOVA BW, all ns; One-way ANOVA

Fat mass, all ns; One-way ANOVA Lean mass, all ns. **(B)** Delta MRI= MRI performed 12 weeks after TAM injection (total 26 weeks on HFD) minus baseline MRI data; One-way ANOVA BW Cre vs. FIKi ns, Cre vs. SIRT3ki $p < 0.05$, FIKi vs. SIRT3ki $p < 0.05$; One-way ANOVA Fat mass Cre vs. FIKi ns, Cre vs. SIRT3ki $p < 0.05$, FIKi vs. SIRT3ki $p < 0.05$; One-way ANOVA Lean mass, all ns. **(C)** Body weight gain 9 and 12 weeks after the last TAM injection (total 23 or 26 weeks on HFD, respectively) ($n = 4-7$); 2-way ANOVA, genotype ns, time $p < 0.0001$, genotype x time ns, followed by Tukey's multiple comparison test at 9 w, all ns, at 12 w: Cre vs. FIKi ns, Cre vs. SIRT3ki $p = 0.0564$, FIKi vs. SIRT3ki $p < 0.05$. One-way ANOVA 9 w, all ns; One-way ANOVA 12 w, Cre vs. FIKi ns, Cre vs. SIRT3ki $p < 0.05$, FIKi vs. SIRT3ki $p < 0.05$. **(D)** Manually collected food intake data in the 13th week after the last TAM injection (total 27 weeks on HFD) ($n = 4-7$); 2-way ANOVA, genotype ns, time $p < 0.0001$, genotype x time ns. One-way ANOVA 24 h, all ns; One-way ANOVA 12 h dark, all ns; One-way ANOVA 12 h light, all ns. Data are presented as means \pm SEM; ns = not significant; * = $p < 0.05$.

The astrocyte-specific knock-in of SIRT3 in SIRT3ki animals was successful as assessed at the mRNA level.

Twelve weeks after the last TAM injection the primary isolated astrocyte fraction from SIRTki and FIKi animals on HFD showed a similar purity profile for all samples (FIKi and SIRT3ki), which was in line with the profile observed in the validation of the isolation method, except for a greater oligodendrocyte contamination (Figure 12A and Figure 1, respectively). Although an increased SIRT3 expression in primary isolated astrocytes of SIRTki mice compared to the control FIKi mice was not detected at the mRNA level, a greater mRNA expression was found for the SIRT3flag gene in SIRT3ki mice (Figure 12B).

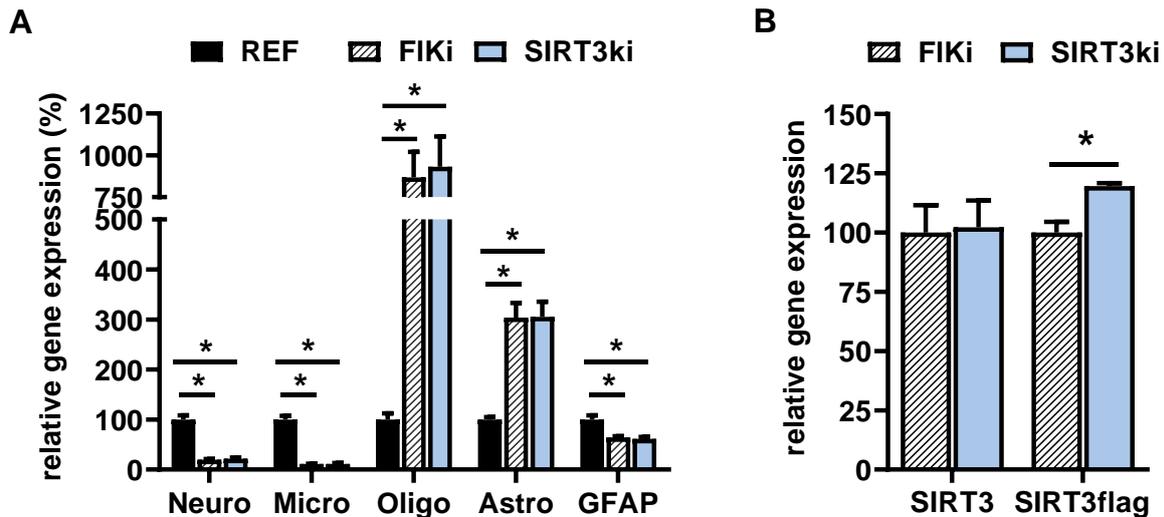


Figure 12: Astrocyte-specific knockin of SIRT3 in SIRT3ki animals was successful as assessed at the mRNA level. Astrocyte isolation efficiency was equal for SIRT3ki or control animals.

(A) Relative mRNA expression of a specific neuronal (Neuro, Syt1: Synaptogamin-1), microglial (Micro, Aif1: Allograft Inflammatory Factor 1), oligodendrocyte (Oligo, Gjc2: gap junctional intercellular communication 2) and astrocyte (Astro, Vim: Vimentin and Gfap: Glial Fibrillary Acidic Protein) genes in the fraction of primary isolated astrocytes (AS) of SIRT3ki ($n = 4$) and FIKi ($n = 4$) animals relative to whole brain lysate (REF) from a wild type mouse ($n = 1$, SEM corresponds to technical triplicates). All animals fed HFD, all animals at age of 32 weeks, 24 weeks on HFD and 12 weeks after TAM injection (normalized to GAPDH). Student t-test of FIKi vs. REF and SIRT3ki vs. REF, for all $p < 0.05$. **(B)** Relative mRNA expression of SIRT3 and SIRT3flag in the fraction of primary isolated astrocytes (AS) of SIRT3ki ($n = 4$) and FIKi ($n = 4$) animals (normalized to GAPDH), Student t-test ns, $p < 0.05$ respectively. Results are presented as means \pm SEM; ns = not significant; * = $p < 0.05$.

SIRT3 knock-out study on control diet

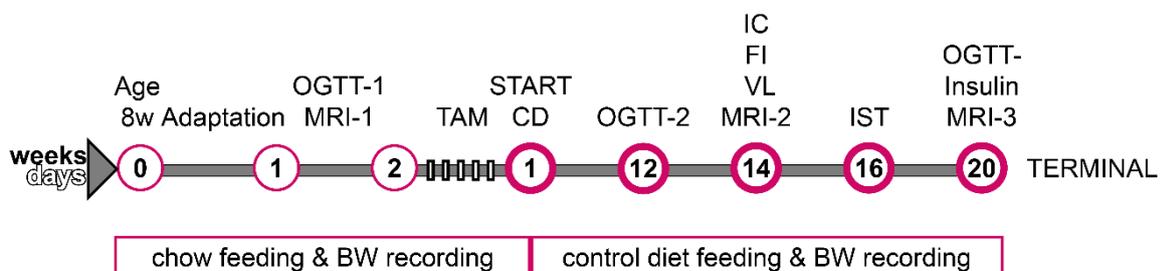


Figure 13: Experimental design of SIRT3ko on control diet

Schematic timeline of the experiments. Measurements and tests: BW = body weight; CD = control diet; FI = food intake; IC = indirect calorimetry; IST = insulin sensitivity test; MRI = magnetic resonance imaging; OGTT = oral glucose tolerance test; TAM = tamoxifen; VL = voluntary locomotion; w = weeks.

An improved glucose tolerance was observed in SIRT3ko compared to control animals (Cre and Flko mice) when fed CD

To examine the glucose tolerance of all genotypes, we performed a first OGTT with approximately 9-10 weeks old mice on chow diet prior to the TAM injections. This OGTT-1 revealed a similar glucose tolerance of all genotypes (Figure 14A). The second OGTT (OGTT-2), performed 12 weeks after the switch to CD, equivalent to 12 weeks after the last TAM injection, revealed a significantly faster glucose uptake in SIRT3ko mice than in control mice at 15 and 30 min after the glucose bolus (Figure 14B). The IST performed 16 weeks after the last TAM injection revealed no difference in the glucose response to insulin between SIRT3ki and control mice (Figure 14C). The OGTT-3 performed 20 weeks after the last TAM injection, in which we also measured insulin at baseline and 15 and 120 min after the glucose bolus, did not reveal any differences in the glucose response to insulin among the three genotypes (Figure 14D).

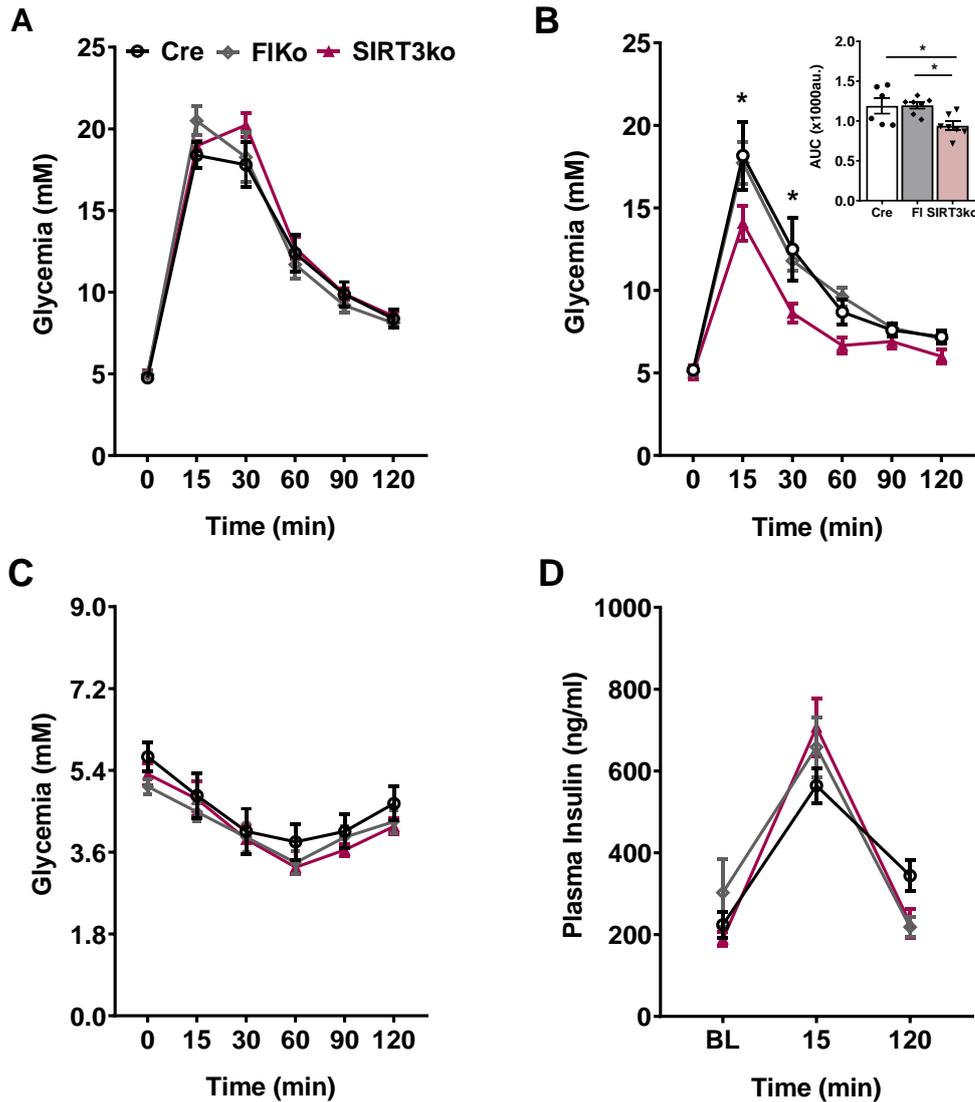


Figure 14: An improved glucose tolerance of SIRT3ko compared to control animals (Cre and FIKo mice) was observed on CD

A-B: Oral glucose tolerance tests (OGTT) (n=6-8). **(A)** OGTT-1: Tail blood glucose values measured at the time points indicated after an oral bolus of glucose (2 g/kg/BW), animals on chow, before TAM injection; 2-way ANOVA, genotype ns, time $p < 0.0001$, genotype x time ns. **(B)** OGTT-2: Tail blood glucose values measured at the time points indicated after an oral bolus of glucose (2 g/kg/BW) after 12 weeks on CD or 12 weeks after the last TAM injection; 2-way ANOVA, genotype $p < 0.05$, time $p < 0.0001$, genotype x time ns, followed by Tukey's multiple comparison test at 15 and 30 min, Cre vs. FIKi ns, Cre vs. SIRT3ki $p < 0.05$, FIKi vs. SIRT3ki $p < 0.05$. Area under the curve (AUC) one-way ANOVA, Cre vs. FIKi ns, Cre vs. SIRT3ki $p < 0.05$, FIKi vs. SIRT3ki $p < 0.05$. **(C)** Insulin sensitivity test (IST), tail blood glucose values measured at the time points indicated after an intraperitoneal injection of insulin (0.3 mU/g body weight) after 16 weeks on CD or 16 weeks after the last TAM injection (n = 6-8); 2-way ANOVA, genotype ns, time $p < 0.0001$, genotype x time ns. **(D)** OGTT-3 performed as in A or B 20 weeks on CD or 20 weeks after TAM injection, tail vein blood plasma was collected at the time points indicated and plasma insulin measured (n = 6-7); Multiple t-test, at

0 min ns, at 15 min ns, at 120 min ns. Data are presented as means \pm SEM; ns = not significant* = $p < 0.05$.

A similar metabolic profile was observed in SIRT3ko and control animals (Cre and FIKo mice) when fed CD

Indirect calorimetry was performed 14 weeks after the last TAM injection, equivalent to 14 weeks after the switch to CD. The data revealed no genotype differences in RER (Figure 15A), EE (Figure 15B), cumulative voluntary locomotor activity or cumulative food intake (Figure 15C and D, respectively).

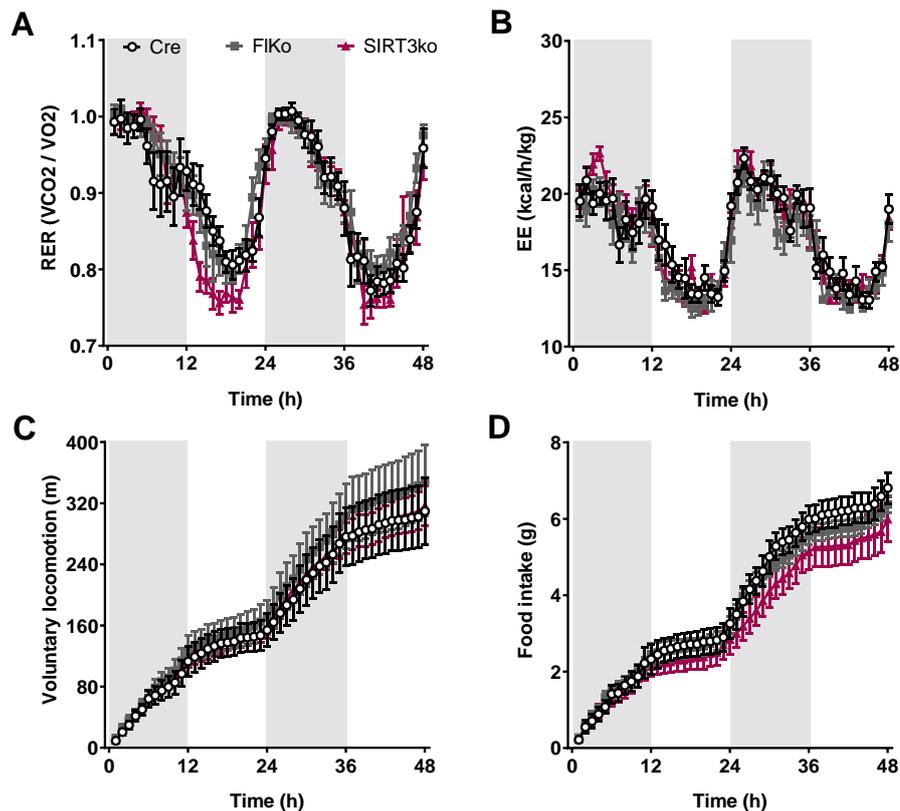


Figure 15: The metabolic profile of SIRT3ko animals and control animals (Cre and FIKo mice) on CD measured 14 weeks after TAM injection was similar.

A-D: Indirect calorimetry data (Sable System) of SIRT3ko animals compared to Cre and FIKo animals 14 weeks after TAM injection and switch to CD ($n = 7-8$). The white and grey background areas represent the light or dark phases, respectively.

(A) Respiratory exchange ratio (RER) as mean values of 1 h bins; 2-way ANOVA, genotype ns, time $p < 0.0001$, genotype \times time ns. **(B)** Energy expenditure (EE) as mean values of 1 h bins, 2-way ANOVA, genotype ns, time $p < 0.0001$, genotype \times time ns. **(C)** Cumulative

locomotor activity of 1 h bins; 2-way ANOVA, genotype ns, time $p < 0.0001$, genotype x time ns. **(D)** Cumulative food intake of 1 h bins; 2-way ANOVA, genotype ns, time $p < 0.0001$, genotype x time $p < 0.05$. Data are presented as means \pm SEM; ns = not significant.

No differences in body composition were observed between SIRT3ko and control animals (Cre and FIKo mice) when fed CD

An Echo MRI performed after 20 weeks CD feeding before TAM injection showed no differences in body composition among all three genotypes Cre, FIKi and SIRT3ko at baseline (Figure 16A). The delta MRI data, which represent the difference between body composition data measured at baseline and 20 weeks after the last TAM injection revealed no difference among all genotypes (Figure 16B). Body weight gain at 12, 16 and 20 weeks after TAM injection also showed no differences among genotypes (Figure 16C).

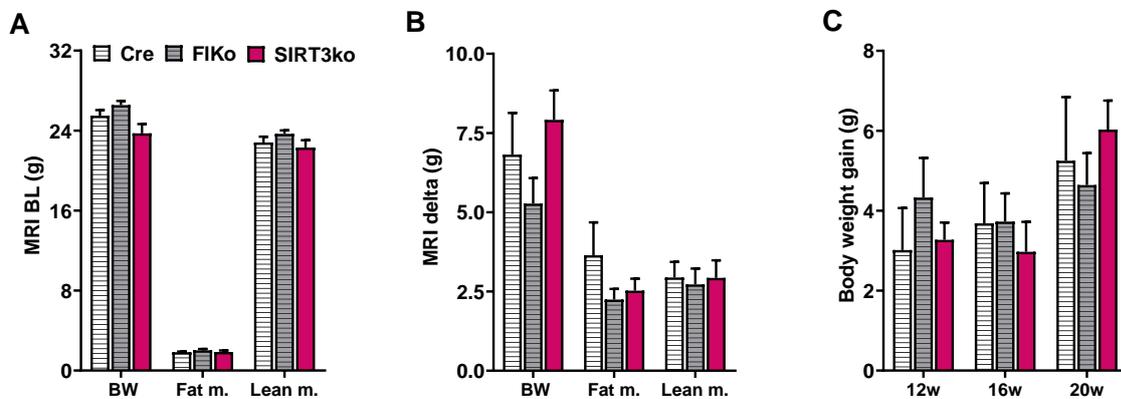


Figure 16: Body composition of SIRT3ko animals on CD measured 20 weeks after TAM injection did not differ from that of control animals (Cre and FIKo mice).

(A-B) Body composition assessed by a mouse Echo MRI ($n = 6-8$). **(A)** Baseline MRI performed before TAM injection, animals on chow, One-way ANOVA, BW all ns; One-way ANOVA Fat mass, all ns; One-way ANOVA Lean mass, all ns. **(B)** Delta MRI= MRI performed 20 weeks after TAM injection and switch to CD minus baseline MRI data; One-way ANOVA BW, all ns; One-way ANOVA Fat mass, all ns; One-way ANOVA Lean mass, all ns. **(C)** Body weight gain 12, 16 and 20 weeks after the last TAM injection or switch to CD ($n = 6-8$); 2-way ANOVA, genotype ns, time $p < 0.0001$, genotype x time $p < 0.05$. One-way ANOVA 12 w, all

ns; One-way ANOVA 16 w, all ns; One-way ANOVA 20 w, all ns. Data are presented as means \pm SEM; ns = not significant.

SIRT3 knock-out study on high-fat diet

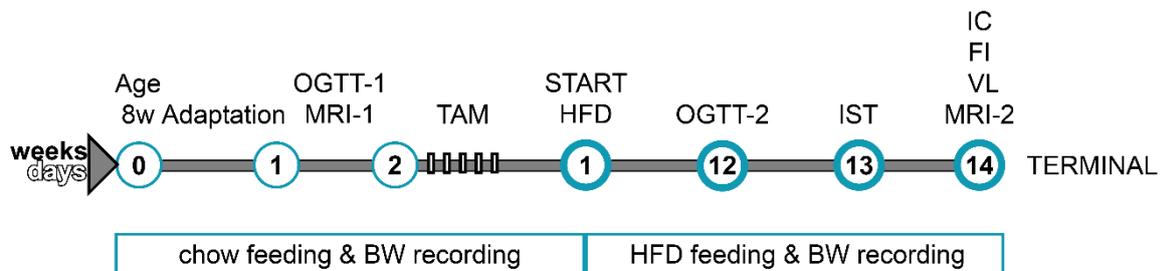


Figure 17: Experimental design of SIRT3ko on high-fat diet

Schematic timeline of the experiment. Measurements and tests: BW = body weight; FI = food intake; HFD = high-fat diet; IC = indirect calorimetry; IST = insulin sensitivity test; MRI = magnetic resonance imaging; OGTT = oral glucose tolerance test; TAM = tamoxifen; VL = voluntary locomotion; w = weeks.

No difference in glucose tolerance was observed between SIRT3ko and control animals (Cre and FIKo mice) when fed HFD

To examine the glucose tolerance of all genotypes before TAM injection, we performed a first OGTT (OGTT-1) with approximately 9-10 weeks old animals on chow diet just prior the start of TAM injections. All animals showed similar glucose tolerance (Figure 17A). A follow-up OGTT-2 was performed 12 weeks after TAM injection or switch to HFD and revealed no difference in glucose tolerance among all genotypes either (Figure 17B). One week later, 13 weeks after TAM injection, an IST showed similar glucose responses to the insulin injection in SIRT3ko animals and control animals (Figure 17C).

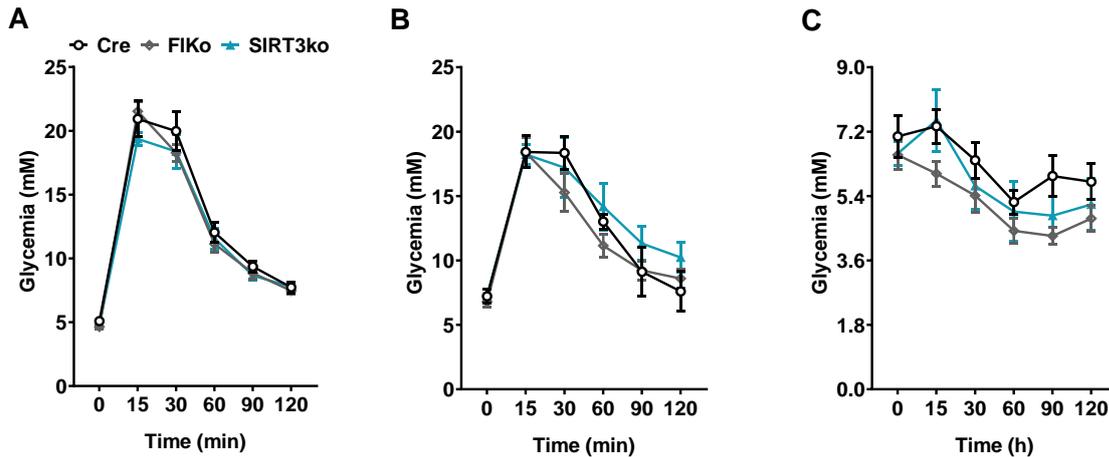


Figure 17: Glucose tolerance of SIRT3ko animals on HFD remained unaffected.

A-B: Oral glucose tolerance tests (OGTT) (n = 6-7).

(A) OGTT-1: Tail blood glucose values measured at the time points indicated after an oral bolus of glucose (2 g/kg/BW) before TAM injection, animals on chow; 2-way ANOVA, genotype ns, time $p < 0.0001$, genotype x time ns. **(B)** OGTT-2: Tail blood glucose values measured at the time points indicated after an oral bolus of glucose (2 g/kg/BW) after 12 weeks on HFD or 12 weeks after the last TAM injection; 2-way ANOVA, genotype ns, time $p < 0.0001$, genotype x time ns. **(C)** Insulin sensitivity test (IST), tail blood glucose values measured at the time points indicated after an intraperitoneal injection of insulin (0.6 mU/g body weight) after 13 weeks on HFD or 13 weeks after the last TAM injection (n = 6-7); 2-way ANOVA, genotype ns, time $p < 0.0001$, genotype x time ns. Data are presented as means \pm SEM; ns = not significant.

No differences in the metabolic profiles were observed between SIRT3ko and control animals (Cre and FIKo mice) when fed HFD

Fourteen weeks after TAM treatment or switch to HFD 48 h indirect calorimetry was performed. The data showed no differences among the genotypes in RER (Figure 18A), EE (Figure 18B), cumulative voluntary locomotor activity or cumulative food intake (Figure 18C and D, respectively).

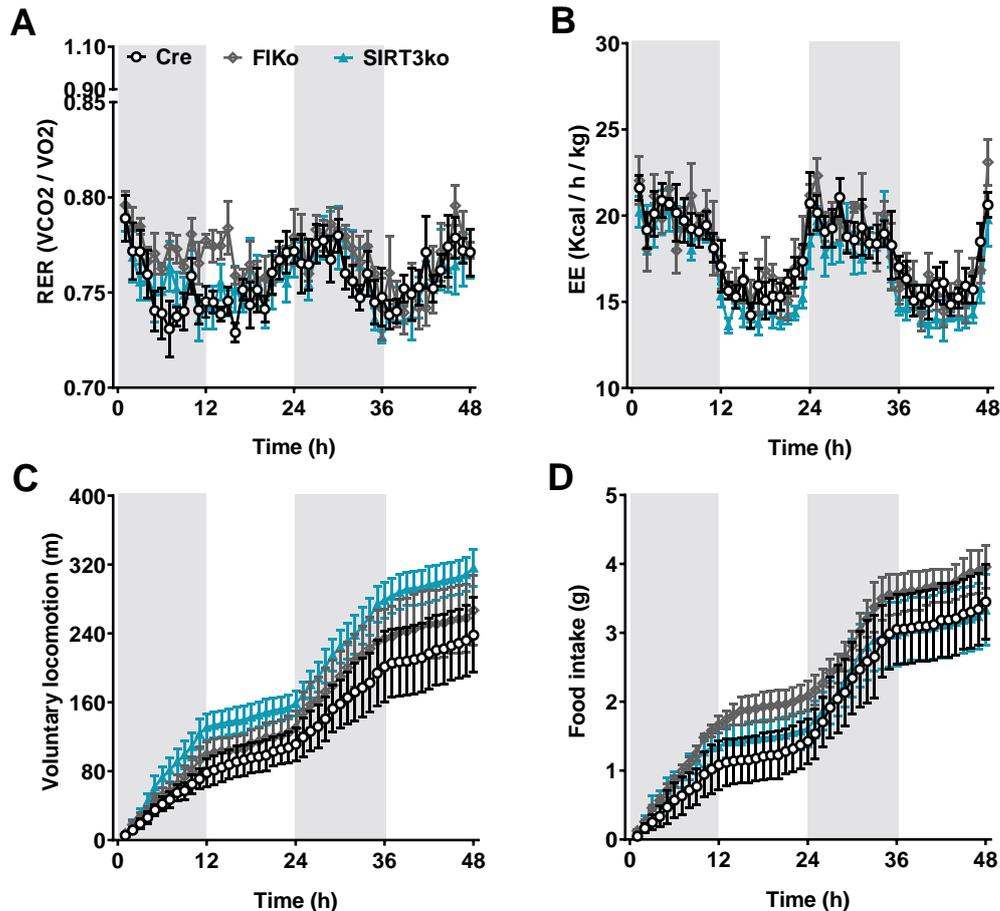


Figure 18: The metabolic profile of SIRT3ko animals and control animals (Cre and FIKo mice) on HFD measured 14 weeks after TAM injection did not differ.

A-D: Indirect calorimetry data (Sable System) of SIRT3ko animals compared to Cre and FIKo animals 14 weeks after TAM injection or switch to HFD ($n = 4-5$). The white and grey background areas represent the light or dark phases, respectively.

(A) Respiratory exchange ratio (RER) as mean values of 1 h bins; 2-way ANOVA, genotype ns, time $p < 0.0001$, genotype x time ns. **(B)** Energy expenditure (EE) as mean values of 1 h bins, 2-way ANOVA, genotype ns, time $p < 0.0001$, genotype x time ns. **(C)** Cumulative locomotor activity of 1 h bins ($n = 4-5$); 2-way ANOVA, genotype ns, time $p < 0.0001$, genotype x time ns. **(D)** Cumulative food intake of 1 h bins ($n = 4-5$); 2-way ANOVA, genotype ns, time $p < 0.0001$, genotype x time ns. Data are presented as means \pm SEM; ns = not significant.

No differences in body composition were observed between SIRT3ko and control animals (Cre and FIKo mice) when fed HFD

Body composition measured at baseline with an echo MRI when the animals were on chow and before TAM injection revealed no differences among all three genotypes

(Cre, FIKo, and SIRT3ko) (Figure 19A). The delta MRI data, which represents the difference between body composition data at baseline and 14 weeks after TAM injection or switch to HFD, revealed no differences among all genotypes (Figure 19B). Also, body weight gain at 4, 8 and 12 weeks after TAM injection showed no differences among genotypes (Figure 19C).

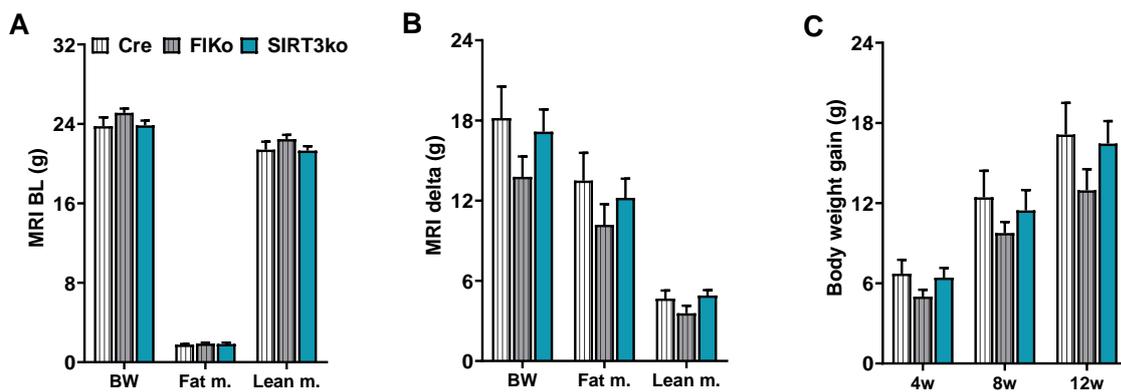


Figure 19: Body composition of SIRT3ko animals and control animals (Cre and FIKo mice) on HFD measured 14 weeks after TAM injection was similar.

(A-B): Body composition assessed by a mouse Echo MRI ($n = 6-8$). **(A)** Baseline MRI performed before TAM injection, animals on chow; One-way ANOVA BW, all ns; One-way ANOVA Fat mass, all ns; One-way ANOVA Lean mass, all ns. **(B)** Delta MRI = MRI performed 14 weeks after TAM injection or switch to HFD minus baseline MRI data; One-way ANOVA BW, all ns; One-way ANOVA Fat mass, all ns; One-way ANOVA Lean mass, all ns. **(C)** Body weight gain 4, 8 and 12 weeks after the last TAM injection or switch to HFD ($n = 6-8$); 2-way ANOVA, genotype ns, time $p < 0.0001$, genotype x time ns. One-way ANOVA 4 w, all ns; One-way ANOVA 8 w, all ns; One-way ANOVA 12 w, all ns. Data are presented as means \pm SEM; ns = not significant.

The astrocyte-specific knock-out of SIRT3 in SIRT3ko animals failed as assessed at the mRNA level

Primary isolated astrocyte fraction from SIRTko, Cre and FIKo animals on chow diet, 12 weeks after TAM injection, revealed an equal purity profile for all samples (CR and SIRT3ko) and was in line with the profile observed during validation of the isolation method (Figure 20A and Figure 1, respectively). A decreased SIRT3 expression in

primary isolated astrocytes of SIRT3ko animals compared to control animals could not be confirmed at the mRNA level (Figure 20B).

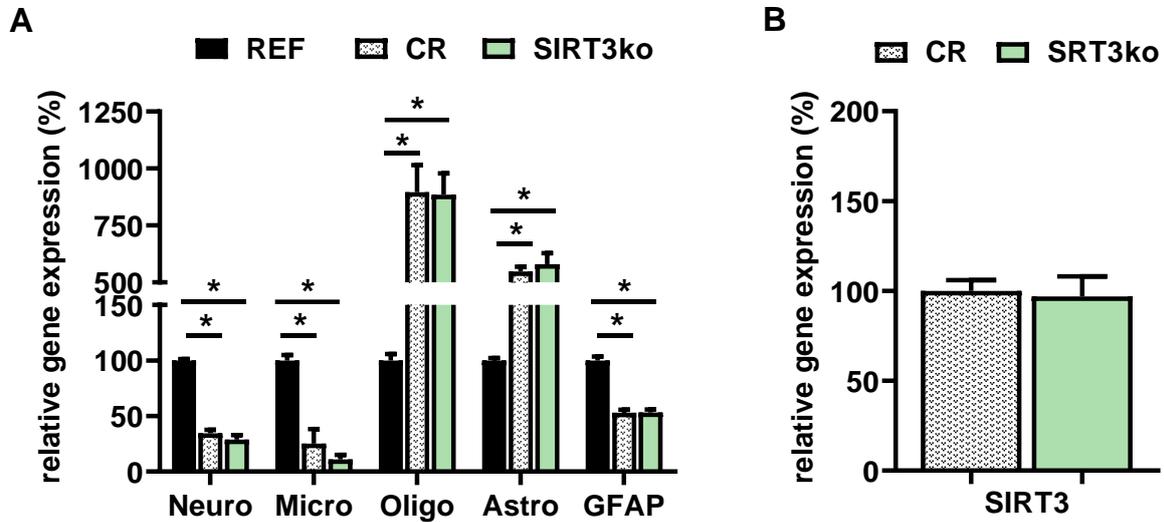


Figure 20: Astrocyte-specific knockdown of SIRT3 in SIRT3ko animals failed as assessed at the mRNA level. Astrocyte isolation efficiency was equal for SIRT3ko and control animals.

(A) Relative mRNA expression of a specific neuronal (Neuro, *Syt1*: Synaptogamin-1), microglial (Micro, *Aif1*: Allograft Inflammatory Factor 1), oligodendrocyte (Oligo, *Gjic2*: gap junctional intercellular communication 2) and astrocyte (Astro, *Vim*: Vimentin and *Gfap*: Glial Fibrillary Acidic Protein) gene in the fraction of primary isolated astrocytes (AS) of SIRT3ko ($n = 4$) and pooled control (CR, Cre ($n = 2$) and FIKo ($n = 2$)) animals relative to whole brain lysate (REF) from a wild type mouse ($n=1$; SEM corresponds to technical triplicates). All animals fed chow, all animals at age of 20 weeks and 12 weeks after TAM injection (normalized to GAPDH). Student t-test of CR vs. REF and SIRT3ko vs. REF, for all $p < 0.05$. **(B)** Relative mRNA expression of SIRT3 in the fraction of primary isolated astrocytes (AS) of SIRT3ko ($n=4$) and pooled control (CR, Cre ($n=2$) and FIKo ($n=2$)) animals (normalized to GAPDH), Student t-test ns. Results are presented as means \pm SEM; ns = not significant; * = $p < 0.05$.

Discussion

Astrocytes, the most abundant glia cells, are literally the rising stars in governing not only brain, but also whole body energy homeostasis (1). Yet, little is known to which extent the response of astrocyte metabolism to nutrient availability affects metabolic signaling within the brain and beyond. Sirtuin-3 (SIRT3), a key regulatory enzyme of mitochondrial metabolism, modulates mitochondrial responses to nutrient availability (26). In this study, we attempted to challenge astrocyte metabolism by overexpressing or downregulating SIRT3 in mice fed a low-fat control diet (CD) or a high-fat diet (HFD) and we phenotyped these transgenic mice with respect to several metabolic parameters. We found that the inducible astrocyte-specific SIRT3 knock-out (SIRT3ko) had no significant effect on whole-body energy homeostasis neither under low-fat CD, nor under HFD feeding conditions. This was also true for mice with an astrocyte-specific SIRT3 overexpression (SIRT3ki) on the low-fat diet, but introduction of SIRT3 overexpression in mice fed HFD provoked changes in energy homeostasis.

Tamoxifen-induced astrocyte-specific overexpression of SIRT3 in adult mice in a physiologically healthy state on the regular CD did not elicit changes in metabolic parameters measured up to 6 weeks after tamoxifen injection. Neither glucose homeostasis, body composition, plasma metabolites (fasted and fed states), energy expenditure and food intake, nor activity differed among the genotypes. SIRT3ki animals showed the same phenotype as the control animals, indicating that with low-fat feeding SIRT3 overexpression in astrocytes has no effect on whole-body energy homeostasis. The complex metabolism of astrocytes and the redundant functions of SIRT3 targets in metabolic regulation leave room for many speculations about the reason for the missing phenotype. First, to our knowledge, there are no studies so far reporting on beneficial or harmful effects on energy homeostasis of manipulated SIRT3

expression in any single tissue in a physiologically healthy state. Combined with our results, this argues for an inconspicuous role of SIRT3 in mitochondrial metabolism under normal conditions, independent of the cell type. Nevertheless, SIRT3 overexpression supposedly increases overall cellular energy turnover and consequently alters mitochondrial release of metabolites and molecules such as Ca^{2+} , ATP, NAD^+ , NADH and NO, which again regulate numerous signaling pathways (27). ATP, for instance, is released by astrocytes and functions as a gliotransmitter, thus actively regulating synaptic properties (28). It was therefore reasonable to speculate that SIRT3 overexpression might have an influence on astrocyte metabolism and signaling.

When adult mice were fed HFD for 12 weeks before astrocyte-specific overexpression of SIRT3 was induced, SIRT3^{ki} animals exhibited a distinct metabolic phenotype. Interestingly, SIRT3^{ki} animals displayed a higher respiratory exchange ratio (RER) and lower locomotor activity as well as energy expenditure (EE), but increased food intake (FI) compared to control animals. This suggests on one hand that SIRT3 overexpression can modify astrocyte metabolism and on the other hand that astrocyte metabolism can affect the overall central nervous system regulation of energy homeostasis. The findings also support the general idea that SIRT3 has a more prominent role in maintaining mitochondrial homeostasis after stress, in this case HFD exposure (29), than under normal conditions. Taken together, the observed phenotype reflects the picture of activated central anabolic neuronal circuits that stimulate eating, which may be related to an activation of agouti-related peptide (AgRP) and neuropeptide Y (NPY) and a simultaneous inhibition of pro-opiomelanocortin (POMC)/cocaine and amphetamine-regulated transcript (CART) neurons in the hypothalamic arcuate nucleus (ARC) (30). Further, SIRT3^{ki} animals displayed less

locomotor activity than control animals. Here, a possible explanation might be the inhibition of orexin-A and B neurons in the lateral hypothalamic area (LHA), which are known to promote locomotor activity (31). Melanin-concentrating hormone (MCH) could contribute as well, a neuropeptide also localized in the LHA and activated by anabolic signaling from the ARC, increases food intake and decreases locomotor activity (32, 33). A stimulation of the ARC in SIRT3ki mice might also be involved in the higher RER and enhanced fat storage of SIRT3ki mice compared to control animals. Cavalcanti-de-Albuquerque et al. (2016) showed that prolonged AgRP activation rapidly increased RER and carbohydrate utilization while decreasing fat utilization (34). This effect was coupled to metabolic shifts towards lipogenesis in well-fed animals.

We found SIRT3ki mice to be better able to regulate their blood glucose levels in response to exogenous glucose or insulin than control mice, but they also exhibited an enhanced insulin secretion upon a glucose bolus. No differences in other pre- and post-prandial plasma metabolites were found between SIRT3ki and control animals. Also, SIRT3 mice gained more weight and accrued more fat, presumably promoted by the increased insulin secretion in addition to food intake. These changes in glucose homeostasis may also be related to AgRP activation. Activation of AgRP neurons supposedly first raises insulin secretion and then impairs systemic insulin sensitivity and glucose tolerance (35). This appears similar to what we observed. We saw improved glucose tolerance in an OGTT, but most likely mainly because of increased insulin secretion. SIRT3ki animals may therefore develop insulin resistance earlier than control animals. In sum, the observed phenotype suggests an activation of anabolic circuits, stimulating food intake and sparing energy stores.

The most prominent feature of SIRT3 activation is the downregulation of glycolytic pathways and the concurrent activation of fatty acid oxidation (FAO) pathways and ketogenesis (KG) (26). Global SIRT3ko studies revealed reduced ketone bodies (KB) in the plasma of HFD fed mice (36), and hepatic overexpression of SIRT3 showed increased mitochondrial FAO (37). Therefore, astrocyte SIRT3 overexpression may also lead to an increased KB production. The role of KB in the CNS regulation of energy homeostasis is controversial (38-40). The observed discrepancies may be partly related to the different experimental approaches, i.e., exogenous KB infusion vs. inhibition of endogenous KB production. Other differences, such as the brain regions studied or the feeding regimen employed, may also contribute. One study that measured KB via microdialysis in the VMH of low and high-fat diet-fed rats concluded that KB produced by astrocytes during HFD feeding have an anorectic effect (13). Consistent with this interpretation, pharmacological inhibition of 3-hydroxy-3-methylglutaryl-CoA synthase-2, the regulatory enzyme of the rate-limiting step in KG, in the VMH and ARC, transiently abolished the observed reduction in food intake when animals were consuming HFD. Carneiro et al. (2016), on the other hand, infused KB for 24 h through a catheter inserted in the carotid artery, i.e., targeting the brain, in mice on chow and found a stimulation of hypothalamic orexigenic neuropeptides as well as increased insulinemia. These authors concluded that KB had an orexigenic effect (41). Assuming that astrocytes of SIRT3ki mice overproduced KB, our observations of enhanced insulin secretion, food intake and weight gain appear to fit these findings, but we did neither assess astrocyte KB production nor the effects of SIRT3ki on hypothalamic neuropeptides, and our mice were on HFD, whereas their mice were on chow. Another major difference is that we introduced the overexpression of SIRT3 in astrocytes, which normally should be downregulated during HFD feeding (42-44). In the study of Carneiro et al., mice were in a normal metabolic state. In this

situation, KB, which are typically produced in the liver during fasting, stimulated FI when they were infused towards the brain. In Le Foll and colleagues' microdialysis study, the rats were on HFD, and astrocyte-derived KB inhibited FI. On a HFD, KB are already produced in the periphery and presumably taken up and produced, at least to some extent, by astrocytes as well. In this case, SIRT3 overexpression would only enhance the already ongoing KB production in the astrocytes. Therefore, our mouse phenotype should have matched the observations of Le Foll et al., i.e., astrocyte-derived KB should have inhibited FI.

We can only speculate about reasons for this discrepancy. Of course, we manipulated SIRT3, not KB. SIRT3 is upregulated during fasting and downregulated during HFD feeding (42-47). During prolonged fasting, the body depends mainly on fatty acids and KB to cover its energy needs, whereas on a normal HFD the body has an energy surplus of fat, but also enough glucose. SIRT3 deacetylates and thereby activates about 1/5 of all mitochondrial enzymes (29). Increased proteome acetylation is found with caloric restriction (CR) and HFD feeding (43, 48). However, if we look at a specific SIRT3 target, i.e., long-chain acyl-CoA dehydrogenase (LCAD), which is the major enzyme responsible for the first step of long-chain fatty acid (LCFA) beta-oxidation, it is deacetylated during CR, but not during HFD (43, 47), consistent with the upregulation and downregulation of SIRT3 in these situations. Not much is known about the regulators of SIRT3 expression or activity. SIRT3 activity depends on NAD⁺, which is increased during CR but not during HFD (49, 50). Peroxisome proliferator-activated receptor gamma coactivator 1-alpha (PGC-1 α), a key regulator of SIRT3 and energy metabolism is also suppressed during HFD (51-53). In sum, it looks as if changes in SIRT3 protein expression represent the significant differences between CR and HFD-fed state. Thus, by shaping mitochondrial acetylation SIRT3 presumably

regulates the overall metabolic effect (29). In our animals eating the HFD, the upregulation of SIRT3 in astrocytes may have prevailed compared to the downregulation by HFD exposure, and hence contributed to changes comparable to the observations of Carneiro and colleagues, i.e., a stimulation of FI with a concomitant decrease in EE.

We also attempted to examine possible metabolic consequences of a reduced astrocyte SIRT3 expression in CD- and HFD-fed mice. SIRT3 knock-out mice (SIRT3ko) on control diet displayed no metabolic differences in any of the parameters measured, except for a better glucose response upon an OGTT measured 12 weeks after the induction of the knock-out. The faster glucose uptake in the OGTT suggests greater insulin sensitivity, but we can only speculate how and why this effect occurred. Overall, a decreased SIRT3 expression in astrocytes does not seem to play a major role in astrocyte metabolism when mice are fed CD. Also when SIRT3ko mice were switched to HFD immediately after TAM treatment, no metabolic differences compared to control animals were observed up to 14 weeks after TAM injection. Therefore, also in this situation astrocyte SIRT3 does not seem to play a major role in the regulation of energy homeostasis. Global SIRT3ko mice on HFD exhibited an exacerbated metabolic syndrome (20). Our data therefore suggest that the knock-out in astrocytes is not crucial for this effect.

The major limitation of all interpretations of the SIRT3ko findings is of course that we were not able to validate the astrocyte-specific knock-out, i.e., we can not be sure that astrocyte SIRT3 was really diminished. This is most likely due to our astrocyte isolation method, which did not target specifically GFAP expressing astrocytes, which account for only ~15 % (observed by staining) of all astrocytes depending on the brain region (54, 55). Consequently, changes in SIRT3 expression could not be detected in the

non-specific GFAP astrocyte fraction. Nevertheless, the additional flag binding to SIRT3 in the SIRT3 overexpression model allowed for the verification of an astrocyte SIRT3 overexpression. Other important limitations of our study, which also hamper interpretation of the SIRT3ki findings, are the lack of central nervous system KB measurements and that our gene-manipulation method did not allow for targeting specific brain regions.

Taken together, our findings indicate that astrocyte SIRT3 does not play a major role in CNS metabolic signaling and whole-body energy homeostasis. Only under conditions of chronic HFD exposure, astrocyte SIRT3 overexpression, presumably through its effects on astrocyte metabolism, produced some effects, but overall these were negative (increased food intake, body weight and body fat, hypersecretion of insulin) rather than positive. Unless the technical limitations mentioned above can be overcome, our observations scarcely warrant further investigations into the mechanisms of astrocyte SIRT3 regulation and actions in relation to the development of obesity.

References

1. **García-Cáceres C, Balland E, Prevot V, Luquet S, Woods SC, Koch M, et al.** Role of astrocytes, microglia, and tanycytes in brain control of systemic metabolism. *Nature Neuroscience*. 2018.
2. **Garcia-Caceres C, Fuente-Martin E, Argente J, Chowen JA.** Emerging role of glial cells in the control of body weight. *Mol Metab*. 2012;1(1-2):37-46.
3. **Weber B, Barros LF.** The Astrocyte: Powerhouse and Recycling Center. *Cold Spring Harbor Perspectives in Biology*. 2015;7(12).
4. **Wyss MT, Jolivet R, Buck A, Magistretti PJ, Weber B.** In vivo evidence for lactate as a neuronal energy source. *Journal of Neuroscience*. 2011;31(20):7477-85.
5. **Dringen R, Gebhardt R, Hamprecht B.** Glycogen in astrocytes: possible function as lactate supply for neighboring cells. *Brain Research*. 1993;623(2):208-14.
6. **Blazquez C, Sanchez C, Daza A, Galve-Roperh I, Guzman M.** The stimulation of ketogenesis by cannabinoids in cultured astrocytes defines carnitine palmitoyltransferase I as a new ceramide-activated enzyme. *Journal of Neurochemistry*. 1999;72(4):1759-68.
7. **Parsons MP, Hirasawa M.** ATP-sensitive potassium channel-mediated lactate effect on orexin neurons: implications for brain energetics during arousal. *Journal of Neuroscience*. 2010;30(24):8061-70.
8. **Kasser TR, Deutch A, Martin RJ.** Uptake and utilization of metabolites in specific brain sites relative to feeding status. *Physiology and Behavior*. 1986;36(6):1161-5.
9. **Mitchell RW, Hatch GM.** Fatty acid transport into the brain: Of fatty acid fables and lipid tails. *Prostaglandins, Leukotrienes and Essential Fatty Acids (PLEFA)*. 2011;85(5):293-302.
10. **Nalecz KA, Miecz D, Berezowski V, Cecchelli R.** Carnitine: transport and physiological functions in the brain. *Molecular Aspects of Medicine*. 2004;25(5-6):551-67.
11. **Kleman AM, Yuan JY, Aja S, Ronnett GV, Landree LE.** Physiological glucose is critical for optimized neuronal viability and AMPK responsiveness in vitro. *Journal of Neuroscience Methods*. 2008;167(2):292-301.
12. **Aja S, Bi S, Knipp SB, McFadden JM, Ronnett GV, Kuhajda FP, et al.** Intracerebroventricular C75 decreases meal frequency and reduces AgRP gene expression in rats. *American Journal of Physiology: Regulatory, Integrative and Comparative Physiology*. 2006;291(1):R148-54.

13. **Le Foll C, Dunn-Meynell AA, Miziorko HM, Levin BE.** Regulation of hypothalamic neuronal sensing and food intake by ketone bodies and fatty acids. *Diabetes*. 2014;63(4):1259-69.
14. **Gao Y, Layritz C, Legutko B, Eichmann TO, Laperrousaz E, Moulle VS, et al.** Disruption of Lipid Uptake in Astroglia Exacerbates Diet-Induced Obesity. *Diabetes*. 2017;66(10):2555-63.
15. **Yang L, Qi Y, Yang Y.** Astrocytes Control Food Intake by Inhibiting AGRP Neuron Activity via Adenosine A1 Receptors. *Cell Reports*. 2015;11(5):798-807.
16. **Kim JG, Suyama S, Koch M, Jin S, Argente-Arizon P, Argente J, et al.** Leptin signaling in astrocytes regulates hypothalamic neuronal circuits and feeding. *Nature Neuroscience*. 2014;17(7):908-10.
17. **Douglass JD, Dorfman MD, Fasnacht R, Shaffer LD, Thaler JP.** Astrocyte IKK β /NF- κ B signaling is required for diet-induced obesity and hypothalamic inflammation. *Mol Metab*. 2017;6(4):366-73.
18. **Garcia-Caceres C, Quarta C, Varela L, Gao Y, Gruber T, Legutko B, et al.** Astrocytic Insulin Signaling Couples Brain Glucose Uptake with Nutrient Availability. *Cell*. 2016;166(4):867-80.
19. **Parihar P, Solanki I, Mansuri ML, Parihar MS.** Mitochondrial sirtuins: emerging roles in metabolic regulations, energy homeostasis and diseases. *Experimental Gerontology*. 2015;61:130-41.
20. **Kincaid B, Bossy-Wetzel E.** Forever young: SIRT3 a shield against mitochondrial meltdown, aging, and neurodegeneration. *Frontiers in Aging Neuroscience*. 2013;5:48.
21. **Hirschey MD, Shimazu T, Jing E, Grueter CA, Collins AM, Auouizerat B, et al.** SIRT3 deficiency and mitochondrial protein hyperacetylation accelerate the development of the metabolic syndrome. *Molecular Cell*. 2011;44(2):177-90.
22. **Yoshino J, Imai S.** Mitochondrial SIRT3: a new potential therapeutic target for metabolic syndrome. *Molecular Cell*. 2011;44(2):170-1.
23. **Brown KD, Maqsood S, Huang J-Y, Pan Y, Harkcom W, Li W, et al.** Activation of SIRT3 by the NAD⁺ precursor nicotinamide riboside protects from noise-induced hearing loss. *Cell Metabolism*. 2014;20(6):1059-68.
24. **Hirrlinger PG, Scheller A, Braun C, Hirrlinger J, Kirchhoff F.** Temporal control of gene recombination in astrocytes by transgenic expression of the tamoxifen-inducible DNA recombinase variant CreERT2. *Glia*. 2006;54(1):11-20.
25. **Foo LC.** Purification and culture of astrocytes. *Cold Spring Harb Protoc*. 2013;2013(6):485-7.
26. **Nogueiras R, Habegger KM, Chaudhary N, Finan B, Banks AS, Dietrich MO, et al.** Sirtuin 1 and sirtuin 3: physiological modulators of metabolism. *Physiological Reviews*. 2012;92(3):1479-514.

27. **Verdin E, Hirschey MD, Finley LW, Haigis MC.** Sirtuin regulation of mitochondria: energy production, apoptosis, and signaling. *Trends in Biochemical Sciences.* 2010;35(12):669-75.
28. **Volterra A, Meldolesi J.** Astrocytes, from brain glue to communication elements: the revolution continues. *Nature Reviews: Neuroscience.* 2005;6(8):626-40.
29. **Hirschey MD, Shimazu T, Huang JY, Schwer B, Verdin E.** SIRT3 regulates mitochondrial protein acetylation and intermediary metabolism. *Cold Spring Harbor Symposia on Quantitative Biology.* 2011;76:267-77.
30. **Schwartz MW, Woods SC, Porte D, Jr., Seeley RJ, Baskin DG.** Central nervous system control of food intake. *Nature.* 2000;404(6778):661-71.
31. **Samson WK, Bagley SL, Ferguson AV, White MM.** Orexin receptor subtype activation and locomotor behaviour in the rat. *Acta Physiologica (Oxford, England).* 2010;198(3):313-24.
32. **Ludwig DS, Tritos NA, Mastaitis JW, Kulkarni R, Kokkotou E, Elmquist J, et al.** Melanin-concentrating hormone overexpression in transgenic mice leads to obesity and insulin resistance. *Journal of Clinical Investigation.* 2001;107(3):379-86.
33. **Broberger C, De Lecea L, Sutcliffe JG, Hokfelt T.** Hypocretin/orexin- and melanin-concentrating hormone-expressing cells form distinct populations in the rodent lateral hypothalamus: relationship to the neuropeptide Y and agouti gene-related protein systems. *Journal of Comparative Neurology.* 1998;402(4):460-74.
34. **Albuquerque J, R Zimmer M, Bober J, Dietrich M.** Rapid shift in substrate utilization driven by hypothalamic AgRP neurons 2016.
35. **Steculorum SM, Ruud J, Karakasilioti I, Backes H, Engstrom Ruud L, Timper K, et al.** AgRP Neurons Control Systemic Insulin Sensitivity via Myostatin Expression in Brown Adipose Tissue. *Cell.* 2016;165(1):125-38.
36. **Shimazu T, Hirschey MD, Hua L, Dittenhafer-Reed KE, Schwer B, Lombard DB, et al.** SIRT3 deacetylates mitochondrial 3-hydroxy-3-methylglutaryl CoA synthase 2 and regulates ketone body production. *Cell Metabolism.* 2010;12(6):654-61.
37. **Nassir F, Arndt JJ, Johnson SA, Ibdah JA.** Regulation of mitochondrial trifunctional protein modulates nonalcoholic fatty liver disease in mice. *Journal of Lipid Research.* 2018;59(6):967-73.
38. **Davis JD, Wirtshafter D, Asin KE, Brief D.** Sustained intracerebroventricular infusion of brain fuels reduces body weight and food intake in rats. *Science.* 1981;212(4490):81-3.
39. **Sun M, Martin RJ, Edwards GL.** ICV beta-hydroxybutyrate: effects on food intake, body composition, and body weight in rats. *Physiology and Behavior.* 1997;61(3):433-6.

40. **Arase K, Fisler JS, Shargill NS, York DA, Bray GA.** Intracerebroventricular infusions of 3-OHB and insulin in a rat model of dietary obesity. *American Journal of Physiology*. 1988;255(6 Pt 2):R974-81.
41. **Carneiro L, Geller S, Hébert A, Repond C, Fioramonti X, Leloup C, et al.** Hypothalamic sensing of ketone bodies after prolonged cerebral exposure leads to metabolic control dysregulation. *Scientific Reports*. 2016;6:34909.
42. **Bao J, Scott I, Lu Z, Pang L, Dimond CC, Gius D, et al.** SIRT3 is regulated by nutrient excess and modulates hepatic susceptibility to lipotoxicity. *Free Radical Biology and Medicine*. 2010;49(7):1230-7.
43. **Hirschey MD, Shimazu T, Jing E, Grueter CA, Collins AM, Aouizerat B, et al.** SIRT3 deficiency and mitochondrial protein hyperacetylation accelerate the development of the metabolic syndrome. *Molecular Cell*. 2011;44(2):177-90.
44. **Palacios OM, Carmona JJ, Michan S, Chen KY, Manabe Y, Ward JL, 3rd, et al.** Diet and exercise signals regulate SIRT3 and activate AMPK and PGC-1alpha in skeletal muscle. *Aging*. 2009;1(9):771-83.
45. **Edgett BA, Hughes MC, Matusiak JB, Perry CG, Simpson CA, Gurd BJ.** SIRT3 gene expression but not SIRT3 subcellular localization is altered in response to fasting and exercise in human skeletal muscle. *Experimental Physiology*. 2016;101(8):1101-13.
46. **Shi T, Wang F, Stieren E, Tong Q.** SIRT3, a mitochondrial sirtuin deacetylase, regulates mitochondrial function and thermogenesis in brown adipocytes. *Journal of Biological Chemistry*. 2005;280(14):13560-7.
47. **Hirschey MD, Shimazu T, Goetzman E, Jing E, Schwer B, Lombard DB, et al.** SIRT3 regulates mitochondrial fatty-acid oxidation by reversible enzyme deacetylation. *Nature*. 2010;464(7285):121-5.
48. **Schwer B, Eckersdorff M, Li Y, Silva JC, Fermin D, Kurtev MV, et al.** Calorie restriction alters mitochondrial protein acetylation. *Aging Cell*. 2009;8(5):604-6.
49. **Lin SJ, Defossez PA, Guarente L.** Requirement of NAD and SIR2 for life-span extension by calorie restriction in *Saccharomyces cerevisiae*. *Science*. 2000;289(5487):2126-8.
50. **Bitterman KJ, Anderson RM, Cohen HY, Latorre-Esteves M, Sinclair DA.** Inhibition of silencing and accelerated aging by nicotinamide, a putative negative regulator of yeast sir2 and human SIRT1. *Journal of Biological Chemistry*. 2002;277(47):45099-107.
51. **Crunkhorn S, Dearie F, Mantzoros C, Gami H, da Silva WS, Espinoza D, et al.** Peroxisome proliferator activator receptor gamma coactivator-1 expression is reduced in obesity: potential pathogenic role of saturated fatty acids and p38 mitogen-activated protein kinase activation. *Journal of Biological Chemistry*. 2007;282(21):15439-50.

52. **Li X, Monks B, Ge Q, Birnbaum MJ.** Akt/PKB regulates hepatic metabolism by directly inhibiting PGC-1alpha transcription coactivator. *Nature*. 2007;447(7147):1012-6.
53. **Kong X, Wang R, Xue Y, Liu X, Zhang H, Chen Y, et al.** Sirtuin 3, a new target of PGC-1alpha, plays an important role in the suppression of ROS and mitochondrial biogenesis. *PloS One*. 2010;5(7):e11707.
54. **Bushong EA, Martone ME, Jones YZ, Ellisman MH.** Protoplasmic astrocytes in CA1 stratum radiatum occupy separate anatomical domains. *Journal of Neuroscience*. 2002;22(1):183-92.
55. **Reeves AM, Shigetomi E, Khakh BS.** Bulk loading of calcium indicator dyes to study astrocyte physiology: key limitations and improvements using morphological maps. *Journal of Neuroscience*. 2011;31(25):9353-8.

CHAPTER 4: GENERAL DISCUSSION

1. Overview of the findings

The two projects presented in this thesis aimed at contributing to a better understanding of the possible involvement of intracellular metabolism in the sensing and signaling of energy availability by vagal afferent nerves (VAN) and astrocytes in the regulation of energy homeostasis.

The first study used a rat model of viral vector-mediated RNA interference in the nodose ganglia (NG) to address the role of VAN MCT2 in the control of eating. MCT2 is a crucial transporter for the uptake of monocarboxylates such as lactate and KB into cells as well as of pyruvate into the mitochondria. The results indicate that VAN MCT2 is involved in eating control if the organism is acutely challenged by food deprivation or high-fat diet (HFD) exposure. These findings indirectly support the hypothesis of a peripheral metabolic contribution to the control of food intake by VAN signaling. They extend previous findings and ideas in suggesting that the VAN do not only pick up some kind of metabolic or other signal from compounds released by other cells (e.g., from hepatocytes or enteroendocrine cells) acting on VAN cell membrane receptors (e.g. GPCR), but rather that VAN metabolism itself constitutes the signaling mechanism.

The second study used a mouse model with conditional knock-in or knock-out of SIRT3 specifically in GFAP expressing astrocytes to examine whether manipulations of astrocyte metabolism, in particular FAO and ketogenesis, would affect energy homeostasis in a physiologically healthy state and in DIO. SIRT3 is a vital posttranslational regulatory enzyme of mitochondrial metabolism; it adjusts and controls mitochondrial responses to nutrient availability. The results indicate that astrocyte-specific SIRT3ko does not play a critical role in energy homeostasis in both, low-fat or HFD feeding conditions. SIRT3 overexpression (SIRT3ki) did also not

affect energy homeostasis on a low-fat diet, but caused an increase in body weight and body fat together with lower locomotor activity and energy expenditure and greater food intake as well as an improved glucose tolerance with hypersecretion of insulin when the mice were chronically fed a HFD. These findings suggest that astrocyte SIRT3 is not important for energy homeostasis under normal conditions and with a HFD challenge, and that its enhanced function may even have negative systemic effects.

2. VAN MCT2 in the control of food intake

Today, it is generally accepted that vagal afferent neurons (VAN) play a role in the control of food intake (FI). An additional recent development is the realization that VAN might be more involved in fine-tuning neuronal responses to the nutritional and metabolic status than originally believed (1). Another recent development is that vagal afferent nerve “blockade”, which actually appears to result in an afferent stimulation, is proposed as an obesity treatment (2, 3). Furthermore, the same VAN fibers can obviously transmit orexigenic or anorexigenic signals, triggered by different substances (e.g. mercaptoacetate and CCK), and they possess substantial plasticity, regulating receptor density and expression of neuromediators according to nutritional status (1, 4, 5). Nevertheless, it remains to be clarified whether metabolic metering of ingested macronutrients, in particular carbohydrates and fats, can also modulate VAN signaling that controls FI.

While SDA, the most specific method to disconnect all subdiaphragmatic vagal afferents, provided evidence for the necessity of intact VAN for signal transduction of anorexigenic GI peptides such as CCK, it also showed that intact VAN are not necessary for the FI inhibiting effects of direct or indirect FAO stimulators such as Wy-14643, OEA and DGAT-1i (5, 6). This suggests that the observed increase in FAO or ketogenesis in the duodenum or jejunum is not essential for the FI inhibitory effect of those compounds and/or that these processes or the resulting signaling molecules do not affect VAN activity (6-9). Interestingly, the eating inhibitory effect of intraperitoneally (IP) injected OEA was just recently proposed to be a side effect of the concomitant locomotor impairment (10). Thus, even if these substances have been shown to enhance fatty acid oxidation, their eating inhibitory effects may be related to other mechanisms. The failure of SDA to block these effects therefore does not necessarily

argue against a VAN mediation of a FAO- or ketone body-derived signal that inhibits eating.

Our MCT2 knockdown manipulated metabolite transport and did not interfere with specific intracellular metabolic pathways. Our findings therefore only indicate, but do not prove, that the VAN signal that caused the behavioral changes resulted from intracellular metabolism of BHB or lactate/pyruvate. It is conceivable that MCT2 could act as a receptor in addition to its transporter function. This has been shown for the CD36 fatty acid transporter, which is involved in hypothalamic neuronal FA sensing (11, 12). Recently the term “transceptor” or “sensor” has been coined for membrane-proteins that combine both **transport** and **receptor**-like signaling function (13, 14). As MCT2`s features are still partly unclear, it may also have such a transceptor function.

Glucose can stimulate or inhibit glucose-sensing neurons in different ways. Two pathways have been identified that can activate glucose-excited neurons. Either neuronal depolarization is triggered by the elevation of the ATP/ADP ratio inactivating ATP-sensitive K⁺ (K_{ATP}) channels (15, 16), or by AMP-activated protein kinase (AMPK) and a K_{ATP}-independent channel (17, 18). Grabauskas and colleagues reported that a subset of gastric VAN or NG neurons requires intracellular glucose metabolism for glucose sensing (19). They showed that GLUT3, glukokinase (GK) and K_{ATP} channels are required for VAN or NG glucosensing. Intracellular metabolization of KB could trigger neuronal depolarization by the same pathways. Glucose can also interact with a sodium-cotransporter and trigger membrane depolarization without intracellular glucose metabolism (20), but to our knowledge, such an effect has not been shown for neuronal signaling induced by lactate or KB. In any case, follow-up experiments should involve silencing lactate dehydrogenase and 3-hydroxybutyrate dehydrogenase, which catalyze the first oxidative step to pyruvate or acetoacetate, respectively. This could

reveal whether the sensing occurs through lactate or BHB metabolism, if the attenuated lactate or KB utilization would regenerate the phenotype that we observed in our MCT2kd animals.

The study of Grabauskas et al. also shows that VAN are polymodal, relaying and integrating mechanical and metabolic signals. This is relevant because our data indicate that VAN function as metabolic sensors in particular when the system is challenged, i.e., this function might come into play when a particularly large meal has been ingested, as observed after a prior food deprivation with the subsequent initial hyperphagia, or when the body is acutely confronted with HFD. In both cases, a positive synergistic interaction of the metabolic signal with mechanical or peptidergic stimuli appears feasible. A metabolic-peptidergic interaction in hepatic branch VAN was shown by Burcelin and colleagues, reporting that the GLP-1 receptor is needed for the proper function of hepatportal glucose sensing (21).

Interestingly, MCT2 expression in hypothalamic nuclei has been shown to be enhanced by HFD feeding (22, 23), and prolonged fasting leads to MCT2 upregulation in the brainstem (24). This raises the possibility that these metabolic states of the organism also affect VAN MCT2 expression. If so, an upregulated MCT2 expression in response to fasting and HFD exposure could be yet another reason for the stronger effects of the VAN MCT2 knockdown on eating behavior in the challenged states of our rats. Thus, the MCT2 knockdown might have markedly attenuated the natural increase in MCT2 expression occurring in the control animals, which might have increased the difference in MCT2 expression between control and MCT2kd rats. MCT2 appears to be predominantly localized in the PDS area of several glutamatergic synapses in several brain areas (25, 26), suggesting that this synaptic localization ensures an adequate supply of energy substrates to postsynaptic terminals upon

excitation. We found MCT2 to be expressed all over the NG neurons, which allows for the speculation that VAN MCT2 might also be close to the central synapse of the pseudobipolar VAN. At least with high circulating lactate and/or KB levels, the VAN MCT2^{kd} might therefore also influence signaling at the central synapse of the VAN neurons (27, 28).

To summarize, we demonstrated for the first time that VAN MCT2 is involved in the control of eating under certain conditions, but further studies are necessary to identify the exact mechanisms involved. Accumulating evidence indicates that MCT2 expression is regulated to adjust monocarboxylate supply to demand and to link neuroenergetics to synaptic transmission. Our findings therefore make MCT2 a promising candidate to study its potential role in VAN energostatic nutrient sensing.

3. Astrocyte SIRT3 in energy homeostasis

Our data presented in CHAPTER 3 questioned a major role of astrocyte SIRT3 in the regulation of energy homeostasis, but suggested some capability of astrocyte SIRT3 to influence whole-body energy homeostasis under certain conditions. This does not add much to the accumulating evidence for a role of astrocytes in energy homeostasis. From a more general perspective, our data reiterate that it matters under which conditions the expression and function of an enzyme, in our case SIRT3, is manipulated.

For any interpretation of these findings, however, the top priority is a proper validation of astrocyte-specific SIRT3 overexpression or downregulation. We originally aimed at isolating vital astrocytes, from SIRT3^{ki/ko} animals, to capture their metabolic status and thus allowing for a metabolic characterization via the Sea-horse metabolic flux analyzer. Therefore, we attempted to use the immune-panning isolation method described by Foo et al. (29). As the isolation of astrocytes from adult mice turned out to be harder than anticipated, we combined it with the microbeads isolation method. Unfortunately, the microbeads isolation targets the ASCA-antigen and thus separates specifically ASCA-expressing, but not GFAP-expressing, astrocytes. The fact that only ~15% of all astrocytes express GFAP (30, 31) and that our isolation did not specifically target GFAP astrocytes explain the extremely low GFAP-expression measured at the mRNA level. For the other astrocyte markers examined, we found an approximately 4-fold increase in gene expression compared to control. If we take the pool of the astrocytes with the 4-fold marker expression as the 100% of all astrocytes in the brain, a 0.5-fold expression equals 12.5 %, which is close to the expected 15 % GFAP expressing astrocytes, thus indirectly validating our isolation method. Isolated astrocytes were almost devoid of neurons and microglia, but were substantially

contaminated with oligodendrocytes. This incomplete dissociation of astrocytes and oligodendrocyte was confirmed by the high mRNA expression of gap junction gamma-2 (Gjc2), which encodes connexin-47, a protein involved in the gap junction coupling between astrocytes and oligodendrocytes and among oligodendrocytes. This oligodendrocyte contamination “diluted” the astrocyte pool and compromised the validation of manipulated SIRT3 expression. Moreover, only about ~15% of astrocytes express GFAP (30, 31), and in the case of the SIRT3ki we had to use heterozygous mice because a genotyping verification of the homozygous SIRT3ki is impossible. This hampered the validation of the transgenic mouse model. Nonetheless, the flagged SIRT3ki allowed us to detect a small SIRT3 overexpression of 20% in isolated astrocytes of SIRT3ki animals on HFD. In contrast, measuring SIRT3 (without a flag) expression did not capture the presumably small differences in SIRT3 overexpression or downregulation (although the SIRT3ko model was homozygous for SIRT3). In sum, the difficulties to assess SIRT3 expression at the mRNA level emphasize that a verification of SIRT3 expression at the protein level with this astrocyte isolation method is illusive. Therefore, a functional validation of the model was impossible.

A possible way to overcome these difficulties would be to achieve a single cell suspension via the immune-panning method and then to FACS sort the cells directly using a GFAP antibody. A pure GFAP cell population might allow for the detection of manipulated SIRT3 expression on the mRNA and protein level. In case of confirmed differences at the protein level, detection of the acetylation level of all proteins would provide a direct functional test. A downregulation of SIRT3 expression would be expected to lead to increased acetylation, whereas the SIRT3ki should decrease acetylation of all proteins (32). Should these tests fail, mass spectrometry would be the next approach to screen for the acetylation profile of GFAP positive cells.

After a successful validation, the first experiment should be to test for the exclusive targeting of GFAP-expressing astrocytes by our CreERT2-loxP system. This is important because GFAP is also expressed in various other tissues relevant for metabolic control. For instance, it was detected in stellate cells from rat pancreas (33) and rat liver (34). Another important experiment would be to establish SIRT3ki/ko efficiency timelines by examining the up- or downregulation of SIRT3 after tamoxifen injection on a weekly basis. Astrocytes, unlike neurons, can replicate, and especially in animals on HFD astrocytes develop astrogliosis and perhaps apoptosis (35). It is therefore crucial to validate how long the TAM induction of SIRT3 lasts and if a subsequent 2nd TAM injection is necessary to prolong the modulated SIRT3 expression.

Most of the knowledge about SIRT3 expression and function so far relies on the examination of peripheral metabolic tissues. Those data show SIRT3 is upregulated during fasting or caloric restriction as well as during short-term HFD feeding, but downregulated with long-term HFD exposure (32). The same regulation pattern might apply to astrocytes, but this needs to be examined before any conclusions can be drawn.

If our transgenic manipulation had the desired effect, the obvious follow-up experiments for the SIRT3ki-HFD study would be: 1) Punctures of the most prominent hypothalamic nuclei involved in EH, and mRNA screening for up- and downregulation of their neuropeptides would show whether our speculation on upregulated anabolic neuropeptides, explaining the increased FI and EE observed, is correct. This is important because our transgenic mouse-line targets GFAP expressing astrocytes in the whole brain. 2) Metabolic sensing neurons display a great heterogeneity in cell-type, function and location. For instance, glucose-sensing neurons are not only found

in the hypothalamus, but also in the basal ganglia, medulla and amygdala (15). We do not know which effects the metabolic challenge of all astrocytes might exert. Therefore, a future experiment should include viral targeting of specific brain areas, starting with the hypothalamus, to localize the origin of the observed phenotype. 3) Although SIRT3 is known for upregulating FAO and KG (36), we have to test for increased KB production, which could be done by microdialysis. It is already known that KB are able to modulate neuronal activity (37, 38), but we modulated SIRT3 activity, which has several other targets; hence we cannot exclude that other mechanisms contributed to the observed phenotype. Therefore, if the SIRT3ki does enhance KB production, targeted inhibition of KB production in SIRT3ki animals could provide some clarification. Nevertheless, an enhanced FAO and KG are only one big effect of increased SIRT3 activity. The other important effect is SIRT3 scavenging of reactive oxygen species (ROS) (39-42). Chronic ROS overproduction in the brain is associated with type 2 diabetes (43, 44). ROS signaling in the hypothalamic regulation of EH was studied intensively in the last 10-20 years (45), indicating that increased ROS production in the hypothalamus upon increased mitochondrial respiration due to glucose or lipids is able to inhibit FI (46-48). Increased ROS activates POMC neurons whereas decreased ROS levels were found to activate NPY/AgRP neurons (49). If, in our case the astrocyte-SIRT3ki attenuated ROS production, as it supposedly does according to other studies (39-41), ROS might be another signaling molecule contributing to our observed phenotype.

Some of these speculations might be worth investigating. Because a global SIRT3ko has been shown to exacerbate the DIO-induced metabolic phenotype (50, 51), our original assumption was that SIRT3 upregulation in astrocytes might have beneficial effects with respect to energy homeostasis. Contrary to this assumption, astrocyte

SIRT3 overexpression in DIO mice aggravated the DIO-induced metabolic phenotype. The “natural” downregulation of SIRT3 in astrocytes upon long-term HFD exposure may therefore represent a “protective response”. In the previous paragraphs, I picked only two likely candidate signaling molecules modulated by SIRT3, i.e., KB and ROS, to speculate on possible links to and explanations for the phenotype that we observed. Clearly, there are more than these two candidates, and in the end, most likely a combination of several factors leads to the observed phenotype in response to SIRT3 manipulations.

The OGTT and IST revealed a faster glucose uptake in SIRTki compared to control mice, but also an increased insulin secretion. We could further pursue these data by performing a euglycemic clamp or analyze metabolic tissue for insulin pathway markers via western-blot after insulin administration to examine if insulin sensitivity is affected. The development of insulin resistance and the increase in adiposity due to increased FI and decreased EE may accelerate the development of the metabolic syndrome in SIRT3ki animals compared to control animals.

Finally, the lack of a phenotype in SIRT3ki and SIRT3ko animals on the control diet as well as in SIRT3ko animals on the HFD may be due to our GFAP-promotor. GFAP is not just an astrocyte marker, but also a marker for astrocyte activation (35, 52, 53). HFD exposure leads to astrogliosis, which is presumably accompanied by an increased expression of GFAP. The use of the GFAP promoter in this situation may lead to a greater percentage of over- or under-expression reflected in the phenotype that we saw in HFD-fed SIRT3ki mice. The lack of an effect in our mice on the CD may therefore also be related to the particularly small number of GFAP-positive astrocytes under this condition. The assumption of an astrogliosis effect on GFAP gene regulation is supported by a study in GFAP^{CreERT}dTomato mice, showing a minimal Cre-mediated

recombination when the mice were on control diet, but a markedly increased recombination when the mice were injected with TAM after 6 weeks of HFD intake (54).

The lack of a phenotype in SIRT3^{ki} animals on CD and SIRT3^{ko} on both diets might therefore simply be due to inefficient Cre-recombination and SIRT3 over- or downregulation. This would in effect limit any interpretation with respect to the role of astrocyte SIRT3 at the given metabolic states (to avoid confusion, it is important to emphasize that the SIRT3^{ki} flag validation refers to SIRT3^{ki} animals on HFD).

All in all, SIRT3 in astrocytes presumably does not play a major role in CNS metabolic sensing in the regulation of energy homeostasis, but given the many limitations of the employed experimental techniques (see above), this interpretation may underestimate the function of astrocyte SIRT3 and can certainly not be extended to astrocyte fatty acid oxidation and KG. If the technical problems can be solved, our findings suggest some directions that future studies might take.

4. References

1. **de Lartigue G, Diepenbroek C.** Novel developments in vagal afferent nutrient sensing and its role in energy homeostasis. *Current Opinion in Pharmacology.* 2016;31:38-43.
2. **Apovian CM, Shah SN, Wolfe BM, Ikramuddin S, Miller CJ, Tweden KS, et al.** Two-Year Outcomes of Vagal Nerve Blocking (vBloc) for the Treatment of Obesity in the ReCharge Trial. *Obesity Surgery.* 2017;27(1):169-76.
3. **Johannessen H, Revesz D, Kodama Y, Cassie N, Skibicka KP, Barrett P, et al.** Vagal Blocking for Obesity Control: a Possible Mechanism-Of-Action. *Obesity Surgery.* 2017;27(1):177-85.
4. **de Lartigue G, Xu C.** Mechanisms of vagal plasticity influencing feeding behavior. *Brain Research.* 2018;1693:146-50.
5. **Raybould HE.** Mechanisms of CCK signaling from gut to brain. *Current Opinion in Pharmacology.* 2007;7(6):570-4.
6. **Mansouri A, Langhans W.** Enterocyte-afferent nerve interactions in dietary fat sensing. *Diabetes, Obesity & Metabolism.* 2014;16 Suppl 1:61-7.
7. **Azari EK, Ramachandran D, Weibel S, Arnold M, Romano A, Gaetani S, et al.** Vagal afferents are not necessary for the satiety effect of the gut lipid messenger oleoylethanolamide. *American Journal of Physiology: Regulatory, Integrative and Comparative Physiology.* 2014;307(2):R167-78.
8. **Karimian Azari E, Leitner C, Jaggi T, Langhans W, Mansouri A.** Possible Role of Intestinal Fatty Acid Oxidation in the Eating-Inhibitory Effect of the PPAR- α Agonist Wy-14643 in High-Fat Diet Fed Rats. *PloS One.* 2013;8(9):e74869.
9. **Schober G, Arnold M, Birtles S, Buckett LK, Pacheco-López G, Turnbull AV, et al.** Diacylglycerol acyltransferase-1 inhibition enhances intestinal fatty acid oxidation and reduces energy intake in rats. *Journal of Lipid Research.* 2013;54(5):1369-84.
10. **Fedele S, Arnold M, Krieger JP, Wolfstädter B, Meyer U, Langhans W, et al.** Oleoylethanolamide-induced anorexia in rats is associated with locomotor impairment. *Physiological Reports.* 2018;6(3):e13517.
11. **Le Foll C, Dunn-Meynell A, Musatov S, Magnan C, Levin BE.** FAT/CD36: a major regulator of neuronal fatty acid sensing and energy homeostasis in rats and mice. *Diabetes.* 2013;62(8):2709-16.
12. **Le Foll C, Irani BG, Magnan C, Dunn-Meynell AA, Levin BE.** Characteristics and mechanisms of hypothalamic neuronal fatty acid sensing. *American Journal of Physiology: Regulatory, Integrative and Comparative Physiology.* 2009;297(3):R655-64.

13. **Diallinas G.** Transceptors as a functional link of transporters and receptors. *Microbial cell (Graz, Austria)*. 2017;4(3):69-73.
14. **Wang Y-P, Lei Q-Y.** Metabolite sensing and signaling in cell metabolism. *Signal Transduction and Targeted Therapy*. 2018;3(1):30.
15. **Levin BE, Kang L, Sanders NM, Dunn-Meynell AA.** Role of Neuronal Glucosensing in the Regulation of Energy Homeostasis. *Diabetes*. 2006;55(Supplement 2):S122.
16. **Rowe IC, Treherne JM, Ashford ML.** Activation by intracellular ATP of a potassium channel in neurons from rat basomedial hypothalamus. *The Journal of Physiology*. 1996;490 (Pt 1)(Pt 1):97-113.
17. **Claret M, Smith MA, Batterham RL, Selman C, Choudhury AI, Fryer LGD, et al.** AMPK is essential for energy homeostasis regulation and glucose sensing by POMC and AgRP neurons. *The Journal of clinical investigation*. 2007;117(8):2325-36.
18. **Fioramonti X, Lorsignol A, Taupignon A, Penicaud L.** A new ATP-sensitive K⁺ channel-independent mechanism is involved in glucose-excited neurons of mouse arcuate nucleus. *Diabetes*. 2004;53(11):2767-75.
19. **Grabauskas G, Zhou S-Y, Lu Y, Song I, Owyang C.** Essential elements for glucosensing by gastric vagal afferents: immunocytochemistry and electrophysiology studies in the rat. *Endocrinology*. 2013;154(1):296-307.
20. **O'Malley D, Reimann F, Simpson AK, Gribble FM.** Sodium-coupled glucose cotransporters contribute to hypothalamic glucose sensing. *Diabetes*. 2006;55(12):3381-6.
21. **Burcelin R, Da Costa A, Drucker D, Thorens B.** Glucose Competence of the Hepatoportal Vein Sensor Requires the Presence of an Activated Glucagon-Like Peptide-1 Receptor. *Diabetes*. 2001;50(8):1720.
22. **Pierre K, Parent A, Jayet P-Y, Halestrap AP, Scherrer U, Pellerin L.** Enhanced expression of three monocarboxylate transporter isoforms in the brain of obese mice. *The Journal of Physiology*. 2007;583(Pt 2):469-86.
23. **Cortes-Campos C, Elizondo R, Carril C, Martinez F, Boric K, Nualart F, et al.** MCT2 expression and lactate influx in anorexigenic and orexigenic neurons of the arcuate nucleus. *PLoS One*. 2013;8(4):e62532.
24. **Matsuyama S, Ohkura S, Iwata K, Uenoyama Y, Tsukamura H, Maeda K, et al.** Food deprivation induces monocarboxylate transporter 2 expression in the brainstem of female rat. *J Reprod Dev*. 2009;55(3):256-61.
25. **Bergersen L, Waerhaug O, Helm J, Thomas M, Laake P, Davies AJ, et al.** A novel postsynaptic density protein: the monocarboxylate transporter MCT2 is co-localized with delta-glutamate receptors in postsynaptic densities of parallel fiber-Purkinje cell synapses. *Experimental Brain Research*. 2001;136(4):523-34.

26. **Pierre K, Magistretti PJ, Pellerin L.** MCT2 is a Major Neuronal Monocarboxylate Transporter in the Adult Mouse Brain. *Journal of Cerebral Blood Flow and Metabolism.* 2002;22(5):586-95.
27. **Pierre K, Chatton JY, Parent A, Repond C, Gardoni F, Di Luca M, et al.** Linking supply to demand: the neuronal monocarboxylate transporter MCT2 and the alpha-amino-3-hydroxyl-5-methyl-4-isoxazole-propionic acid receptor GluR2/3 subunit are associated in a common trafficking process. *European Journal of Neuroscience.* 2009;29(10):1951-63.
28. **Bergersen LH, Magistretti PJ, Pellerin L.** Selective postsynaptic co-localization of MCT2 with AMPA receptor GluR2/3 subunits at excitatory synapses exhibiting AMPA receptor trafficking. *Cerebral Cortex.* 2005;15(4):361-70.
29. **Foo LC.** Purification and culture of astrocytes. *Cold Spring Harb Protoc.* 2013;2013(6):485-7.
30. **Bushong EA, Martone ME, Jones YZ, Ellisman MH.** Protoplasmic astrocytes in CA1 stratum radiatum occupy separate anatomical domains. *Journal of Neuroscience.* 2002;22(1):183-92.
31. **Reeves AM, Shigetomi E, Khakh BS.** Bulk loading of calcium indicator dyes to study astrocyte physiology: key limitations and improvements using morphological maps. *Journal of Neuroscience.* 2011;31(25):9353-8.
32. **Hirschey MD, Shimazu T, Huang JY, Schwer B, Verdin E.** SIRT3 regulates mitochondrial protein acetylation and intermediary metabolism. *Cold Spring Harbor Symposia on Quantitative Biology.* 2011;76:267-77.
33. **Apte MV, Haber PS, Applegate TL, Norton ID, McCaughan GW, Korsten MA, et al.** Periacinar stellate shaped cells in rat pancreas: identification, isolation, and culture. *Gut.* 1998;43(1):128-33.
34. **Maubach G, Lim MCC, Zhang C-Y, Zhuo L.** GFAP promoter directs lacZ expression specifically in a rat hepatic stellate cell line. *World Journal of Gastroenterology.* 2006;12(5):723-30.
35. **Sofroniew MV, Vinters HV.** Astrocytes: biology and pathology. *Acta Neuropathologica.* 2010;119(1):7-35.
36. **Hirschey MD, Shimazu T, Goetzman E, Jing E, Schwer B, Lombard DB, et al.** SIRT3 regulates mitochondrial fatty-acid oxidation by reversible enzyme deacetylation. *Nature.* 2010;464(7285):121-5.
37. **Minami T, Shimizu N, Duan S, Oomura Y.** Hypothalamic neuronal activity responses to 3-hydroxybutyric acid, an endogenous organic acid. *Brain Research.* 1990;509(2):351-4.
38. **Le Foll C, Dunn-Meynell AA, Miziorko HM, Levin BE.** Regulation of hypothalamic neuronal sensing and food intake by ketone bodies and fatty acids. *Diabetes.* 2014;63(4):1259-69.

39. **Chen Y, Zhang J, Lin Y, Lei Q, Guan KL, Zhao S, et al.** Tumour suppressor SIRT3 deacetylates and activates manganese superoxide dismutase to scavenge ROS. *EMBO Rep.* 2011;12(6):534-41.
40. **Qiu X, Brown K, Hirschey MD, Verdin E, Chen D.** Calorie restriction reduces oxidative stress by SIRT3-mediated SOD2 activation. *Cell Metabolism.* 2010;12(6):662-7.
41. **Ansari A, Rahman MS, Saha SK, Saikot FK, Deep A, Kim K-H.** Function of the SIRT3 mitochondrial deacetylase in cellular physiology, cancer, and neurodegenerative disease. *Aging Cell.* 2017;16(1):4-16.
42. **Bause AS, Haigis MC.** SIRT3 regulation of mitochondrial oxidative stress. *Experimental Gerontology.* 2013;48(7):634-9.
43. **Ahmad W, Ijaz B, Shabbiri K, Ahmed F, Rehman S.** Oxidative toxicity in diabetes and Alzheimer's disease: mechanisms behind ROS/ RNS generation. *Journal of Biomedical Science.* 2017;24(1):76.
44. **Manoharan S, Guillemin GJ, Abiramasundari RS, Essa MM, Akbar M, Akbar MD.** The Role of Reactive Oxygen Species in the Pathogenesis of Alzheimer's Disease, Parkinson's Disease, and Huntington's Disease: A Mini Review. *Oxidative Medicine and Cellular Longevity.* 2016;2016:15.
45. **Drougard A, Fournel A, Valet P, Knauf C.** Impact of hypothalamic reactive oxygen species in the regulation of energy metabolism and food intake. *Frontiers in Neuroscience.* 2015;9:56-.
46. **Carneiro L, Allard C, Guissard C, Fioramonti X, Turrel-Cuzin C, Bailbé D, et al.** Importance of Mitochondrial Dynamin-Related Protein 1 in Hypothalamic Glucose Sensitivity in Rats. *Antioxidants & Redox Signaling.* 2012;17(3):433-44.
47. **Benani A, Troy S, Carmona MC, Fioramonti X, Lorsignol A, Leloup C, et al.** Role for mitochondrial reactive oxygen species in brain lipid sensing: redox regulation of food intake. *Diabetes.* 2007;56(1):152-60.
48. **Leloup C, Magnan C, Benani A, Bonnet E, Alquier T, Offer G, et al.** Mitochondrial reactive oxygen species are required for hypothalamic glucose sensing. *Diabetes.* 2006;55(7):2084-90.
49. **Andrews ZB, Liu ZW, Wallingford N, Erion DM, Borok E, Friedman JM, et al.** UCP2 mediates ghrelin's action on NPY/AgRP neurons by lowering free radicals. *Nature.* 2008;454(7206):846-51.
50. **Hirschey MD, Shimazu T, Jing E, Grueter CA, Collins AM, Auizerat B, et al.** SIRT3 deficiency and mitochondrial protein hyperacetylation accelerate the development of the metabolic syndrome. *Molecular Cell.* 2011;44(2):177-90.
51. **Yoshino J, Imai S.** Mitochondrial SIRT3: a new potential therapeutic target for metabolic syndrome. *Molecular Cell.* 2011;44(2):170-1.

52. **Brahmachari S, Fung YK, Pahan K.** Induction of glial fibrillary acidic protein expression in astrocytes by nitric oxide. *The Journal of neuroscience : the official journal of the Society for Neuroscience.* 2006;26(18):4930-9.
53. **Eng LF, Ghirnikar RS.** GFAP and astrogliosis. *Brain Pathology.* 1994;4(3):229-37.
54. **Douglass JD, Dorfman MD, Fasnacht R, Shaffer LD, Thaler JP.** Astrocyte IKK β /NF- κ B signaling is required for diet-induced obesity and hypothalamic inflammation. *Mol Metab.* 2017;6(4):366-73.

CURRICULUM VITAE

Master of Science

NADJA WEISSFELD

date of birth 18th of February 1988
nationality German
E-mail nadja.weissfeld@gmail.com

EDUCATION

- Since Jun. 2015 **Doctoral candidate in Physiology and Behavior**
ETH Zurich, Switzerland
- * Enrolled at Zurich Life Science Graduate School
Program: Integrative Molecular Medicine
- May 2015 **Master of Science in Biochemistry and Molecular Biology**
Apr. 2011 University of Potsdam (Germany)
- * Successful participation in the “International Genetically Engineered Machine Competition 2011” (iGEM)
 - * Master Thesis at ETH Zurich
- Feb. 2011 **Bachelor of Science in Applied Life Sciences**
Oct. 2007 University of Applied Sciences, Kaiserslautern (Germany)
- * Including a semester at University of Florida, Gainesville, USA
 - * Bachelor Thesis at Robert Koch Institute, Berlin, Germany
- March 2007 **High-school diploma**
Johann-Wolfgang Goethe Gymnasium, Germersheim, Germany

RESEARCH & WORK EXPERIENCE

- Since Jun. 2015 **Doctoral candidate**
Institute of Food, Nutrition and Health, Laboratory of Physiology and Behavior, ETH Zurich, Switzerland
- * Thesis title: “Brain metabolic sensing and energy homeostasis”
 - * Supervisor: Prof. Dr. Wolfgang Langhans
 - * Co-advisor: Dr. Abdelhak Mansouri

- May 2015 **Master`s project**
Dez.2013 Institute of Brain Research, Laboratory of Neuronal Regeneration and Repair, ETH & UZH Zurich, Switzerland
- * Thesis title: “Development of inducible gene expression and novel behavior tools to study motor memory engrams in the rat striatum”
 - * Supervisor: Prof. Dr. Martin E. Schwab
 - * Co-advisor: Dr. Alice Mosberger
- Jul. 2013 **Internship**
University Medical Center, Department of Neuropathology, RWTH Aachen, Germany
- * Topic of research: “Understanding the neuropathological features in ALS by immunohistochemical approach”
- Feb. 2013 **Work experience**
Oct. 2012 Department of Biochemistry and Molecular Biology, University of Potsdam, Germany
- * Supervision of the practical course “Methods of Biochemistry and Molecular Biology” for undergraduate students
- Dec. 2012 **Work experience**
Jun. 2011 Department of Biochemistry and Molecular Biology, University of Potsdam, Germany
- * Administrative assistance at the project GoFORSYS and active cooperation on the 7th Workshop-Molecular Interactions- in October 2011, Berlin
- Nov. 2011 **Research project**
Apr. 2011 Department of Biotechnology, University of Potsdam, Germany
- * “International Genetically Engineered Machine Competition 2011” (iGEM), Team Potsdam Bioware
 - * Topic of research: “Modification, selection and production of cyclic peptides for therapy”
 - * Gold award at the European Jamboree in Amsterdam
 - * Participated in the final competition at the Massachusetts Institute of Technology, Boston, USA
- Jan. 2011 **Bachelor project**
Jun. 2010 Department of Neurodegenerative Diseases, Robert Koch Institute, Berlin, Germany
- * Thesis title: “Interaction between Prion protein and Amyloid beta”
 - * Supervisor: Dr. Michael Baier
- Feb. 2010 **Research project**
Nov. 2009 Department of Microsystem Technology, University of Applied Sciences Kaiserslautern, Germany

- * Topic of research: "Encapsulation, electrical and electrochemical characterization of ion sensitive field-effect transistors in Dip-Chip design"

Nov. 2009 **Internship**

Aug. 2009 University of Florida, Biomedical Engineering Department,
Gainesville, USA

- * Topic of research: "Comparison of neural cell growth on micro printed surface polymers"

POSTER PRESENTATION

Meeting: Society for the Study of Ingestive Behavior Annual Meeting, July 2018, Bonita spring, Florida, USA

- * "Knockdown of the monocarboxylate transporter-2 in nodose ganglia increases food intake and body weight in rats fed a high-fat diet"
Nadja Weissfeld, Wolfgang Langhans and Myrtha Arnold
- * "SIRT3 overexpression in astrocytes affects glucose metabolism and energy homeostasis"
Nadja Weissfeld, Wolfgang Langhans and Abdelhak Mansouri

PUBLICATIONS

- * Mosberger AC, Miehbrandt JC, **Bjelopoljak N**, Schneider MP, Wahl AS, Ineichen BV, et al.
Axotomized Corticospinal Neurons Increase Supra-Lesional Innervation and Remain Crucial for Skilled Reaching after Bilateral Pyramidotomy. *Cerebral Cortex*. 2018;28(2):625-43
- * Ramachandran D, Clara R, Fedele S, Michel L, Burkard J, Kaufman S, **et al.**
Enhancing enterocyte fatty acid oxidation in mice affects glycemic control depending on dietary fat. *Scientific Reports*. 2018;8(1):10818
- * Langhans W, Adan R, Arnold M, Banks WA, Card JP, Dailey MJ, **et al.** New horizons for future research - Critical issues to consider for maximizing research excellence and impact. *Mol Metab*. 2018;14:53-9.

